BRNO UNIVERSITY OF TECHNOLOGY
VYSOKÉ UČENÍ TECHNICKÉ V BRNĚ

FACULTY OF CHEMISTRY
FAKULTA CHEMICKÁ

INSTITUTE OF CHEMISTRY AND TECHNOLOGY OF ENVIRONMENTAL PROTECTION
ÚSTAV CHEMIE A TECHNOLOGIE OCHRANY ŽIVOTNÍHO PROSTŘEDÍ

STUDY OF THE INTERACTION OF HAZARDOUS METAL – MICROPLASTIC

STUDIUM INTERAKCE RIZIKOVÝ KOV – MIKROPLAST

MASTER'S THESIS
DIPLOMOVÁ PRÁCE

AUTHOR **Bc. LENKA SINČÁKOVÁ**
AUTOR PRÁCE

SUPERVISOR **Mgr. HELENA DOLEŽALOVÁ WEISSMANNOVÁ, Ph.D.**
VEDOUCÍ PRÁCE

BRNO 2024

BRNO UNIVERSITY OF TECHNOLOGY
FACULTY OF CHEMISTRY

Assignment Master's Thesis

Project no.:	FCH-DIP1872/2022	Academic year: 2023/24
Department:	Institute of Chemistry and Technology of Environmental Protection	
Student:	**Bc. Lenka Sinčáková**	
Study programme:	Environmental Chemistry and Technology	
Field of study:	no specialisation	
Head of thesis:	**Mgr. Helena Doležalová Weissmannová, Ph.D.**	

Title of Master's Thesis:

Study of the interaction of hazardous metal – microplastic

Master's Thesis:

1. Analysis of the current state of knowledge focused on the issue of the interaction of hazardous metals with microplastics in the aquatic or terrestrial environment.
2. Sorption experiments.
3. Analysis of model samples of hazardous metal – microplastic systems.
4. Evaluation of data and interpretation of results.

Deadline for Master's Thesis delivery: 6.5.2024:

Master's Thesis should be submitted to the institute's secretariat in a number of copies as set by the dean This specification is part of Master's Thesis

Bc. Lenka Sinčáková student	Mgr. Helena Doležalová Weissmannová, Ph.D. Head of thesis	prof. Ing. Jozef Krajčovič, Ph.D. Head of department

In Brno dated 1.2.2024

prof. Ing. Michal Veselý, CSc.
Dean

Abstract

Microplastics are ubiqitous in the aquatic environmet and serve as a vector of wide range of contaminants, including heavy metals. This thesis aimed to examine the adsorption processes of five heavy metals (Pb, Hg, Zn, Cu and Cd) onto polyethylene terephtalate (PET), common river and sea pollutant. There has not been found a clear trend with regard to the influence of the size of the microplastics on the adsorption process. The salinity of the environment, on the other hand, has been found to have a profound impact on the adsorption process, with the observable decline of the adsorbed amounts in the environment with high ionic strength. The analysed heavy metals have been sorted in ascending order by its adsorption on PET as follows: Hg < Cd < Zn < Pb < Cu.

Abstrakt

Mikroplasty, široko zastúpené vo vodnom prostredí, slúžia ako vektor širokej škály kontaminantov, vrátane ťažkých kovov. Táto práca sa zaoberá adsorpciou piatich ťažkých kovov (Pb, Hg, Zn, Cu and Cd) na polyetylén tereftalát (PET), rozšírený polutant riek a morí. Pokiaľ ide o vplyv veľkosti mikroplastov na proces adsorpcie, nebol zistený jasný trend. Salinita prostredia má značný vplyv na adsorpčný proces s pozorovateľným poklesom adsorbovaných množstiev v prostredí s vysokou iónovou silou. Analyzované ťažké kovy boli zoradené vzostupne podľa ich schopnosti adsorpcie na PET nasledovne: Hg < Cd < Zn < Pb < Cu.

Keywords

microplastics, MPs, polyethylene terephtalate, PET, heavy metals, HMs, pollution, Pb, Hg, Zn, Cu, Cd, adsorption, atomic absorption spectrometry, AAS, Fourier transform infrared spectrometry, FTIR, fresh water, sea water, Langmuir isotherm, Freundlich isotherm, Temkin isotherm

Kľúčové slová

mikroplasty, MPs, polyetylén tereftalát, PET, ťažké kovy, HMs, znečistenie, Pb, Hg, Zn, Cu, Cd, adsorpcia, atómová absorpčná spektrometria, AAS, infračervená spektrometria s Fourierovou transformáciou, FTIR, sladká voda, morská voda, Langmuirova izoterma, Freundlichova izoterma, Temkinova izoterma

Reference

SINČÁKOVÁ, Lenka. *Study of the interaction of hazardous metal – microplastic.* Brno, 2024. Master's thesis. Brno University of Technology, Faculty of Chemistry. Supervisor Mgr. Helena Doležalová Weissmannová, Ph.D.

Rozšírený abstrakt

Znečistenie životného prostredia mikroplastami sa v posledných rokoch stalo celospoločenským problémom, ktorého negatívne dôsledky dosahujú naprieč celými ekosystémami. V neposlednom rade má ich prítomnosť aj priame následky pre človeka, ktorý je na dennej báze vystavený kontaktu s nimi. Jedným z hlavných hrozieb mikroplastov je ich schopnosť adsorbovať na svoj povrch kontaminanty zo svojho okolia, ako sú organické polutanty či ťažké kovy. Mikroplasty sa stávajú súčasťou potravy vodných živočíchov a postupne sa dostávajú do potravinových reťazcov. V tráviacich systémoch živočíchov potom môže dochádzať k desorpcii naviazaných polutantov a ich toxickému pôsobeniu na organizmy.

Táto práca sa zameriava na skúmanie adsorpčného správania piatich bežných ťažkých kovov (olova, ortuti, zinku, medi a kadmia) na polyetyléntereftalátové (PET) mikroplasty pomocou adsorpčnej atómovej spektrometrie (AAS). Napriek tomu, že PET má v porovnaní s inými polymérmi pomerne nízku adsorpčnú schopnosť pre polutanty, ide o široko používaný polymér nachádzajúci sa v mnohých spotrebných produktoch, najmä obalových materiáloch, a pre tento experiment bol vybraný pre svoj častý výskyt v životnom prostredí. Všetky adsorpčné experimenty sa uskutočnili v prostredí sladkej aj morskej vody a PET mikroplasty boli rozdelené do dvoch frakcií na základe veľkosti častíc ($< 0,63\ \mu m$ a $0,63\ \mu m - 1\ mm$), a následne bol skúmaný vplyv salinity a veľkosti aktívneho povrchu na adsorpčný proces.

Experimentálne výsledky odhalili komplexné interakcie medzi ťažkými kovmi a PET mikroplastmi. Zatiaľ čo v súvislosti s veľkosťou mikroplastickej frakcie na adsorpciu naprieč rôznymi kovmi nebol pozorovaný žiaden trend, a teda iné faktory mali prvadepodobne prevládajúci vplyv, salinita prostredia významne ovplyvnila proces adsorpcie. So zvyšujúcou sa iónovou silou výrazne klesala adsorpcia, pravdepodobne kvôli konkurencii o väzbové miesta, elektrostatickému odpudzovaniu a tvorbe komplexov. Modelovanie adsorpčných izoteriem ukázalo odlišné preferencie pre adsorpčné modely medzi študovanými kovmi. Zatiaľ čo adsorpcia zinku sa riadila Freundlichovým adsorpčným modelom, adsorpcia ortute a kadmia sa riadila Langmuirovým adsorpčným modelom a adsorpcia olova a medi sa riadila Temkinovým adsopčným modelom. Linearizačné a nelinearizačné metódy boli použité k optimalizácii kriviek, pričom druhé spomenuté vykazovali lepšie výsledky. Podľa adsorpčnej kapacity PET pre jednotlivé kovy je možné ich zoradiť vzostupne nasledovne: Hg < Cd < Zn < Pb < Cu.

Výsledky následnej analýzy pomocou infračervenej spektroskopie s Fourierovou transformáciou (FTIR) korelovali s výsledkami predchádzajúcich adsorpčných experimentov a poskytli pohľad na chemickú povahu adsorpčných procesov a potvrdili zmeny vo funkčných skupinách spojených s väzbou ťažkých kovov. K najväčším zmenám dochádzalo v oblastiach $1500 - 1400\ cm^{-1}$ a $450 - 400\ cm^{-1}$.

Táto práca prispieva k pochopeniu adsorpcie ťažkých kovov na mikroplasty v rôznych typoch prostredia. Pozorované rozdiely v adsorpčnom správaní podčiarkujú dôležitosť zohľadnenia environmentálnych faktorov pri hodnotení interakcií znečisťujúcich látok a mikroplastov a zdôrazňujú potrebu ďalšieho výskumu v podmienkach, ktoré sa čo najviac približujú tým reálnym.

Study of the interaction of hazardous metal – microplastic

Declaration

I hereby declare that this Master's thesis was prepared as an original work by the author under the supervision of Mgr. Helena Doležalová Weismannová, Ph.D. I have listed all the literary sources, publications and other sources, which were used during the preparation of this thesis.

.....
Lenka Sinčáková
May 2, 2024

Acknowledgements

Here I would like to thank my supervisor, Mgr. Helena Doležalová Weismannová, Ph.D., for her support, advice and suggestions.

Contents

List of Figures

Chapter 1

Introduction

Plastic is a material of ever-growing popularity owing to its wide array of useful properties. The very properties that contribute to popularity of plastic (low density, durability), however, also make it persistent pollutant in the environment. Apart from aesthetic impact, plastics pose a direct threat to marine fauna by accumulation, entrapment, entanglement, choking and suffocation. Additionally, they act as a source of organic and anorganic contaminants to fauna, as animals often confuse plastic particles for food. Such contaminants include plasticisers added to the plastic during manufacture and hydrophobic organic compounds (PCBs and PAHs) adsorbed to the surface from the environment.

Among the adsorbed contaminants of concern are heavy metals, which have been in the scientific spotlight for significantly shorter time than hydrophobic organic compounds. A vast variety of metal ions have been shown to sorb to plastics in the aquatic environment, with interactions between the two leading to alterations in bioaccumulation and toxicity of the two contaminants. The effects on organisms differ greatly, from synergistic effects to microplastics (MPs) acting as a chelating agents to heavy metals, lowering their toxicity in the environment.

Polyethylene terephtalate (PET) is a polyester with diverse range of applications, including packaging industry, clothing and electronic industry. Although it has a faily low sorption capacity to environamntal pollutants compared to other polymers, it is particularly prevalent in the environment, which can be contributed to its widespread use in drinking bottles manufacture, among others.

The adsorption of heavy metals on microplastics is influenced by a number of factors, with the active surface of MPs and salinity of the environment being an important ones. In this thesis, adsorption process of 5 heavy metals (Pb, Hg, Zn, Cu and Cd) on PET is being analyzed, using the atomic absorption spectrometry (AAS). PET was used in two fractions ($< \ 0,63\ \mu m$ and $0,63\ \mu m - 1\ mm$) and the adsorption experiments were carried out in both the freshwater and seawater (both laboratory prepared). MPs with smaller particle size were expected to exhibit larger adsorption capacity due to increased specific surface area, while presence of salts in sea water was expected to lead to competition for binding sites, complexation and electrostatic shielding, resulting in reduction of the adsorption process. Fourier transform infrared spectrometry (FTIR) was used as an additional method to confirm the chemical changes associated with the adsorption process.

Chapter 2

Theoretical part

2.1 Microplastics in Aquatic Ecosystems

Plastic is a generic term for man-made polymers prepared by polymerization of monomers from oil or gas (alternatively from coal, natural gasses, cellulose or latex from trees) [43]. Since becoming widely available in 1940s and 1950s, plastics have been consistently growing in popularity up to their current annual levels of consumption [26]. The overview of the plastic production and use since it became widely available can be seen in Figure 2.1. Rivers carry around $70 - 80$ % of environmental plastics, leading to their extensive deposition in world's oceans. The estimated consumption of plastic for 2050 is 33 billion tons [55]. The vast benefits of plastics include weight reduction, better facilitation of manipulation of material and improvement of energy efficiency in vehicles, to name a few [26].

According to State of The Science White Paper by Environmental Protection Agency (EPA) (2016), plastic particles are the most abundant type of debris encountered in the marine environment with estimated $60-80$ % of all marine debris being plastic and more than 90 % of all floating debris being plastic. The volume of plastics entering the marine environment has increased as much as three to four orders of magnitude since its mass production began in the 1940s and 1950s [8].

Microplastics and nanoplastics exhibit different properties than their corresponding bulk materials and thus represent a major concern in terms of their biological and ecological implications. These „smaller" plastic particles came to the scientific spotlight in 1970s after being indentified as major component in ocean floor debris [3].

Until recently, interactions between metals and plastic debris have not been considered a problem, as polymers are generally thought of as an inert material. Nevertheless, loss of metal to plastic containers is a common problem during sample storage or during experiments involving spiking of metal standards [26].

Nowadays, global production of plastics is on the rise, with environmental protection being of great importance and significant concern. Microplastics have been detected in aquatic, terrestrial and atmospheric environments (aquatic environment being the most explored), as well as in biota.

The negative effects of plastic debris on biota are of both physical and chemical nature, therefore, the plastic debris potentially acts as a multiple stressor to organisms. The physi-

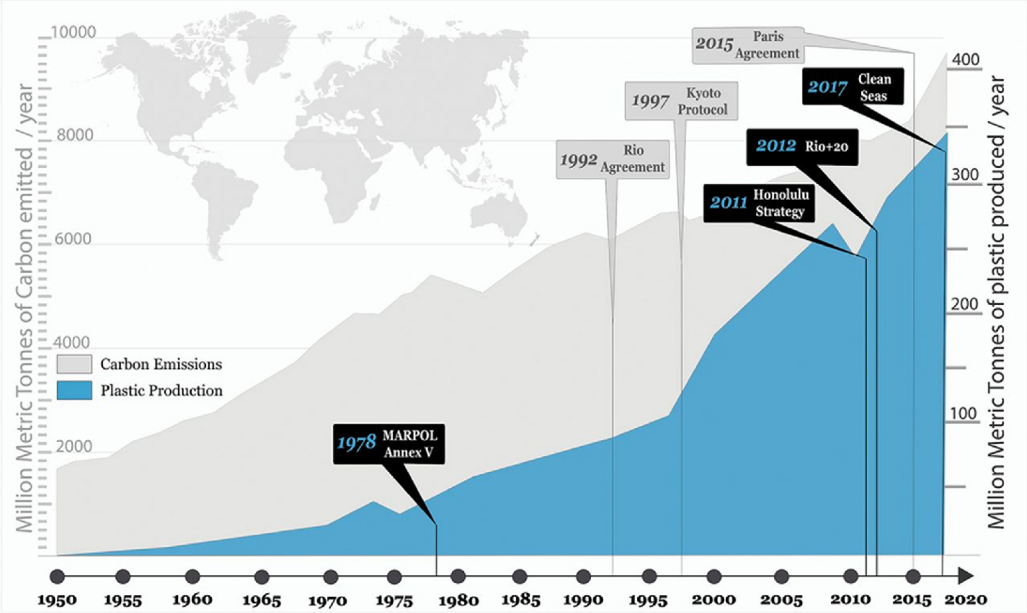

Figure 2.1: The overview of plastic production and consumption throughout the years 1950 - 2020. Taken from [23].

cal negative effects include ingestion, entaglement and smothering [47] [50] [21]. The chemical negative effects are a result of the presence of chemicals of two types: (i) additives and polymeric raw materials and (ii) chemicals absorbed from the surrounding ambience [13].

In light of the aforementioned facts, great efforts are being made to develop new methods for microplastics removal from the environment and mitigating its effects. The most common methods include absorption, filtration, biological degradation and chemical treatment processes. For removing micro and nanoplastics (MNPs) from wastewater (main entering point of MNPs to the environment), membrane bioreactors have been in use for the treatment of primary effluent coupled with various tertiary treatment technologies, such as disc filters, rapid sand filtration and dissolved air flotation for the treatment of secondary effluent. Photocatalyc, Fenton and ozone and peroxide based treatments are also being researched for the MNPs removal. The percentage of removal from waste waters with the combined use of this techniques is around $70 - 86$ % [50].

2.1.1 Definition and classification

Plastic debris can be divided into four categories: megaplastic (> 50 cm), macroplastic ($5 - 50$ cm), mesoplastic ($0,5 - 5$ cm) and microplastic ($< 0,5$ cm).These particles are often further degraded into even smaller particles – nanoplastics [50] [40] [57]. The International Organization for Standardization has defined nanoparticles as objects with their external dimensions falling into nanoscale ($1 - 100$ nm) [3] [60]. The size classification of plastics is provided in Figure 2.2. MNPs come in various shapes (pellets, fragments, fibers) and colours. Polyethylene (PE), polyprophelene (PP) and polystyrene (PS) are among the most common ones [34] [60].

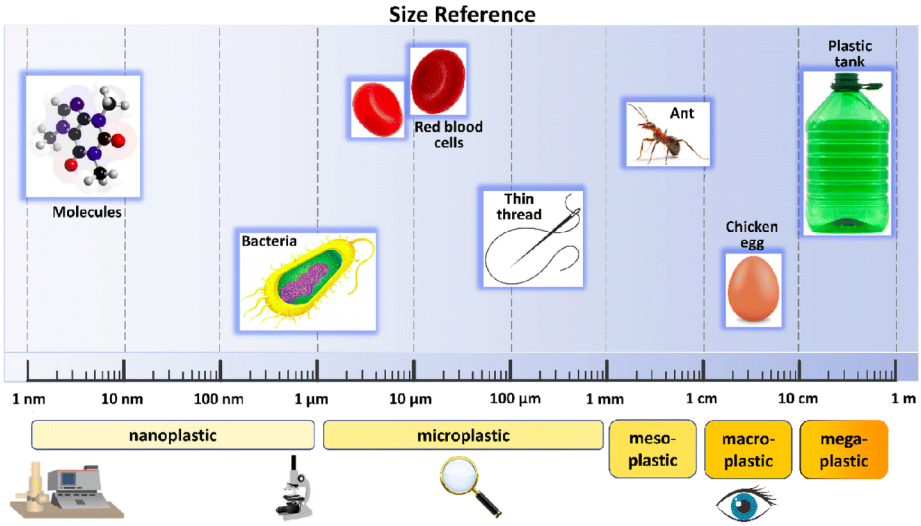

Figure 2.2: Size classification of different plastic types with the size reference to other real-world objects. Taken from [50].

Primary microplastics are plastics manufactured in size of a microplastics, typically for the purpose of use as an abrasive medium in both the cleaning industry and home cleaning products (facial cleansers, toothpaste, etc.). The second type is secondary microplastics, which get to the environment by breaking bigger sized plastics into smaller pieces, typically as a result of weathering through UV induced degradation, hydrolysis, biodegaradation or by mechanical degradation [34] [54] [23].

2.1.2 Origin

Primary MNPs are basically sourced from plastic pellets and personal care products containing microbeads. They are also used in other special applications, such as blasting agents in sandblasting or carriers for delivering active pharmaceutical agents [3] [17] [35].

Microbeads are microplastics (PE, PP, PS) serving as exfoliating agents not only in cosmetics, but aso in biomedical and other health-science applications. They have been found in marine water since 1990s [15] and come in various shapes – mostly spherical, but also elliptical and thread-like, and besides being used as scrubber agents, they can be also used as film-forming and hydrophilic agents. Their properties create a ball-bearing effect, resulting in spreadability and silky texture, desired qualities in cosmetic applications. Another application is a substitute for natural materials like pumice stone and activated carbon. Coloured microbeads are used for esthetic purposes. They pass through sewage treatment plants unhindered, making them a problematic source of MPs in water bodies. Estimated 11 % of MPs in North Sea are microbeads [3] [35].

Secondary microplastics are produced via different environmental degradation processes – biodegradation, chemical degradation (photooxidation, corrosion) or physical degradation (temperature, wave action, erosion). Primary sources of plastics are land-based, contributing an estimated 80 % of the total plastic debris to the environment. The major sources of secondary MPs include municipal wastes – farming films, plastic bags and bottles, fishing

gears, vehicle tire wear and mulching foils. Secondary MPs account for most of the MPs found in the environment [3] [17] [8].

Resin pellets (granulate) are another major source of MPs. They either come as pre-preduction material used in plastic manufacture, or as a by-product of plastic recycling (during cleaning, crushing, melting, sorting and molding) [3]. Landfills and waste incineration also contribute to the MNPs pollution [50].

Due to increasing number of vehicles worlwide, vehicle tire wear and road markings abrasions are of particular concern. Another notable source of microplastics is shedding from synthetic textile fibers during washing and drying process, with approximately 124 to 308 mg of microplastics being released per kg of washed fabric. Construction industry is also among the top sources of microplastics worlwide, as well as materials and cargo lost from the ships [3] [17].

A summary of the major sources of different types of MPs is presented in Figure 2.3.

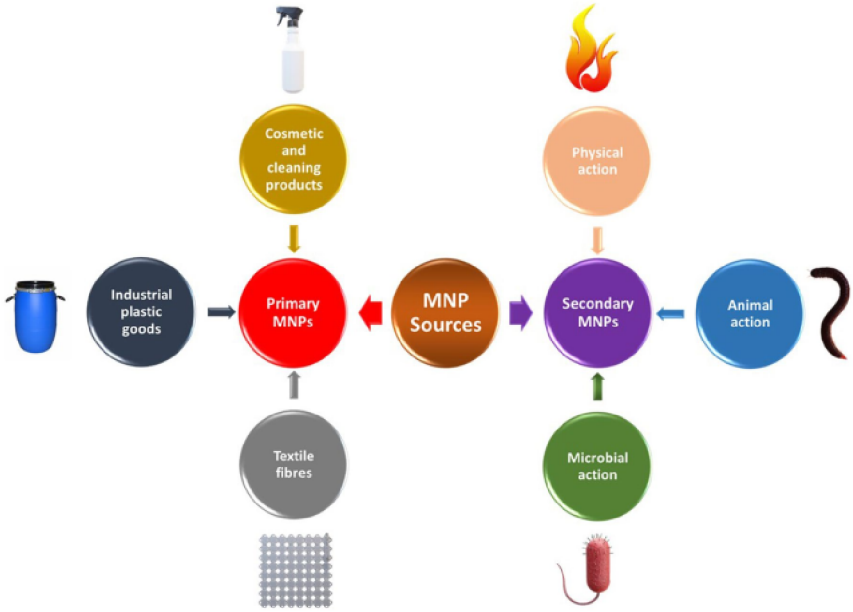

Figure 2.3: The overview of major sources for both the primary and the secondary microplastics in the environment. Taken from [3].

2.1.3 Occurence and transport

MPs pollute aquatic, terrestrial and atmopheric environments, which are all interconnected via diverse networks of source-pathway-sink connections that influence the flux and retention of MPs in the environment. The biogeochemical cycle of microplastics transport across various components of environment are shown in Figure 2.4. Nevertheless, majority of studies conducted in last decades is aimed at the aquatic pollution [3].

Plastic waste is usually generated (i) by the inhabitants, varying according to their habits, geographic location and existing infrastructures; (ii) from waste management and treatment, (iii) from industrial and manufacturing plants. Once MNPs enter the environment,

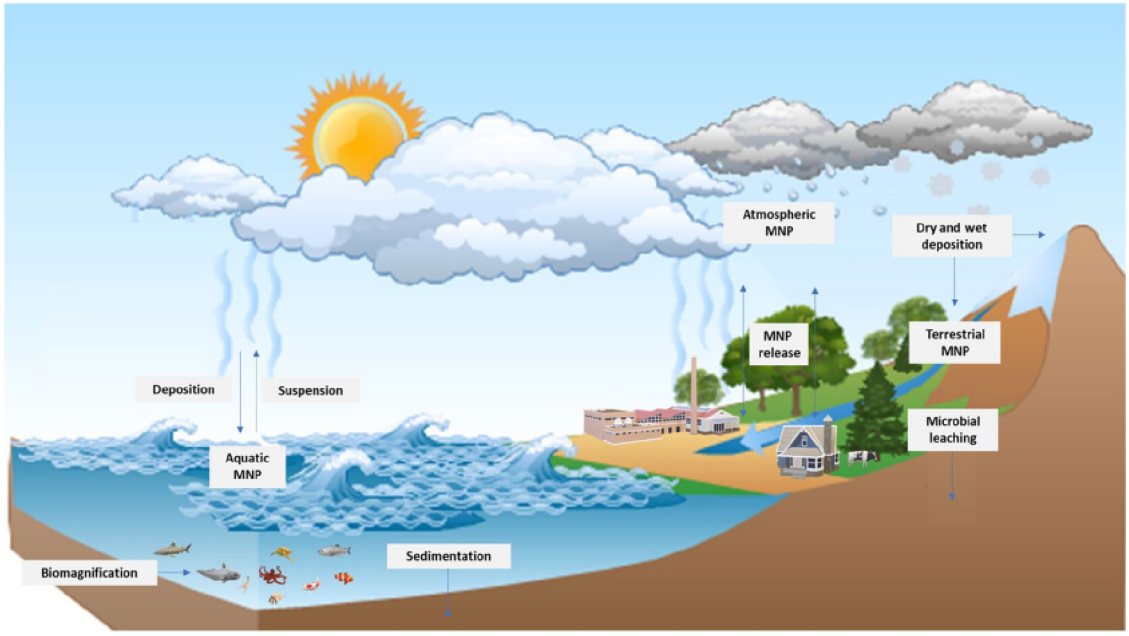

Figure 2.4: The biogeochemical cycle of microplastics across aquatic, terrestrial and atmospheric environment. Taken from [3].

it is transported by wind, washed off from land by rainfall, and subsequently transported in fresh and seawater. Most of consumer plastics are buoyant in seawater [17] [50] [33].

Land-based microplastics are mainly introduced into water bodies through wastewater treatment plant (WWTP) effluent and industrial discharge. Apart from WWTPs, a major source of MNPs in the environment is drainage system overflow. MNPs can either float on the water's surface or settle on the waterbeds, posing ecological risks. In polar regions, melting sea ice is releasing trapped microplastics. Microplastics are found in both natural and human-made water cycles, including municipal sewage and wastewater treatment plants, where they come from various sources like domestic washing and personal care products [15] [8] [33].

The spatial concentration of aqueous microplastics is primarily influenced by land use patterns, while the longitudinal distribution in flowing water is affected by microplastic density, land use, and hydrodynamic factors like flow dynamics and tidal exchanges. Rivers transport plastic particles over longer distances, with microplastics settling when there is a decrease in energy flow, such as in riverbeds. Lakes, characterized by low water flow and high sedimentation rates, accumulate microplastics [15] [50]. The net transport of plastic to and within the ocean can be exacerbated by extreme weather events such as floods, tsunamis, hurricanes, and tornados [8]. Figure 2.5 shows spatial distribution of plastic debris in world's oceans.

The shape, size, and density of microplastics impact their dispersal through natural currents, with large, dense particles sinking easily, irregular-shaped ones getting retained underwater, and spherical-shaped ones remaining on the surface. Most of these micro-fragments can accumulate in the central oceanic regions (termed "gyres" - a systems of ocean currents that move in a circular pattern). So-called "Stokes drifts" generate the transport of MP

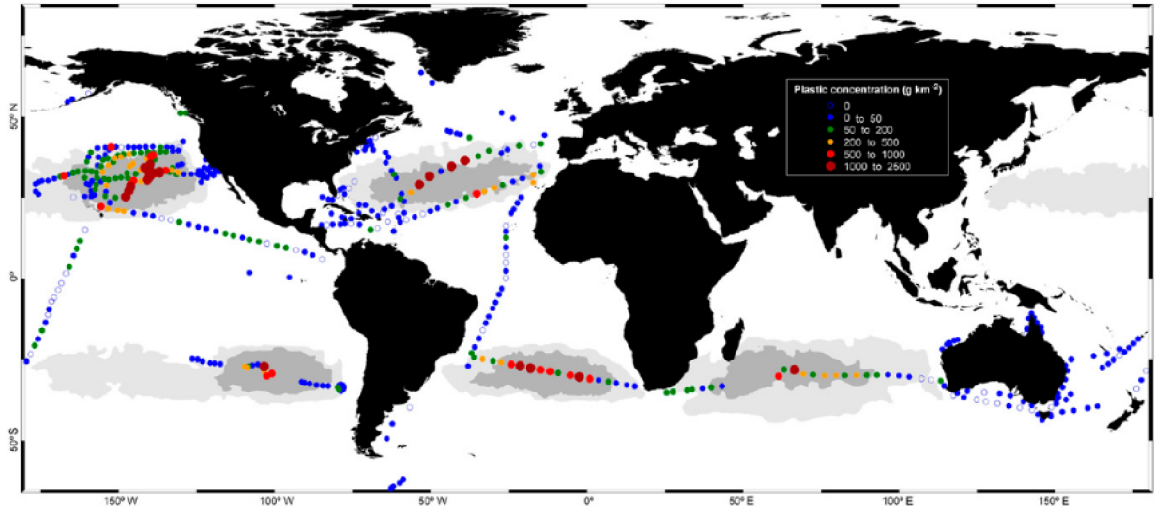

Figure 2.5: The spatial trends of plastic debris in world's oceans. Taken from [43].

from the open sea to shallow coastal waters. A phenomenon of biofouling is often observed: organisms collonise the surface of plastic fragments and form biofilms, which results in aggregates forming and the speed of sedimenting increasing rapidly [15] [50] [8].

2.1.4 Toxicological effects

Several studies of aquatic organisms have shown the harmful, if not lethal effects of microplastics at the individual, cellular, and molecular levels. The summary of recorded effects of microplastics on organisms on different levels is provided in Figure 2.6. Aquatic organisms and aquatic-dependent wildlife can be selective in the types, forms, colors, and sizes of plastics they ingest depending on their foraging technique and diet. The toxicity of microplastics may depend on the size, shape, and surface coating of the particles [55] [8]. The unmodified polymers were shown in vitro to affect cell viability, inflammatory gene expression, and cell morphology. The ability to interfere with cell processes enhances greatly when charge is introduced to the MNPs particles. MNPs were shown to be uptaken by different cell lines (tested on macrophage *RAW 264,7* and epithelial cells *BEAS-2B*). Is it assumed that the MNPs cause oxidative stress, which is the main cause of metabolic disorders and local inflammations [3].

Ways of exposure of human body to MNPs include consumption of sea salt, consumption of MNPs in drinking water (90000 MNPs particles consumed from bottled water compared to 4000 consumed when relying on tap water), alcohol, sugar or seafood. The uptake from cosmetic products have not yet been properly tested. The bioavailability (oral) for PS in mammalian models (rats) was estimated as 10 %, for blood, bone marrow, liver and spleen it was estimated to be around 4 % [3] [15].

To ensure the safety of sea food for human consumption, bioindicator organisms, such as the lugworm (*Arenicola marina*) for sediment toxicity tests or the mussel (*Mytilus galloprovincialis*) for marine pollution are used. Due to their large surface area, they are able to interfere with lipid metabolism and transportation and distort the structual integrity

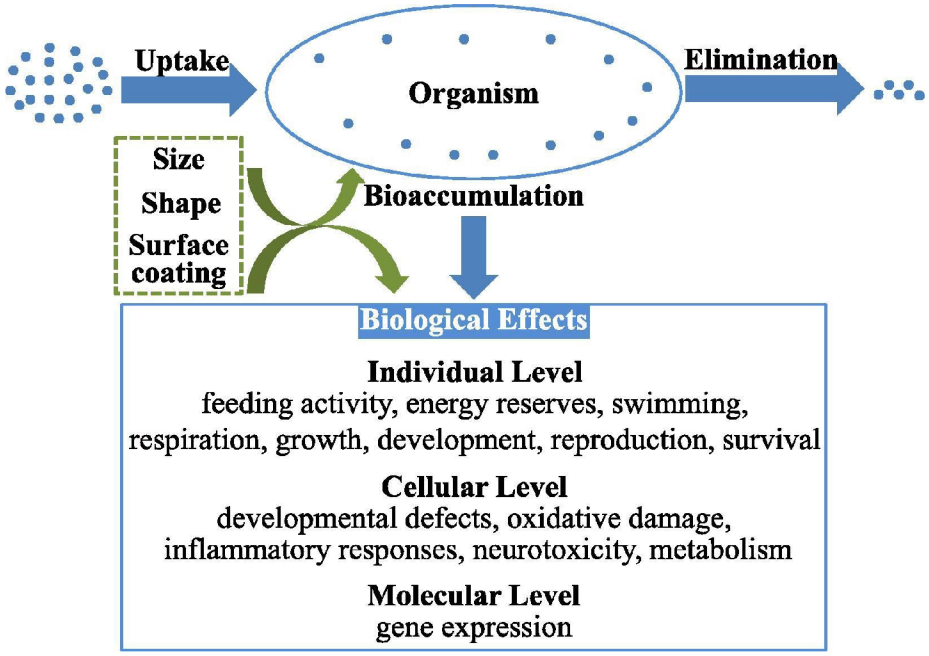

Figure 2.6: The effects of microplastics on organisms on individual, cellular and molecular level. Taken from [55].

of proteins by changing secondary structures, inducing protein misfolding and affecting integrity anf function of the membrane by interaction with metallic ions [3].

They can also, due to their small size, potentially impact immune mechanisms during pregnancy, growth-factor signaling during implantation, and interactions between the embryo and uterus. Placental exposure to microplastics and the transgenerational effects of plasticizers on metabolism and reproduction have been observed. In vitro exposure to microplastics has been shown to increase genetic variability in human peripheral blood lymphocytes. Even low concentrations of microplastics can have this effect. While microplastics smaller than 20 μm can penetrate few organs, practices of 10 μm size can have access to sensitive organs, including the placenta, liver, and brain, through cell membranes and blood-brain barrier [15].

Chemical additives like plasticizers, heat stabilizers, antioxidants, and colorants are commonly used in polymer manufacturing to enhance product performance, such as mechanical and thermal resistance. Plasticizers are complex chemical products that have low vapor pressure, are insoluble in liquids, are chemically stable, and which are inserted between molecular chains to reduce their forces of physical attraction and increase their mobility, workability or distensibility. Among the additives of concern, bisphenol A (BPA), phtalates, some of the brominated flame retardants and heavy metals are of particular concern [15] [13] [60]. According to the UN Globally Harmonized System (GHS) over 50 % of all plastic types contain hazardous monomers, additives and byproducts [29]. The topic of heavy metals as a plastic additive is discussed later in section 2.4 in this thesis.

2.1.5 Accumulation and fate in the aquatic environment

Due to the heterogenity of MPs, as well as organic matter often adsorbed on their surface and the microorganisms that tend to collonise them, they have the propensity to form both homo- or hetero-aggregates [3] [17]. It is well-known that a wide range of wild animals confuse plastic debris for food and ingest it. This animals include amphipods, copepods, lugworms, barnacles, mussels, decapod crustaceans, seabirds, fish, and turtles [55] [35]. Low-density (i.e. buoyant) microplastics are ingested by pelagic filter feeders while high-density microplastics tend to be ingested by benthic deposit feeders. In most cases, MNPs are excreted rapidly, for for very small MNPs, translocation from the GIT to the circulatory system was observed [17]. Possible routes and interactions of MNPs with organisms are depicted in Figure 2.7.

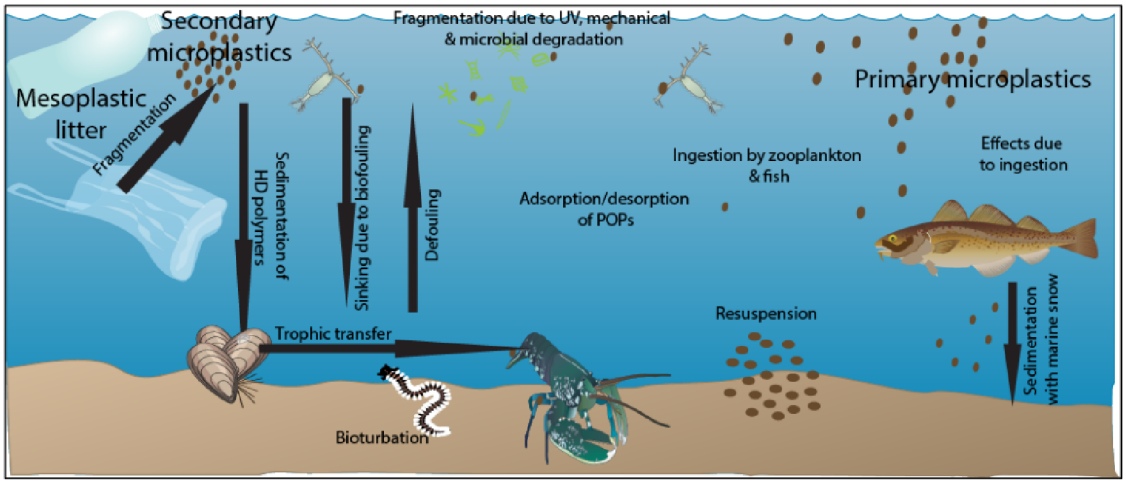

Figure 2.7: Potential pathways of MNPs in marine environment, including biological interactions. Taken from [43].

The four main factors that can play a role in MNPs degradation are biodegradation, hydrolysis, photodegradation and thermooxidative degradation [3]. Disintegration of common polymers such as low-density polyethylene (LDPE), high-density polyethylene (HDPE) and PP on the surface is mainly initiated by UV radiation. In the water, wave turbulences and wave action, as well as freeze-thaw cycles, tend to be of bigger importance [17].

Among others, biodegradation has been studied extensively in past years as a promising way of degrading MNPs. Biodegaradation is defined as a breakdown of complex polymers by microorganisms (archaea, bacteria, fungi), into non-toxic products that are reintroduced into biogeochemical cycles. The mechanisms include biodeterioration, biofragmentation, assimilation and mineralization [3].

The first step is attachment of organisms to the surface of the polymer. Subsequently, the chemical activities of microorganisms coupled with external processes (light, temperature, chemicals) depolymerase the material into oligomers or monomers that are taken up into the cells by active or passive transport. Assimilative transport is faciliated by various molecules, such as monooxygenases and porins. Lastly, the monomers are broken down into oxidized metabolites (CH_4, CO_2, H_2O, N_2) (the final products being a function of the respiration condition of a microbe). *Bacillus* and *Pseudomonas* bacterial species have been found to

be the most promising with regard to biodegradation in an estuary. For petroleum-based MNPs, *Zalerion maritimum* and *Aspergillus flavus* are a promising fungi species [3].

2.1.6 PET

In the experimental part of this thesis, polyethylene terephtalate was used. Polyethylene terephthalate (PET) is a chemically stable polyester made by transesterification reaction between ethylene glycol and dimethyl terephtalate. It has a diverse range of applications, including food and drink containers, electronic components, and clothing fibers. The use of PET has significantly increased in recent decades. Recycled PET bottles are commonly used to make fleece garments and plastic bottles (Figure 2.8) (Table 2.1) [16] [46].

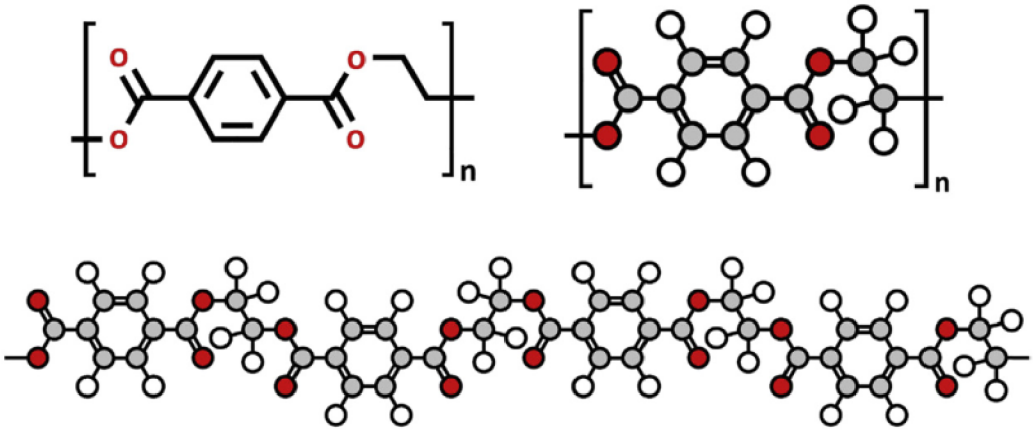

Figure 2.8: Molecular formula of polyethylene terephtalate. Taken from [16].

It possesses several key characteristics, making it an important polymeric material in use:

- PET is colourless and can be transparent (if amorphous) or translucent (if semi-crystalline);
- PET is lightweight;
- PET is thermoplastics, robust, semi-rigid to rigid, mechanically-resistant to impact, and stretchable during processing;
- PET shows gas-barrier properties against moisture and CO_2;
- PET is extremely inert compared to the other plastics, and free from plasticizers (on the contrary, in the case of PVC the use of plasticizers is essential);
- in order to improve specific properties, PET can be blended with other polymers (e.g., with polycarbonate (PC), PP, PP copolymers, and polybutylene terephthalate (PBT)) or surface modified (through physical and chemical treatments);
- PET can be copolymerized (e.g., PET-G) [44].

chemical formula	$(C_{10}H_8O_4)_n$
abbreviation	PET or PETE
number	01
classification	thermoplastic
molecular orientation in solid phase	semi-crystalline
monomers	terephtalic acid, ethylene glycol
general properties	transparency to visible light and microwaves; very good resistance to ageing, wear and heat; lightweight, impact and shatter resistant; good gas and moisture barrier properties;

Table 2.1: Overview of PET properties [16].

2.2 Heavy metals

There has been an ongoing discussion regarding the definition of the term „heavy metals“, which are defined by their high atomic weight or high density. Heavy metals are commonly defined as elements with a specific weight of more than 5 g/cm^3. Those metals that are at least 5 times denser than water are also categorized as heavy metals. These include essential metals such as Mo, Mn, Cu, Ni, Fe, and Zn, as well as non-essential metals like Cd, Ni, As, Hg, and Pb. The assumption that heaviness and toxicity are interconnected extends to metalloids like arsenic, which can induce toxicity even at low levels of exposure. It is worth noting that some metalloids and lighter metals, like selenium, arsenic, and aluminum, can be toxic and are thus included in the category of heavy metals, even though traditionally not all heavy metals are toxic (e.g., gold) [11] [49] [32].

Heavy metals constitute a relatively large portion of periodic table and are present in all sorts of habitats in the environment and are of either natural, or anthropogenic origin. Many of them exhibit toxic properties and some of them are a vital part of living organisms, such as manganese, copper and zinc [30]. Lead, thallium, cadmium and antimony are commonly found as a byproduct and waste from industrial production. Heavy metals (HMs) can cause toxicity in certain areas of human body, such as nephrotoxicity, neurotoxicity, hepatotoxicity, skin toxicity and cardiovascular toxicity. Among treatment procedures developed, various natural products have been in use, together with novel nanotechnological approaches [41].

2.2.1 Properties

Metalloids have a tendency to form covalent bonds and exhibit toxicological properties as a direct consequence. This property allows them to bind covalently with organic groups, forming lipophilic ions and compounds, leading to potentially toxic effects when they bind to nonmetallic elements of cellular macromolecules. Examples of lyophilic compounds include tributyltin oxide and methylated forms of arsenic, both highly toxic. Lead and mercury, binding to sulfhydryl groups of proteins, exemplify the binding to nonmetallic elements [11].

Heavy metals can enter the human body through ingestion of contaminated food, inhalation from the atmosphere, drinking contaminated water, and skin contact from various

sources [11]. Human exposure to toxic heavy metals comes mostly from vegetables, which accounts approximately to 90 % of the overall intake (the rest coming from skin contact and breathing of polluted air) [41]. These metals are nonbiodegradable and cannot be broken down. Organisms may detoxify metal ions by hiding the active element within a protein or depositing them in intracellular granules for excretion. Bioaccumulation of heavy metals in the human system can lead to biological and physiological complications [11].

Some heavy metals are essential elements necessary for life, required for various biochemical and physiological functions. However, they can be toxic in large amounts. These elements play crucial roles in maintaining skeletal structure, regulating acid-base equilibrium, and serving as constituents of enzymes, structural proteins, and hormones [11] [41]. The relationship between concentration of essential elements in the human body and its performance is depicted in Figure 2.9.

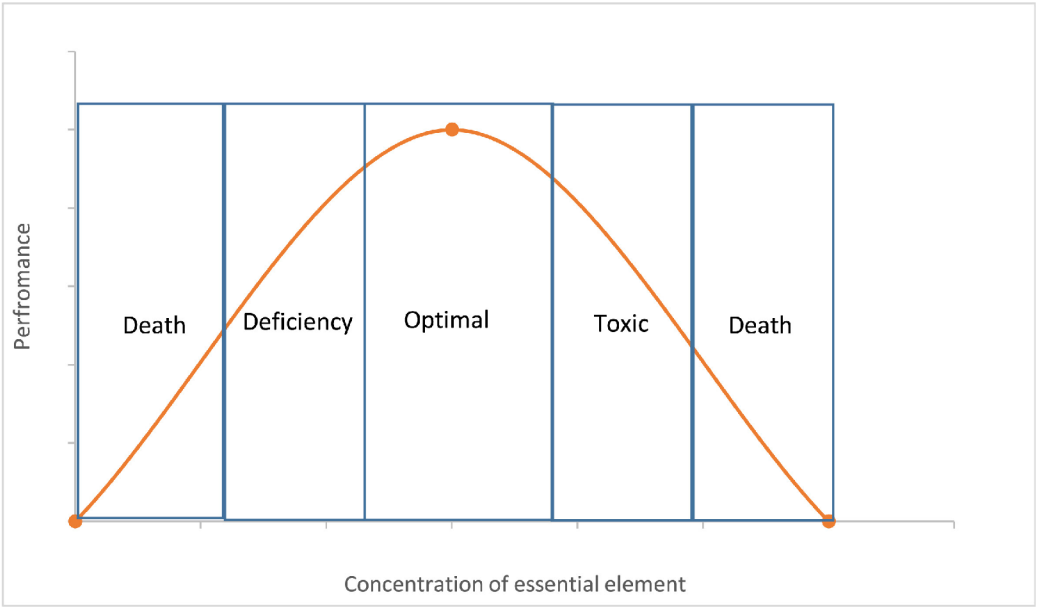

Figure 2.9: The relationship between concentration of essential heavy metals in the body and performance. Taken from [11].

Nonessential metals do not have a key role in the body, but they may cause toxicity by affecting the levels of essential elements. The dispersion of these metals into the environment, including the atmosphere, waters, and soils, is a consequence of their widespread use in agriculture, industry, medicine, and other sectors [11] [41].

2.2.2 Heavy metals in the environment - entry, transport and fate

Heavy metals are present in the Earth's crust since its formation. However, the significant increase in human activities such as mining, smelting, foundries, and other metal-based industries, has led to a substantial rise in metallic substances in both terrestrial and aquatic environments. Other industrial sources include coal burning in power plants, petroleum combustion, nuclear power stations and high tension lines, plastics, textiles, microelectronics, wood preservation, and paper-processing plants. Agricultural practices, including the use of pesticides, insecticides, and fertilizers, further contribute to this pollution. Natural

processes like volcanic activity, metal corrosion and sediment resuspension can also contribute to heavy metal pollution [11] [49] [7]. While plastics in the marine environment have received the most attention to date, investigations also indicate that plastics readily accumulate in freshwater environments [8].

Heavy metals are also categorized as trace elements due to their presence in trace concentrations (less than 10 ppm) in various environmental matrices. Their bioavailability is influenced by physical factors such as temperature, phase association, adsorption, and sequestration. Additionally, chemical factors, including speciation at thermodynamic equilibrium, complexation kinetics, lipid solubility, and octanol/water partition coefficients, impact their behavior. Biological factors, such as species characteristics, trophic interactions, and biochemical/physiological adaptation, also play a crucial role [49].

Heavy metals pollution is persistent and long-term, they are non-biodegradable and have a long half-life. Heavy metals have the capacity to engage in reactions with other elements in the soil or sediment, leading to the formation or degradation of compounds that may become more toxic. An illustration of this phenomenon is the creation of the toxic methylmercury through the interaction of inorganic mercury with bacteria present in water, sediment, and soil. Soil contamination with heavy metals and their subsequent absorption and bioaccumulation in food crops is of substantial concern, especially in developing countries. Heavy metals concentration is influenced by soil type, plant genotype and their interactions. Metals are bound more to the soil if the clay content, organic matter and the pH are higher. In the water domain, the solubility of metals is primarily influenced by the water's pH. When streams containing heavy metals enter the sea, the acidity level increases, causing the solubility of the metals to decrease, resulting in their precipitation towards the seabed. Phytoremediation and intercropping are ways in which heavy metals can be absorbed and removed from the soils, sediments and waters [41] [11] [33]. The overview of common heavy metals pathways in the environment is provided in Figure 2.10.

2.2.3 Effects and toxicity

The global health risks associated with heavy metal pollution are a major concern due to the toxicity, carcinogenicity, bioaccumulation, and complex mechanisms involving multiple sources and pathways. Several shocking incidents of heavy metal pollution have occurred globally, including Japan's Minamata disease caused by mercury pollution, Itai-itai disease induced by cadmium pollution, health issues from arsenic contamination in Bangladesh, and lead poisoning in children. While emissions of heavy metals have decreased in many developed countries since the end of the 20th century, the health risks associated with heavy metals persist. In some less developed countries, these risks are increasing due to complex exposures from multiple sources through various processes and pathways [24].

Certain metals like cobalt (Co), copper (Cu), chromium (Cr), iron (Fe), magnesium (Mg), manganese (Mn), molybdenum (Mo), nickel (Ni), selenium (Se), and zinc (Zn) are essential nutrients crucial for various biochemical and physiological functions. An insufficient supply of these micronutrients can lead to various deficiency diseases or syndromes [49]. Several elements, such as chromium and copper, exhibit a relatively narrow concentration range where they can have beneficial effects, but beyond this range, they become hazardous [30].

The transfer of metals from soil to plants is a significant concern for food safety. Consuming food crops grown in contaminated soils represents a major pathway for human exposure

Figure 2.10: Pathways, sources and interactions of heavy metals in the environment. Taken from [41].

to these metals through the food chain, with Cd, As and Pb being the most concerning metals regarding soil-to-plant exposure in health risk assesment. In drinking water, As is a very frequently represented heavy metal, which is a major concern especially in developing countries, such as Bangladesh and Pakistan. Another major source of contaminants and health concerns is dust, with the main pollutants in urban street/road dust and rural dust being Cd, Pb, Zn, Cr, Cu and Mn [24].

Certain metals, such as cadmium, nickel, and arsenic, are known to inhibit DNA repair mechanisms, further contributing to genomic instability. Oxidative effects on DNA include (i) base modification (observed with chromium and nickel), (ii) crosslinking (seen with nickel, copper, and oxidant iron), (iii) strand scission (seen with nickel, cadmium, chromium), and (iv) depurination (observed with copper, chromium, and nickel) [11] [6]. Metal-induced damage can be classified into „direct“ and „indirect“ damage. In direct damage, conformational changes occur to biomolecules due to metal interactions. Indirect damage results from the production of reactive oxygen and nitrogen species, including hydroxyl and superoxide radicals, hydrogen peroxide, nitric oxide, and other endogenous oxidants. Heavy metals, such as iron, copper, nickel, chromium, and cadmium, activate signaling pathways and contribute to the formation of free radicals, leading to DNA damage, alterations in sulphydryl homeostasis, and lipid peroxidation (Figure 2.11) [11].

Metal-mediated alterations in calcium homeostasis, often due to membrane damage, activate various calcium-dependent systems, including endonucleases. Free radical formation,

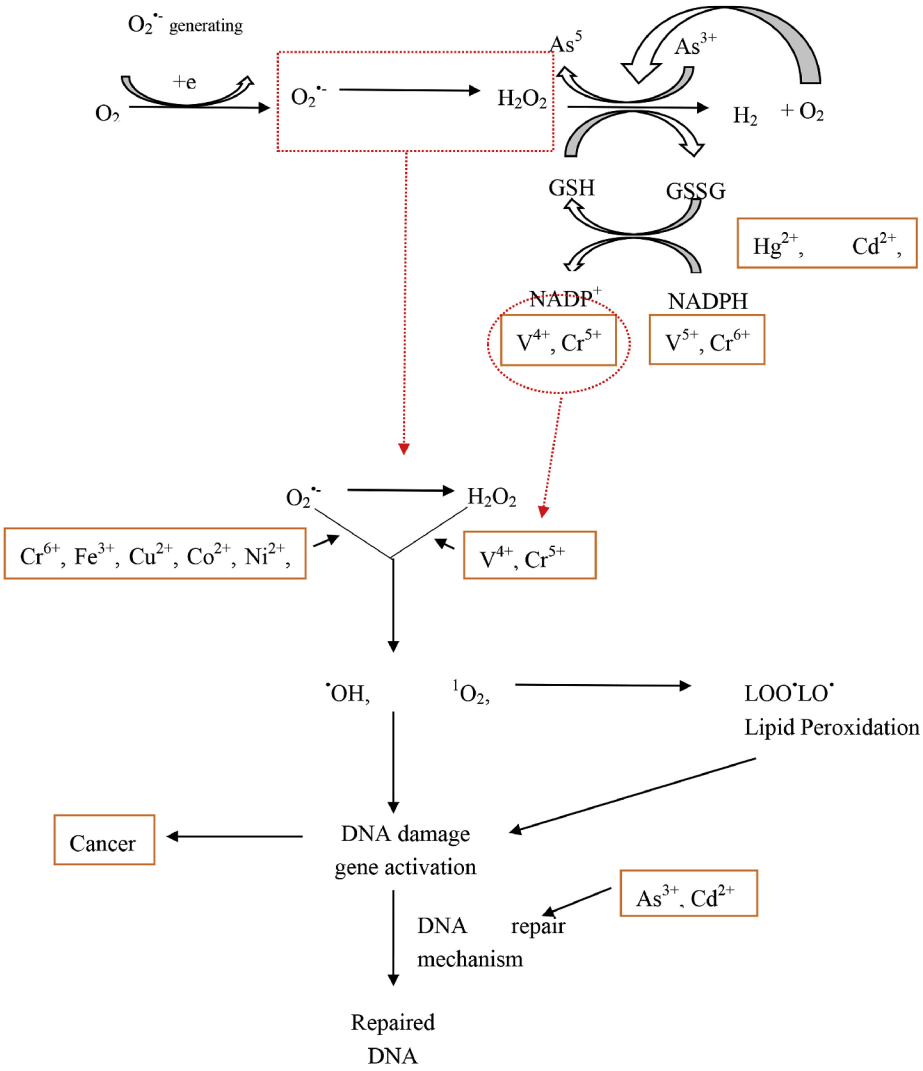

Figure 2.11: Metal-induced oxidative stress pathways. Taken from [11].

particularly investigated for iron, copper, nickel, chromium, and cadmium, is associated with their carcinogenic properties. Iron, copper, vanadium, chromium, and cobalt follow the Fenton reaction (Equation 2.1), primarily linked to cellular structures like mitochondria, microsomes and peroxisomes [11].

$$Me^{n+} + H_2O_2 \rightarrow Me^{(n+1)+} + \cdot OH + OH^- \tag{2.1}$$

Upon entering the body, heavy metals can bind to lipids, proteins, and nucleic acids. The binding to enzymes and proteins frequently involves thiol (–SH) groups, leading to modifications of cysteine residues in proteins (Figure 2.12) [6].

Protection against free radical attacks induced by metals involves various antioxidants, both enzymatic and non-enzymatic. In the context of iron toxicity, antioxidants play a protective role by preventing molecular oxygen and/or peroxides reactions, chelating ferrous ions, facilitating the chelation of iron, maintaining the redox state to render iron incapable of

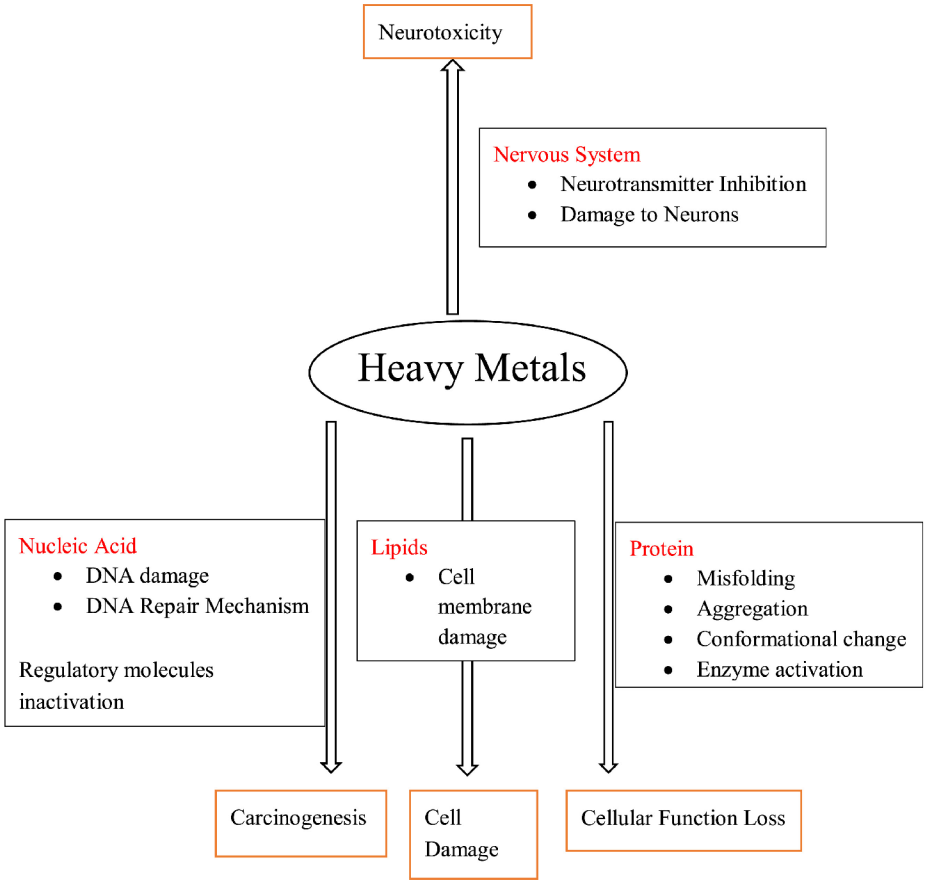

Figure 2.12: Heavy metals pathways of human exposure and consequences of this exposure in human body. Taken from [11].

reducing molecular oxygen, and trapping formed radicals. Thiol compounds, including glutathione, are particularly effective, maintaining the cell's redox state and reducing peroxide to protect the cell. Additionally, non-enzymatic antioxidants like Vitamin E contribute to preventing damage caused by metals in in vitro systems and animals exposed to iron, copper, and cadmium [11].

2.2.4 Characterization of selected heavy metals

The heavy metals which are described in further detail in this subsection include Lead, Mercury, Zinc, Copper and Cadmium, which are subjects of the experimental part of this thesis (see chapter 3). In Table 2.2, the overview of properties, uses, effects on humans and food sources of above mentioned metals is provided.

Lead

Lead is a naturally occurring bluish-gray metal found in small amounts in the earth's crust. While lead is naturally present in the environment, human activities such as burning fossil fuels, mining, and manufacturing contribute to the release of higher concentrations. It is

	Properties	Uses	Effects	Food source
Pb	· density: $11,3\ g/cm^3$ · colour: dull silver-grey · soft · easily worked · ore: galena	· batteries · cable sheeting · lead glass · lead piping · roofing	· hypertension · miscarriages · brain injury · iron deficiency · sperm damage	· grains · seafood · red meat · wine · fruits
Hg	· density: $13,5\ g/cm^3$ · rare in natural state · silvery liquid at 25 $°C$ · 66^{th} most abundant · ore: cinnabar	· barometers · thermometers · gold recovery · tooth fillings · catalyst	· genotoxic · Down's syndrome · irritating · misscariages · Minamata disease	· sea food · mushrooms
Zn	· density: $7,13\ g/cm^3$ · colour: silvery-white · essential · tarnishes in air · ore: sphalerite	· galvanisation · deodorants · batteries · ink · X-ray screens	· anaemia · nausea · fatique · copper deficiency · neutropenia	· lamb · beef · cheese · herring · sunflower
Cu	· density: $8,96\ g/cm^3$ · colour: reddish-gold · easily worked · essential · ore: chalcopyrite	· alloys · wires · plating · coins · pipes	· Wilson's disease · insomnia · anxiety · agitation · restlessness	· liver · oyster · spirulina · lobster · shiitake
Cd	· density: $8,69\ g/cm^3$ · colour: silvery-bluish · found with zinc · 64^{th} most abundant · ore: greenockite	· fertilizer · pesticide · batteries · plating · nuclear reactors	· nephrotoxicity · infertility · bone fracture · DNA impairment · cancer	· shellfish · mussels · seaweed · shrimps · mushrooms

Table 2.2: An overview of properties, uses, effects on humans and most frequent food sources for selected heavy metals [11].

employed in the production of lead–acid batteries, ammunitions, metal products like solder and pipes, and devices used for X-ray shielding [49] [51] [32].

Lead exposure primarily occurs through the inhalation of lead-contaminated dust particles or aerosols and the ingestion of lead-contaminated food and water [49] [30]. Lead (Pb) disturbs various processes, including protein folding, inter- and intracellular signaling, apoptosis, enzyme regulation, and cell adhesion. This is because lead metal ions can replace other monovalent cations like Na^{+} and bivalent cations like Cl^{2+}, Fe^{2+}, etc., disrupting normal cellular functions [32]. In the human body, the highest percentage of lead is absorbed by the kidneys, followed by the liver and other soft tissues like the heart and brain [49].

In cases of chronic lead nephropathy, there are identifiable features such as hyperplasia, interstitial fibrosis, tubular atrophy, renal failure, and glomerulonephritis [41]. However, the major body fraction of lead is stored in the skeleton. The nervous system is particularly vulnerable to lead poisoning. Early symptoms of lead exposure's effects on the central nervous system include headaches, poor attention span, irritability, loss of memory, and dullness [49] [51]. In humans, lead (Pb) can cause two types of anemia. High levels of exposure to lead can result in hemolytic anemia, while prolonged exposure to elevated blood lead levels can lead to Frank anemia [32]. Children absorb $4-5$ times more ingested lead than adults [51]. Experimental studies have suggested that lead is potentially carcinogenic, as it has been found to induce renal tumors in rats and mice. Due to these findings, the International Agency for Research on Cancer (IARC) considers lead as a probable human carcinogen [49] [51].

Chemical precipitation is requently used for elimination of Pb from contaminated liquids. Numerous economical adsorbents, including bagasse pith sulfurized activated carbon, blast furnace sludge, biogas residual slurry, olive mill products, and peanut shell carbon, have been explored for their efficacy and affordability in removing Pb(II) from wastewater [30].

Mercury

Mercury is a heavy metal found in three forms in nature: elemental, inorganic, and organic. Mercury vapor is more hazardous than the liquid form. It also exists in cation forms with oxidation states of +1 (mercurous) or +2 (mercuric). Methylmercury, an organic compound, is commonly encountered in the environment through methylation of inorganic mercury by microorganisms [49] [6] [32]. In Japan and Iraq, it caused so-called Minamata disease [32]. Mercury finds applications in the electrical industry, paint industry, dentistry (in dental amalgams), and various industrial processes, including the production of caustic soda, nuclear reactors, antifungal agents in wood processing, and as a solvent and preservative in pharmaceuticals. Mercury has also had medicinal uses in the past. The industrial demand for mercury peaked in 1964, declining sharply between 1980 and 1994 due to federal bans on mercury additives in paints and pesticides, as well as reduced use in batteries [49] [6] [30].

Mercury toxicity is primarily mediated by its chemical activity and biological properties, indicating the involvement of oxidative stress in its toxic effects. Both inorganic mercury (Hg^{2+}) and methylmercury (MeHg) exhibit sulfhydryl reactivity. Once inside the cell, they form covalent bonds with cysteine residues of proteins, depleting cellular antioxidants. Antioxidant enzymes, crucial for cellular defense, become compromised in the presence of mercury compounds. The interaction of mercury compounds with cellular components

suggests the generation of oxidative damage through the accumulation of reactive oxygen species (ROS), normally counteracted by cellular antioxidants [49] [11] [51]. Mercury has been demonstrated to induce neurotoxicity, nephrotoxicity, hepatotoxicity, and cardiovascular toxicity in humans. Recent research has revealed a connection between levels of mercury in hair and oxidized LDL levels in atherosclerotic lesions, acute coronary failure, and atherosclerosis [41]. The relationship between mercury exposure and carcinogenesis remains controversial. Mercury has been shown to induce the formation of ROS, which are known to cause DNA damage in cells. However, conflicting evidence exists, with other studies not showing a clear association between mercury exposure and genotoxic damage [49] [41].

The excretion rate of mercury and its compounds is influenced by their oxidation state. Elemental and inorganic mercury are primarily eliminated by the kidneys (urine) with minimal excretion through the gastrointestinal tract (feces), exhibiting a half-life of $30-60$ days. On the other hand, organic compounds are excreted through feces, but they undergo enterohepatic recirculation, resulting in a longer half-life of approximately 70 days [51]. Adsorption has emerged as a promising method for mercury removal, boasting simplicity, cost-effectiveness, and high efficiency, making it a notable choice among various developed methods for purifying water contaminated with mercury [30].

Zinc

Zinc is a moderately reactive metal that reacts with oxygen and non-metals to produce hydrogen, along with dilute acids. It is primarily introduced into the environment through industrial activities like mining, coal and waste combustion, and steel processing. It finds widespread use in various industries, including galvanization, paint, batteries, smelting, fertilizers, pesticides, fossil fuel combustion, pigments, polymer stabilizers, and more. Consequently, effluents from these industries often contain significant amounts of zinc [30]. Zinc is considered an essential element, crucial for the activity of more than 300 enzymes. Some of these enzymes include alcohol dehydrogenase, alkaline phosphatase, Cu, Zn-superoxide dismutase, carbonic anhydrase, DNA polymerases, RNA transcriptase, and carboxypeptidase [41] [11].

The antioxidant properties of zinc contribute to the reduction of oxidative stress through mechanisms such as (i) protecting the sulfhydryl groups of enzymes and proteins from oxidation and (ii) preventing the formation of free radicals, thereby reducing the generation of hydroxyl radicals from hydrogen peroxide molecules. Additionally, zinc interacts with the immune system's mechanisms, and the uncontrolled accumulation of zinc and amyloid-β peptide (Aβ) is suggested to result in Aβ-mediated oxidative stress and zinc-induced cytotoxicity [11]. Prolonged exposure to zinc can result in copper malabsorption, impacting immune function, especially in individuals with diabetes mellitus. Severe toxicity manifests as symptoms such as kidney injury, pancreatic damage, liver failure, dehydration, acute gastrointestinal bleeding, septic shock, lethargy, sideroblastic anemia, and dizziness. Inhalation of zinc may induce respiratory issues like dyspnea, airway inflammation, and acute respiratory distress, particularly in occupational settings. Furthermore, chronic exposure to zinc, due to its interference with copper absorption in the gastrointestinal tract, can lead to copper deficiency, resulting in polyneuropathy and affecting bone marrow [51].

The removal process includes adsorption (chemisorption), surface and pore complexation, ion exchange, microprecipitation, condensation of heavy metal hydroxides onto the biosurface, and surface adsorption [30].

Copper

Copper is a versatile metal valued for its excellent qualities, finding applications in electronics, the production of wires, sheets, and tubes, as well as in alloy formation. Copper that is immobile and not readily bioavailable can undergo absorption or precipitation into the soil matrix. As copper typically exists in a cationic form, it creates complexes with negatively charged clay minerals, anionic salts, organic materials, hydroxides, phosphorus, and sulfate [30]. Copper is a vital micronutrient and is involved in numerous physiological functions, including formation of chlorophyll, photosynthesis and carbohydrate and protein metabolism [41]. Copper plays a vital role as an essential cofactor for various oxidative stress-related enzymes, including catalase, superoxide dismutase, peroxidase, cytochrome c oxidases, ferroxidases, monoamine oxidase, and dopamine β-monooxygenase [49] [51]. Hypocupremia, or copper deficiency, is characterized by a serum level below the normal range of $0,64 - 1,56\ \mu g/ml$. Severe hypocupremia may lead to Menkes disease, also known as Menkes kinky hair syndrome [51].

The ability of copper to cycle between its oxidized state, Cu(II), and reduced state, Cu(I), is utilized by cuproenzymes participating in redox reactions. However, this property also renders copper potentially toxic because transitions between Cu(II) and Cu(I) can generate superoxide and hydroxyl radicals. Homeostatic mechanisms typically maintain a physiologically essential copper level, involving control over absorption, intracellular transport, cellular uptake and efflux, sequestration/storage, and copper excretion from the body. Gastrointestinal copper absorption is inversely related to dietary intake, and studies indicate that uptake is saturable, influenced by intracellular copper levels [11].

Studies confirm that copper induces DNA strand breaks and oxidizes bases through oxygen free radicals and hydroxyl radicals. Both cupric and cuprous states of copper enhance DNA breakage, particularly through the genotoxic benzene metabolite (1,2,4-benzenetriol), more than iron. Recent findings suggest that the upper limit of copper „free“ pools is significantly less than a single atom for each cell, emphasizing the limited capacity for copper chelation in the cell [11]. Excessive exposure to copper has been associated with cellular damage, leading to Wilson disease in humans, a condition causing neurobehavioural abnormalities, similar to schizophrenia. It also augments zinc-induced neurotoxicity [49] [41]. Increased levels of hepatic copper are also seen in cholestatic liver diseases, where they arise from reduced biliary excretion of copper and are not a causative factor for liver infection [41].

Ion exchange treatment is often used as a means of copper elimination [30].

Cadmium

Cadmium, a silver-white metal finds significant industrial applications due to its robust electrical conductivity, excellent chemical resistance, and low melting point [30]. Its major uses include alloy production, pigments, and batteries, as well as electroplating industry [6] [51] [32]. While the use of cadmium in batteries has experienced significant growth in recent years, its commercial use has decreased in developed countries due to environmental

concerns. It is widely dispersed in the Earth's crust, the highest concentrations of cadmium compounds in the environment are found in sedimentary rocks and marine phosphates [49]. The primary routes of exposure to cadmium are through inhalation, particularly from cigarette smoke. Skin absorption is uncommon, the GI absorption is also very inefficient [6].

Evidence suggests that the intestinal absorption mechanism involves transporter proteins, with studies indicating that the divalent metal transporter I (DMT1) is one of the proteins involved in cadmium absorption through the gastrointestinal tract. Following acute ingestion, symptoms such as abdominal pain, burning sensation, nausea, vomiting, salivation, muscle cramps, vertigo, shock, loss of consciousness, and convulsions typically manifest within $15 - 30$ minutes. Acute cadmium ingestion can lead to gastrointestinal tract erosion, as well as pulmonary, hepatic, or renal injury, and coma, depending on the route of poisoning [49] [41] [11].

Cadmium has neurotoxic effects, inducing neurodegenrative defects such as amyotrophic lateral sclerosis, Parkinson's and Alzheimer's diseases, as well as multiple sclerosis. Cadmium-induced nephrotoxicity gives rise to pronounced clinical manifestations, including glucosuria, a Fanconi-like syndrome, phosphaturia, and aminoaciduria. Occupational and environmental exposure to cadmium can induce immunosuppressive effects, with the nature of these effects depending on the exposure conditions [41] [11]. Cadmium (Cd) causes Itai-Itai disease, primarily affecting women. It impairs tubular and glomerular functions, leading to multiple fractures in bones due to osteoporosis and osteomalacia, where calcium is released from the bones [32]. Cadmium compounds are classified as human carcinogens by several regulatory agencies. Both the IARC and the US National Toxicology Program have concluded that there is sufficient evidence to categorize cadmium as a human carcinogen, with the IARC categorising it as carcinogenic to humans (Group 1) [49] [6] [32].

Biochar treated with MnO_2, which has more hydroxyl groups, a larger surface area, and a higher pore volume, is a primary mechanism for Cd elimination [30].

2.3 Adsorption

Adsorption is a surface process where a molecule or ion (adsorbate) in a gaseous or liquid bulk adheres to the surface of a solid (adsorbent). Unlike absorption, adsorbate does not penetrate the structure of the adsorbent. Desorption is the reverse process, involving the release of molecules from a solid surface. This naturally occurring phenomenon has various industrial applications and can influence processes like enzymatic reactions and ion exchange [5] [19]. It can be considered in various systems depending on the types of phases in contact, including liquid-gas, liquid-liquid, solid-liquid, and solid-gas systems [18].

2.3.1 Types of adsorption

Adsorption can be broadly classified into two main types: physical adsorption (physisorption) and chemical adsorption (chemisorption). In physical adsorption, the adsorbate adheres to the surface of the adsorbent through physical forces such as van der Waals forces. This type of adsorption is characterized by weaker interactions and is typically reversible. On the other hand, chemical adsorption occurs only at a monolayer and involves a stronger

bond where the adsorbate is chemically bound to the surface of the adsorbent. Chemisorption interactions are more specific and can be irreversible [5] [18].

Adsorption, like any chemical reaction, is affected by the environmental conditions, especially temperature, pH, and redox conditions. The surface area of the adsorbent is a crucial factor, with porous substances or those with a higher surface area per unit volume, such as activated carbon and clay, being more effective adsorbents [5].

Physisorption

Physisorption is driven by van der Waals interactions, which are weak electrostatic forces between molecules. When adsorbate molecules approach the surface with low energy, this energy can be dissipated as heat through the vibration of the solid lattice, allowing the molecules to be trapped on the surface. However, if the molecules strike the surface with excessive energy that cannot be dissipated by the adsorbent, they will bounce away, preventing effective adsorption. The balance between attractive forces and energy considerations governs the physisorption process [5].

Physisorption involves a minimal change in enthalpy, typically less than 20 $kJ \cdot mol^{-1}$, resulting in no alteration in the chemical status of the adsorbate or adsorbent. No new chemical bonds are formed, and only a slight increase in the adsorbent's temperature is observed. The physical bond formed during physisorption is highly labile, and the process can easily reverse due to vibrational motion. The lifetime of physisorption is brief, estimated to be around 10^{-8} s at typical environmental temperatures (approximately 20 $°C$), extending to seconds only at very low temperatures (about -170 $°C$) [5] [18].

Physisorption is most relevant at low temperatures, always below the critical temperature of the adsorbate. This process can occur in multiple layers, allowing new adsorbate molecules to adhere to the surface as long as they do not completely shield the electrostatic potential. The strength of adsorption and its duration decrease as the number of layers of adsorbate on the surface increases, with each subsequent layer requiring lower enthalpy for desorption [5] [18].

Chemisorption

In contrast to physisorption, chemisorption involves stronger forces, where the adsorbate forms a genuine chemical bond, typically covalent, with the adsorbent's surface. The change in enthalpy for chemisorption is greater, ranging from 40 to 400 $kJ \cdot mol^{-1}$, and is always negative, signifying a spontaneous process. Chemisorption can be an activated process, requiring a minimum energy for the adsorbate to be sorbed. This activation depends on the presence of an energetic barrier between the physisorbed and chemisorbed states (see Figure 2.13). If this barrier is higher than the energy of the free molecules, the adsorbate will chemically bond to the adsorbent only if it possesses more energy than the barrier; otherwise, it will be desorbed. Conversely, if the barrier is lower than the energy of free molecules, all the physisorbed molecules can rapidly form a chemical bond with the adsorbent surface, leading to a swift occurrence of chemisorption [5] [18].

Due to the higher enthalpy involved, vibrational motions are incapable of breaking the covalent bonds formed during chemisorption. Consequently, the lifetime at environmental

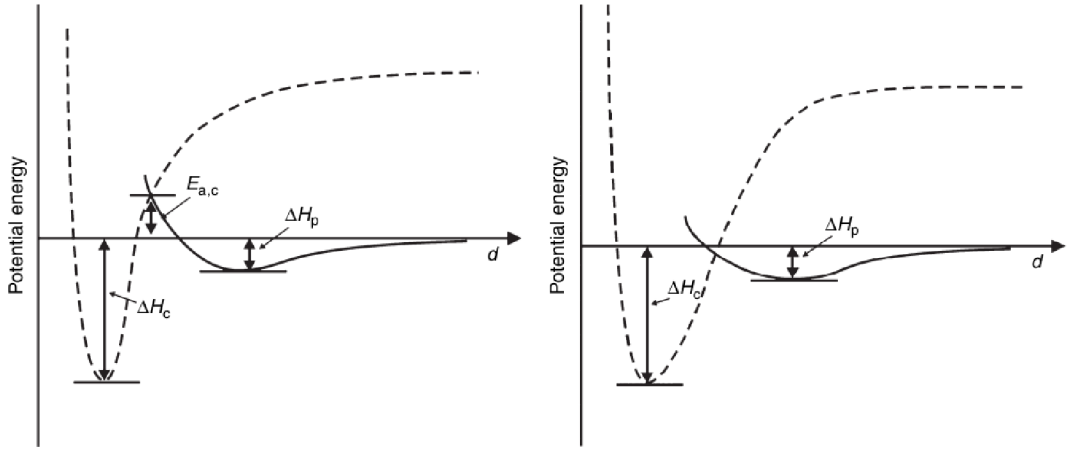

Figure 2.13: The diagram illustrates the energy of adsorption based on the distance (d) of the adsorbate molecule from the surface. The solid line represents physisorption, characterized by low enthalpy (ΔH_p), while the dashed line represents chemisorption, which requires higher energy (ΔH_c). On the left side, there is the case of activated chemisorption, where $E_{a,c}$ is the activation energy for chemisorption. Taken from [5].

temperatures (around 20 $°C$) is on the order of thousands of seconds (i.e., approximately 1 hour), and only at elevated temperatures (100 $°C$) does it decrease to approximately 1 second [5].

Desorption from the chemisorbed state is always an activated process. In order to detach from the surface, molecules need to be supplied with energy to break the covalent bonds. Chemisorption typically involves only a monolayer of adsorbate on the adsorbent surface. Once the entire surface is covered by adsorbate molecules, with no more sites available for bonding, adsorption reaches a dynamic equilibrium with desorption [5].

2.3.2 Isotherms

As discussed in subsection 2.3.1, adsorption typically entails low enthalpy and a brief lifetime, indicating low activation energy for both adsorption and desorption. This results in a rapid attainment of equilibrium unless there are alterations in physicochemical environmental conditions [5].

Therefore, adsorption is time-independent, expressing the connection between the quantity of adsorbate adhered to the adsorbent and the amount present in the environment, typically represented as pressure for gases or concentration for solutions. It depends on adsorbate, adsorbent and the properties of adsorption solution (pH, ionic strength, temperature). Adsorption isotherms, commonly employed, serve to forecast the quantity of adsorbate that can adhere to a solid surface. They aid in determining whether the adsorption mechanism follows linear monolayer coverage or involves multilayer adsorption [5] [19] [12].

For dissolved adsorbate,

$$q = f(C) \tag{2.2}$$

where q $(mg \cdot g^{-1})$ is the mass adsorbed per mass unit of adsorbent and C $(mg \cdot l^{-1})$ is the concentration od adsorbate in the environment. Such dependencies are called isotherms, its name suggesting that they are defined at constant temperature. The most used types are Langmuir (see Equation 2.3) and Freundlich (see Equation 2.4) isotherms [5]. In experimental part of this thesis, Temkin isotherm (see Equation 2.5) was also used.

Langmuir isotherm

Langmuir, credited with developing a theoretical equilibrium isotherm linking the amount of gas sorbed on a surface to the gas pressure, has introduced a widely known and widely used sorption isotherm model:

$$q = q_{max} \frac{K_l C}{1 + K_l C} \tag{2.3}$$

where q_{max} $(mg \cdot g^{-1})$ is the maximum amount of adsorbate in the adsorbent and K_l $(L \cdot mol^{-1})$ is the equilibrium constant related to the enthalpy of the process (large K_l indicates favourable adsorption). In the derivation of equilibrium constants for isotherms like the Langmuir and Freundlich isotherms, the fundamental principle is to establish a balance where, at equilibrium, the rates of molecules' adsorption and desorption are equal. This equality in rates signifies a state where the number of molecules attaching to the adsorbent surface is equivalent to the number detaching from it per unit time. The resulting equilibrium constant reflects this balanced state [5] [12] [19].

At low sorbate concentrations ($C = 0$), it behaves like a linear isotherm, adhering to Henry's law. Conversely, at high sorbate concentrations, it predicts a constant monolayer sorption capacity (q_m), a crucial parameter for comparing adsorbent capacities in the literature [12].

The formulation of the Langmuir isotherm is based on four key hypotheses:

- adsorbate molecules can only attach to specific sites on the surface that meet the necessary conditions for interaction, whether through van der Waals forces or chemical bonds;
- adsorption is limited to a monolayer, meaning each site can only be occupied by one molecule at a time, leading to a saturation shape in the isotherm;
- all sites are assumed to be energetically equivalent, implying that the energy involved in adsorption is the same across all sites;
- the molecules adsorbed are considered to be independent and unable to influence each other or the adsorption and desorption processes [5] [19].

These assumptions collectively describe a homogeneous (albeit discrete) adsorption occurring on the surface. The shape of Langmuir isotherm (see Figure 2.14) depends on parameters, however, ususally the saturation is reached quite fast [5].

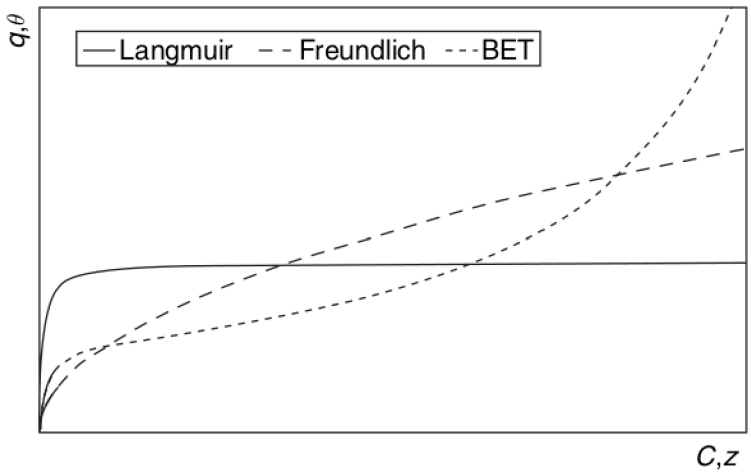

Figure 2.14: The isotherms of Langmuir (solid line), Freundlich (dashed), and BET (dotted) describe the relationship between the amount of adsorbate, expressed as the mass fraction q (or fraction of sites occupied for BET), and its concentration C (or pressure of gaseous adsorbate relative to saturation pressure). These isotherms provide insights into how adsorption varies with changes in concentration or pressure under different conditions. Taken from [5].

Freundlich isotherm

In 1906, Freundlich introduced the earliest known sorption isotherm equation:

$$q = K_f C^{\frac{1}{n}} \tag{2.4}$$

where K_f $(mg \cdot g^{-1})$ is the adsorption coefficient and n is an empirical constant (usually > 1). As opposed to Langmuir (theoretically based), Freundlich model is empirical [5] [53] [12].

The adsorption coefficient (K_f) in the Freundlich model characterizes the partitioning of pollutants between the aqueous solution and MPs. It is influenced by the interactions between organic pollutants and MPs. Additionally, the parameter $1/n$ in the Freundlich model signifies adsorption intensity or surface heterogeneity. A value below 1 indicates favorable adsorption, while values exceeding 1 suggest unfavorable adsorption as available sites on the adsorbent decrease with increasing sorbate concentration [19].

Two important assumptions are being made when considering Freundlich isotherm:

- adsorption is not limited to a monolayer but allows for the attachment of several layers of adsorbate on the adsorbent (the mathematical formulation, however, lacks an asymptote, suggesting that the adsorbent would never saturate and continuously bind to adsorbate, which contradicts real-world observations);
- the energy needed for adsorption is not constant but follows an exponential distribution (the bonding strength is non-uniform, influenced by the physicochemical properties of sites or the number of molecules already adsorbed - as the number of molecules

bound to a site increases, the likelihood of another molecule binding to the same site decreases exponentially due to the progressively higher energy requirement) - this is evident from the Freundlich curve (Figure 2.14), where the slope decreases with increasing adsorbate concentration [5] [19] [12].

The Freundlich isotherm, derived by assuming an exponentially decaying sorption site energy distribution, has faced criticism for lacking a fundamental thermodynamic basis. However, for the special case of $1/n = 1$, it aligns with Henry's law [12].

Parameter values for both isotherms are typically estimated through the interpolation of empirical observations. These parameters change in response to temperature variations, resulting in a decrease in the fraction adsorbed as temperature rises and vice versa. Higher temperatures lead to stronger vibrational motion, increasing the probability of adsorbate breaking weak van der Waals bonds. The slope of both curves decreases, and the Langmuir curve reaches the asymptote for higher concentrations of adsorbate. Empirically, Freundlich's model is often more suitable for describing adsorption from liquid solutions, while Langmuir's model tends to better fit data on adsorption of gases [5].

Temkin isotherm

The derivation of the Temkin isotherm assumes that the adsorption heat of all molecules decreases linearly with the increase in coverage of the adsorbent surface, and that adsorption is characterized by a uniform distribution of binding energies, up to a maximum binding energy. It is generally applied as follows:

$$q = \frac{RT}{b_t} \ln\left(K_t C\right) \tag{2.5}$$

where K_t is the equilibrium binding constant $(L \cdot mol^{-1})$ corresponding to the maximum binding energy, R is the universal gas constant $(8,314\ J \cdot (mol \cdot K)^{-1}$, T is the temperature (K) and b_t is the Temkin isotherm constant related to the adsorption heat $(-)$ [12] [45].

A simpler approach posits that adsorption is directly proportional to the concentration of the adsorbate:

$$q = kC \tag{2.6}$$

where k is the partition coefficient $(L \cdot g^{-1})$ – the ration between the solid phase concentration and the equilibrium concentration in the liquid phase. This straightforward relationship has a notable limitation as q increases rapidly with concentration. Nevertheless, for diluted adsorbate, this model can be applied with minimal or no error, serving as an approximation of the Langmuir model in conditions far from saturation [5] [53].

The partition coefficient's value can be estimated through empirical observation or, for nonionic compounds like organic chemicals, can be determined via

$$k = f_{OC} k_{OC} \tag{2.7}$$

where f_{OC} is the fraction of carbon in the adsorbent and k_{OC} is the partition coefficient of adsorbate in the organic carbon (this can be estimated directly from k_{OW} (octanol-water partition coefficient)). Adsorption is assumed to occur solely on the organic carbon fraction due to the specific affinity of organic chemicals with organic carbon [5].

2.3.3 Adsorption dynamics

While adsorption is commonly viewed as an equilibrium process, there are instances where studying its dynamics is crucial, such as in systems with limited contact between adsorbate and adsorbent (e.g., rains percolating through acid soil). The approach to derive the dynamic law for adsorption is analogous to the theory of two films used for absorption. This involves considering a single film to separate the solution bulk, where adsorbate is uniformly diluted due to eddy diffusion, and a film near the adsorbent surface, where only molecular diffusion occurs (see Figure 2.15) [5].

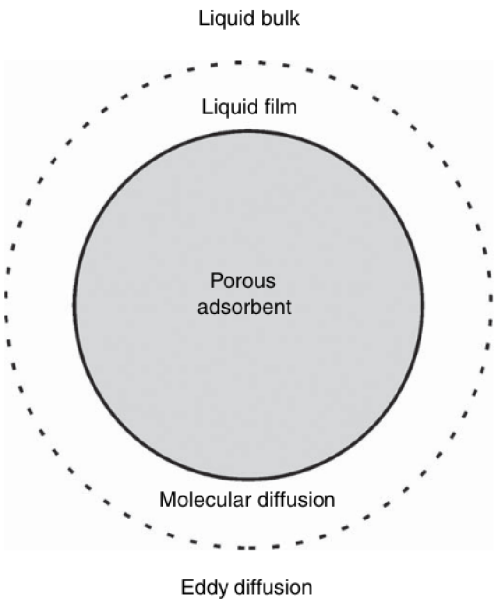

Figure 2.15: The conceptual model employed to formulate the dynamics of adsorption involves a stationary liquid (or gaseous) film, where only molecular diffusion takes place. This film surrounds a particle of porous adsorbent submerged in a liquid (or gaseous) bulk with a constant solute concentration due to eddy diffusion. Taken from [5].

The second film is dispensable as adsorption primarily occurs on the surface without entering the solid structure. However, two resistances impede adsorbate motion: the first is the stagnant film resistance (involving molecular diffusion and dependent on the ratio of molecular diffusivity D_{AB} to the film thickness δ), and the second is the resistance associated with movement into the solid's pores. Complete adsorption to equilibrium requires molecules to navigate through intricate pores to access all available sites [5].

2.3.4 Kinetics of adsorption

Adsorption kinetic models are commonly employed to assess the effectiveness and rate-limiting steps of pollutants' adsorption on MPs (microplastics) and explore the underlying adsorption mechanisms [19]. Over the past decades, various mathematical models have been developed to explain adsorption data, broadly categorized as adsorption reaction models and adsorption diffusion models. While both are used to describe the kinetic process of adsorption, they differ significantly in their nature [28].

Adsorption diffusion models are generally divided into four steps:

1. bulk transport (occurs quickly),
2. film diffusion (occurs slowly),
3. intraparticle diffusion (occurs slowly),
4. adsorption attachment (occurs quickly) [19].

Adsorption reaction models, derived from chemical reaction kinetics, focus on the entire adsorption process without explicitly considering the steps mentioned earlier [28].

The adsorption kinetics of pollutants on MPs are commonly characterized using following models: pseudo-first-order (Equation 2.8), pseudo-second-order (Equation 2.9), intraparticle diffusion (Equation 2.10), and film diffusion (Equation 2.11). The pseudo-first-order and pseudo-second-order models assess the overall adsorption process, while intraparticle diffusion and liquid film diffusion models describe the limiting steps. In cases where the pseudo-first-order and pseudo-second-order models are insufficient to explain the complex adsorption mechanism, they can be complemented by intraparticle and liquid film diffusion models [53] [19].

Pseudo-first-order model

Lagergren (1898) introduced the first-order rate equation to explain the kinetics of liquid-solid phase adsorption. This model, applied to the adsorption of oxalic acid and malonic acid onto charcoal, is considered one of the earliest models linking adsorption rate to adsorption capacity [28].

The pseudo-first-order adsorption model is evaluated by plotting the relationship between adsorption capacity at a specific time (q_t) and that time (t), followed by linear fitting. If the experimental data fits the pseudo-first-order model, it suggests that physical diffusion in a solid-liquid system mainly controls the adsorption process. The correlation coefficient (R^2) and standard error are used to determine the model's goodness of fit. Additionally, assessing the proximity of experimental and theoretical values of the sorbate's adsorption capacities (q) is crucial in model evaluation [19]. The pseudo-first-model is defined:

$$q_t = q\left[1 - \exp(-k_1 t)\right] \tag{2.8}$$

where q_t is the sorption capacity in the solid phase at time t ($mg \cdot g^{-1}$), t is time (day) and k_1 is the psedo-first-order rate constant (day^{-1}) [19] [53] [12].

To fit the equation to experimental data, the equilibrium sorption capacity (q) must be known. However, in many cases, q is unknown, especially in slow chemisorption processes where the amount sorbed is considerably smaller than the equilibrium amount. The pseudo-first-order equation of Lagergren is often limited to the initial 20 to 30 minutes of the sorption process and may not fit well for the entire contact time range. Extrapolating experimental data to $t = \infty$ or treating q as an adjustable parameter determined by trial and error is commonly required in such cases [12].

The term „pseudo-first-order“ is applied to Lagergren's first-order rate equation to differentiate it from kinetic equations based on adsorption capacity rather than solution concentration. This equation has found extensive use in describing the adsorption of pollutants from wastewater in various applications, such as the removal of methylene blue from aqueous solution using broad bean peels and the adsorption of malachite green from aqueous solutions using oil palm trunk fiber [28].

Pseudo-second-order model

In 1995, Ho presented a kinetic model for the adsorption of divalent metal ions onto peat. This model attributes the cation-exchange capacity of peat to chemical bonding between divalent metal ions and polar functional groups on peat, including aldehydes, ketones, acids, and phenolics [28].

If the pseudo-second-order accurately represents the adsorption process, it implies that the sorption mechanism involves chemisorption. Chemisorption entails valency forces, where electrons are shared or exchanged between the sorbent and sorbate [19]. It is defined by:

$$q_t = \frac{q^2 k_2 t}{[1 + k_2(q)t]} \tag{2.9}$$

where k_2 is the pseudo-second-order rate constant (day^{-1}) [53] [19].

The pseudo-second-order kinetic model, proposed in 1995, has emerged as the most extensively examined model for studying the sorption of metal ions and organic pollutants from wastewater. It is utilized to differentiate kinetic equations based on adsorption capacity from those based on solution concentration. This equation has found successful application in describing the adsorption of various substances, including metal ions, dyes, herbicides, oils, and organic compounds, from aqueous solutions [28] [12].

The primary limitation of the pseudo-second-order kinetic model lies in its pseudo-kinetic nature, wherein a distinct rate constant is derived for each alteration in system variables. Hence, it is crucial to establish an equation that correlates the pseudo-rate constant with each variable [12].

Intraparticle diffusion model

In typical liquid/solid adsorption, film diffusion, intraparticle diffusion, and mass action are involved. For physical adsorption, mass action is a rapid process and often negligible for kinetic studies. Consequently, the kinetic process of adsorption is typically controlled by either liquid film diffusion or intraparticle diffusion, where one of these processes serves

as the rate-limiting step. Adsorption diffusion models are constructed to describe the mechanisms of film diffusion and/or intraparticle diffusion in the adsorption process [28].

The intraparticle diffusion model suggests that adsorbates penetrate the pores of the adsorbent material during adsorption. If the fitted curve intersects the origin ($E_i = 0$), it indicates that the rate-limiting step of the adsorption process is solely controlled by intraparticle diffusion. The intraparticle diffusion model (Weber-Morris model) is relative to a diffustion-controlled process:

$$q_t = k_i t^{0,5} + E_i \tag{2.10}$$

where k_i is the intraparticle diffusion rate constant ($mg \cdot g^{-1} \cdot day^{-0,5}$) and E_i is the constant associated with the thickness of the boundary layer ($mg \cdot kg^{-1}$) [53] [19] [28].

Film diffusion model

The film diffusion model, guided by physicochemical interactions like hydrophobic interactions and covalent forces, is employed to anticipate the rate-limiting steps in adsorption processes. The Boyd plot, depicting B_t against time, serves to determine whether the rate-limiting step involves intraparticle or film diffusion. Linearly fitted data points, not passing through the origin, suggest the involvement of both intraparticle and film diffusion in the adsorption process. It is defined by:

$$B_t = -ln(1 - q_t/q) - 0,4977 \tag{2.11}$$

where B_t is Boyd constant [19].

Film diffusion coefficients can be determined through two approaches: the correlation method and the dimensional analysis method. The correlation method involves substituting experimental data into the film diffusion equation to calculate the coefficient. On the other hand, the dimensional analysis method utilizes sorbent and sorbate characteristics along with sorbent terminal velocity for coefficient computation. A comparison between the two methods helps identify the most accurate values for external film mass transfer coefficients [12].

For spherical pellets, Fick's second law can be applied as it takes into account the pellet radius:

$$\frac{\partial C}{\partial t} = D \cdot \frac{\partial^2 C}{\partial x^2} \tag{2.12}$$

where C is the concentration in the solid phase ($mg \cdot g^{-1}$), D is the diffusion coefficient ($cm^2 \cdot day^{-1}$) and x is the distance from the centre of the plastic sphere (cm) [53].

2.4 HM and plastics

Due to several specific properties (small particle size combined with large surface area, hydrophobicity), microplastics tend to adsorb several hydrophopic substances on their sur-

face from the environment [34] [4]. Among substances commonly found adsorbed on the microplastics surface is 78 % of chemicals listed as „priority pollutants“ by Environmental Protection Agency (EPA) (chemicals that have been found bioaccumulative, persistent and/or toxic). Unlike organic compounds, the presence of metals adsorbed on microplastics has been studied for a significantly shorter time [47]. The buoyancy of microplastics is responsible for relatively high exposure of plastic fragments to metals and other contaminants near the water surface microlayer [26]. Metal ions, such as aluminum, antimony, cadmium, chromium, cobalt, copper, iron, lead, manganese, molybdenum, tin, uranium, and zinc, have all been shown to sorb to plastics in the aquatic environment [8].

A study conducted at San Diego bay (California) showed that concentration of some metals were up to several magnitudes of order higher on the plastic pellets than on seawater particulates, indicating that some metals may partition to plastic to a greater extent than to a natural sediment [47]. Another study, conducted at various beaches at south west England, concluded similarly – maximum detected concentration on individual pellets were closed to – in some cases even exceeded – concentrations reported from contaminated estuarine sediment from south west England (between 100 and 400 $\mu g/g$) [26].

The natural processes in the environment lead to modifications in exposed microplastics, leading to phenomena such as increased surface oxidation or formation of micro-cracks on the surface, as well as degradation of MPs into smaller plastic particles, which can augment the adsorption of contaminants on MPs. This is attributed to the increased surface area exposure and heightened chemical reactivity of the MPs. Kinetic models and isotherms of adsorption on such particles show incresed sorption capacity of such particles, compared to pristine microplastics. The mechanisms involved are predominantly influenced by their physical interactions, with key roles played by factors such as partition coefficient, electrostatic interactions, and intermolecular hydrogen bonding. The rate of such modifications and thus also the overall sorption process depends on a variety of different factors, including composition, structure, binding energy and surface properties of MPs, pH, temperature, salinity and ionic strenght of the surrounding medium or presence of organic matter and other substances and its corresponding solubility, redox state, charges and stability [53] [2] [48].

Interactions between microplastics (MPs) and heavy metals can alter their bioaccumulation and toxicity. The adverse effects on organisms may be synergistically exacerbated in a dose- or size-dependent manner when both pollutants are present. Conversely, some studies suggest protective effects, where organisms may be shielded by the interactions between heavy metals and chelating MPs. For instance, PVC was observed to reduce the toxicity of Cd to nematodes, possibly attributed to PVC's high chelating capacity [36]. The presence of microplastics (MPs) in the environment can influence the speciation of metals. MPs can increase the organic-bound fractions of heavy metals through direct adsorption, thereby modifying soil physicochemical and biogeochemical properties, including dissolved organic carbon (DOC) and pH. Additionally, MPs in the soil may reduce the exchangeable, carbonate-bound, and Fe-Mn oxide-bound fractions of metals such as Cu, Cr, and Ni. Conversely, certain studies indicate an increase in diethylenetriaminepentaacetic acid (DTPA)-extractable Cd concentrations in the presence of HDPE, PE, PLA, and PS. These alterations in metal speciation have the potential to impact the bioavailability of metals or metalloids in environmental matrices [36].

Research on the mechanisms of contaminant adsorption on MPs, the fate and transport of MPs with adsorbed contaminants, and the efficiency of MP treatment is scarce, despite the potential impact of MPs with adsorbed contaminants (c-MPs) on the aquatic environment and other co-existing emerging contaminants [2].

Figure 2.16 shows the overview of heavy metals - microplastics interactions in the environment and their effects on biota.

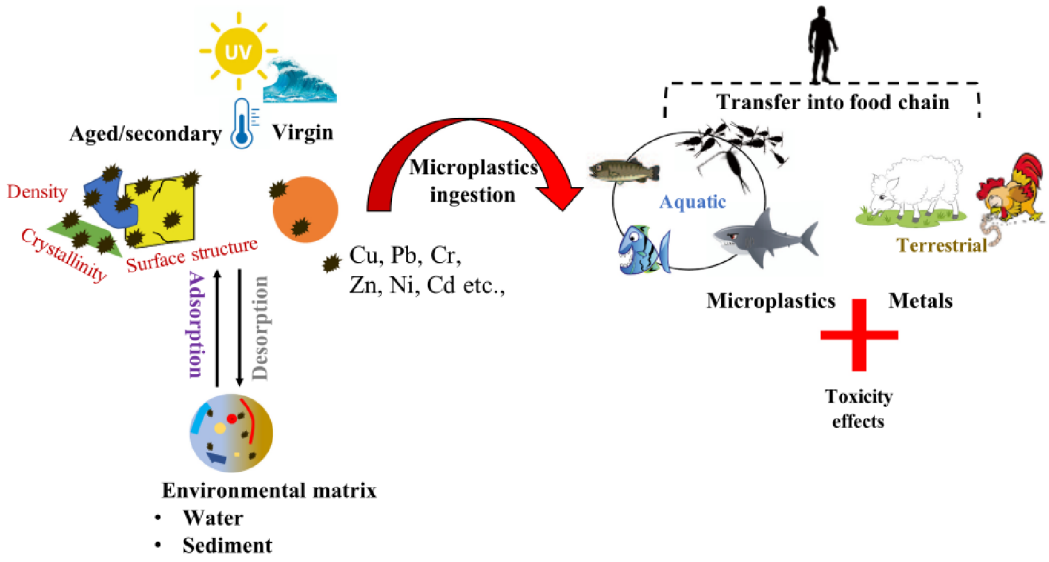

Figure 2.16: Interaction of microplastics with heavy metals in the environment and their effects in biota. Taken from [34].

2.4.1 Sources and stability of HMs in MPs

Heavy metals in environmental microplastics (MPs) primarily originate from two sources. Firstly, during the production of plastic, heavy metals and their compounds are intentionally added to polymers to enhance their properties. An overview of these applications and functions can be seen in Table 2.3. Common heavy metals like Cd and Zn are used as stabilizers and pigments in plastic products, with reported contents of up to 1 % and 10 %, respectively. Secondly, MPs can absorb heavy metals from their surrounding environment, and research indicates variations in metal concentrations on MPs across different sampling locations and times [14] [8].

The heavy metals added during the production of plastics are relatively stable and have minimal tendency to migrate. They are physically retained within plastics as most metallic compounds are added in the liquid phase. However, when plastics break into small fragments through processes like physical abrasion, chemical oxidation, or biodegradation, there is potential for the migration of metals to the surface of microplastics (MPs). Additionally, recycling of waste plastics, especially electronic waste plastics, poses a potential risk of heavy metals overloading and migration during recycling processes and use. The risk increases with more recycling times, leading to accelerated aging and deterioration of mechanical properties in waste plastics [14] [8].

types	functions	heavy metals	purpose
fillers	mineral fillers	$BaSO_4$	fiber composite
	metallic fillers	Al, Ni, Cu, Ag	electronics
property modifiers	colorants	TiO_2, ZnS, Fe_3O_4	colored plastics
	antimicrobials	silver ions	medical devices
	antioxidants	TiO_2, ZnO	UV absorbers
	adhesion promoters	zircoaluminates	car bumpers
	metal deactivators	Cu, Ni	-
	flame retardants	aluminium trihydrate	-
	conductive fillers	metal powders	-
processing aids	lubricants	MoS_2	-
	acid scavengers	metal oxides	-

Table 2.3: Specific functions and species of heavy metals in plastics [14].

Different polymer types inherently contain varying amounts of heavy metals and exhibit distinct adsorption capacities for metals from the environment. Aging and weathering further enhance the adsorption capacity of microplastics (MPs) toward heavy metals, attributed to the increased surface area-to-volume ratio of smaller MP particles. Compared to materials in the surrounding environment, MP particles can concentrate heavy metals at levels $10 - 100$ times higher [31] [37].

In natural environments, microplastics (MPs) exhibit a high affinity for heavy metals in the aqueous phase, rapidly adsorbing them from nearby sources. Studies have shown that metal concentrations in beached pellets are comparable to extraneous solids, and in some cases, they exceed concentrations in local estuarine sediments. Experiments demonstrated that the amount of copper (Cu) and zinc (Zn) adsorbed by PVC fragments and polystyrene (PS) beads was significantly higher than that in seawater. The concentration of heavy metals in MPs, such as cadmium (Cd), lead (Pb), manganese (Mn), and mercury (Hg), was found to be closely related to the level of heavy metal contamination in the surrounding soil environment. However, heavy metals were also observed to be easily desorbed from MPs, suggesting potential ecological risks to organisms [14].

Each type of polymer possesses unique characteristics, and the adsorption mechanism may be altered due to the formation of new adsorption bonds, creating an additional pathway for chemical contaminants to adsorb onto microplastic surfaces. Experimental conditions have shown the sorption of chromium on microplastic particles, with polyethylene microbeads effectively adsorbing chromium from seawater. The rate of adsorption is influenced by factors such as surface area and the reactivity of the metal toward the microplastic particle [42].

In one study, researchers collected MPs from Caribbean beaches in an industrialized city and found that they contained certain metals. Investigation of factors like contact time, solution pH, salinity, and microplastic size revealed pH increase enhancing adsorption rates. Cadmium adsorption onto high-density polyethylene microplastics showed rapid initial adsorption, reaching equilibrium in 90 minutes, with maximum adsorption at the smallest particle size. Cadmium was easily desorbed, and Fourier transform infrared analysis sug-

gested dominant physical interactions. Water parameter modifications can alter microplastic adsorption capability, providing an additional pathway for heavy metal contamination in water bodies and organisms [42].

Earlier studies have also documented the adsorption of metals such as Al, Fe, Mn, Cu, Ag, Zn, Co, Mo, Sb, Sn, and Pb on different microplastics (MPs) present in marine environments in West England, San Diego Bay, California, Portugal, and Croatia. These studies revealed significantly higher accumulation of heavy metals on MPs compared to the surrounding sediment particles or seawater. This heightened accumulation is likely attributed to the larger surface area and increased polarity of the MPs particles. For example, in one study, the presence of PVC and PS particles showed an accumulation of Zn and Cu that was 800 times higher compared to other environmental particles. [31].

Saturation of heavy metal adsorption on microplastic particles occurred after 8 hours at 25 $^{\circ}C$ when exposed to heavy metal concentrations of $0,05\ mg/L$ copper (Cu^{2+}), $0,01\ mg/L$ cadmium (Cd^{2+}), and $0,05\ mg/L$ lead (Pb^{2+}) in another study. High-density polyethylene adsorbed the maximum concentration of copper ($1,62\ \mu g/l$ at $0,5\ h$), higher than those of lead and cadmium. Sample collection at fixed intervals ($4, 6, 8, 10$, and 12 hours) facilitated the analysis of the effect of contact time on the adhered concentration of heavy metals using inductively coupled plasma–mass spectrometry [42].

2.4.2 Interaction mechanisms of HMs and MPs

Numerous studies have highlighted the capacity of different types of microplastics (MPs) to accumulate various heavy metals such as Cr, Co, Ni, Cu, Zn, Cd, Pb, Ag, and Hg. It has been observed that the adsorption of heavy metals on original/virgin MPs without surface modification is almost negligible, as they do not possess any significant porosity on their surface. In contrast, beached/eroded/weathered MPs, as well as those modified through the attachment of organic matter, demonstrate an increased ability to accumulate heavy metals. However, in this interaction, no chemical changes occur that could result in the formation of functional groups on MPs. Therefore, this adsorption is likely a physical interaction between these two species [14] [31] [40].

Plastic is typically white, translucent, or off-white in color; however, discoloration can result from ultraviolet degradation and weathering mechanisms. This discoloration may occur due to chemical precipitation, leading to increased porosity, roughness, and hydrophilicity of the plastic surface, thereby enhancing the adsorption capacity of the polymer [42] [40].

Direct interaction

The direct interaction between microplastics (MPs) and heavy metals primarily involves their interaction under free contact conditions, typically occurring in a liquid medium (Figure 2.17) [14].

All MPs were found to have a pH point of zero charge (pHpzc) around 3, suggesting that in the natural aqueous environment, MPs should exhibit a negative charge on their surface, promoting heavy metals adsorption [38]. The adsorption of heavy metal ions onto microplastics involves either single electrostatic interactions or a combination of electrostatic interactions and surface complexation. Heavy metals form interactions with polar or

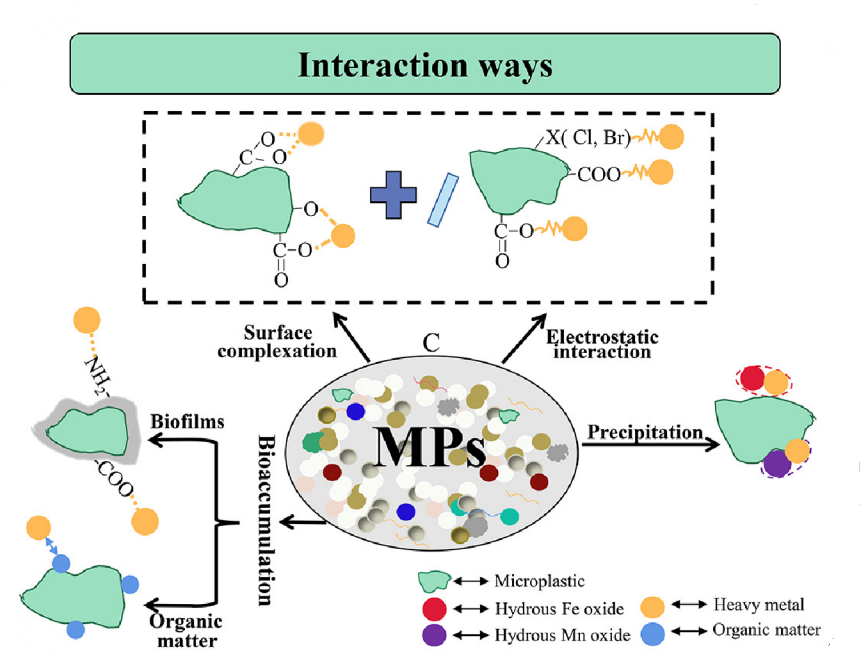

Figure 2.17: Diagram showing the interactions of different types of microplastics with heavy metals, according to contemporary literature. Taken from [14].

charged microplastics through coulombic forces. The plastic surface's polarity is influenced by its inherent physical and chemical properties, such as the presence of chlorine in materials like polyvinyl chloride (PVC) and chlorinated polyethylene (CPE), or the existence of charged contaminants and additives like hexabromocyclododecane (HBCD), a common brominated flame retardant. Additionally, imperfections and photo-oxidative weathering contribute to the formation of oxygen-containing functional groups (aldehydes, ketones, alcohol, carboxylic acids, hydroperoxides), further enhancing the polymer's polarity and inducing a charged surface [14] [42] [31].

In a study exploring the effects of surfactants on the adsorption of Pb^{2+} by three different MPs, the results indicated that the addition of surfactants enhanced the hydrophilicity and increased the negative charge of the MPs. This was considered the primary reason for the observed increase in sorption capacity [22].

Microplastics (MPs) also undergo complex formation through sorption and bioaccumulation by biofilms and natural organic matter, altering their surface area and properties. A long-term study in seawater showed similar metal accumulations on different plastic types, indicating biofilm mediation. Adsorption is enhanced by complexation with biofilm functional groups (-COOH, -NH_2, -phenyl). In soil, MP introduction increased organic heavy metal content, partly due to MP-organic molecule interactions. The attachment of substances to MP surfaces increases charge, roughness, porosity, and hydrophilicity, enhancing heavy metal adsorption on MPs [14] [37] [4]. The distribution of biofilm is similar among different types of plastic, leading to a similar metal adsorption capacity for various polymers. However, HDPE exhibited lower adsorption capability compared to other polymers, implying a reduced bioavailability of metals to aquatic biota through HDPE plastic debris [42].

Additional interactions include precipitation/coprecipitation, where heavy metal ions or their complexes co-precipitate with hydrous oxides of Fe and Mn through adsorption onto these oxides. Although beached pellets have been reported to contain significant concentrations of Fe and Mn, there is limited research on the co-precipitation of heavy metals on microplastics. This gap in studies is attributed partly to the occurrence of coprecipitation in adsorption systems with high concentrations of heavy metal ions [14] [39] [33]. The presumption is that adsorption occurs due to the interaction of bivalent cations and oxyanions with charged regions of plastic or through interactions between neutral metal–organic complexes and the hydrophobic plastic surface [42].

One example involves the surface-initiated free radicals connecting cationic substances on polystyrene spheres, turning them into cationic microplastics capable of efficiently adsorbing anionic pollutants in white papermaking water. The chelating properties of certain groups, such as amines and sulfur, were highlighted in the stability of metal-ligand interactions, exemplified by amine and sulfur chelating resin for Cu(II) and Pb(II) adsorption, with the chelating mechanism of polyethylamine with lead and mercury all being examples of this [59] [37].

Numerous studies have indicated that the adsorption of heavy metals on MPs is primarily governed by specific sorption, particularly surface complexation and cation-π bonding interactions. Analysis of FTIR and X-ray photoelectron spectroscopy (XPS) C 1s spectra for polyamide (PA), PVC, PS, acrylonitrile butadiene styrene (ABS), and PET demonstrated changes in oxygen and carbon functional groups, implying the involvement of oxygen functional groups (e.g., C–O and C–O–C) and cation-π bonding interactions during the Cd^{2+} sorption process [22].

Indirect interaction

Prior research indicates that microplastics (MPs) have the potential to modify soil structure and various physical and chemical properties, including soil bulk density, aggregation stability, water holding capacity, water availability, DOC, and pH. Of these properties, soil DOC content and pH are particularly crucial factors influencing the chemical behavior of heavy metals in soils. Consequently, MPs may influence the bioavailability of heavy metals by altering the physical and chemical properties of the soil [14] [4] [57].

Certain studies have indicated that microplastics (MPs) can heighten the bioavailability of heavy metals in soils and sediments. In one study, the presence of HDPE decreased soil adsorption capacity while increasing the desorption of cadmium (Cd). However, the bioavailability can vary between plants and animals. For example, the coexistence of PE or polylactic acid (PLA) elevated the DTPA-extractable Cd contents in soil without altering Cd concentration in plant tissues. This difference may be attributed to the distinct contact modes and adsorption capacities of animals and plants with heavy metals [14].

However, a recent study contradicted previous findings, stating that the presence of microplastics (MPs) decreased the bioavailability of copper (Cu), chromium (Cr), and nickel (Ni) in soil. This decrease was attributed to the transformation of the speciation of bioavailable heavy metals into organic bound forms. The study suggested that MPs influence heavy metal speciation through adsorption or by altering the physical and chemical properties of the soil. In contrast, when nanoscale zinc oxide (nZnO) and PE, PS, and PLA MPs were co-

exposed through soil cultivation, two different conclusions were drawn. The bioavailability of nZnO was reduced by PE and PS but increased by PLA [14].

These findings suggest that the co-exposure of microplastics (MPs) can either enhance or reduce the bioavailability of heavy metals. The impact of MPs on heavy metal bioavailability varies under different conditions and is influenced by factors like plastic type, the quantity of plastic added, and the concentration and types of heavy metals. To objectively assess the ecological risk arising from the co-exposure of MPs and heavy metals, thorough research is essential. A comprehensive understanding of the indirect impacts resulting from the co-exposure of MPs and heavy metals is crucial for a more accurate ecological risk assessment [14] [4] [57].

2.4.3 Factors influencing adsorption on microplastics

Due to their extensive specific surface area, aging, and surface functional groups, microplastics (MPs) can efficiently serve as carriers for various heavy metals, facilitating their transport and migration across different environmental media. The adsorption process is primarily influenced by the type and characteristics of plastics, the chemical properties of heavy metals, and environmental factors, including pH, salinity, natural organic matter (NOM), and variations in the background concentration of pollutants (Figure 2.18) [14] [42].

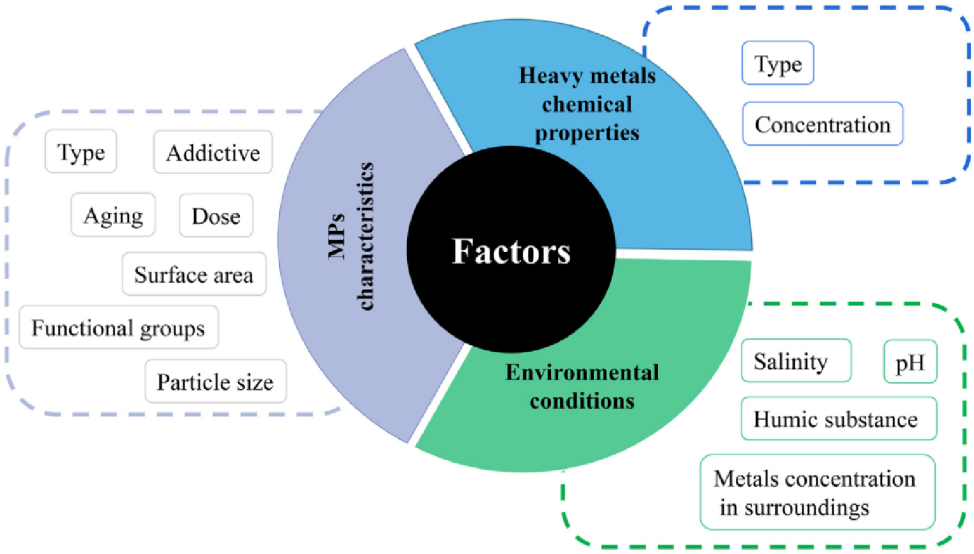

Figure 2.18: Various factors influence the adsorption behavior of heavy metals by microplastics (MPs). The types of MPs considered in these studies include polypropylene (PP), polyethylene (PE), polystyrene (PS), polyvinyl chloride (PVC), polyamide (PA), and polyoxymethylene (POM). It's noteworthy that, with a few exceptions, most tested MPs are virgin polymers without additives. Taken from [14].

MPs characteristics

PP, PE, PS, and PVC are the prominent MPs studied for their heavy metal adsorption behavior, with PE generally exhibiting a higher sorption capacity to environmental pollutants than other plastic types. Previous research highlights that the impact of polymer type is primarily linked to specific surface area and functional groups. In one study, aging and weathering processes not only generated additional surface area on the resin but also introduced various functional groups. This resulted in increased polarity, charge, roughness, and porosity to some extent, influencing the adsorption capacity of microplastics. Other studies revealed varied adsorption capacities for different heavy metals by different plastic types. Nylon MPs' surfaces with O-containing groups interacted with Ni^{2+}, Cu^{2+}, and Zn^{2+}. Plastic additives, like hexabromocyclododecane (HBCD), were found to enhance Pb(II) adsorption onto HBCD-PS MPs, increasing absorbed Pb(II) onto PS from 0 to $0,760\ \mu mol/g$. In another study, modifying polytetrafluoroethylene (PTFE) fibers through radiation grafting to introduce C=O and -OH functional groups significantly enhanced the removal efficiency of Cu(II) [14] [59] [39]. Specific surface area (surface to mass ratio) of plastic more accurately evaluates its ability to carry contaminants [39] [58].

A study conducted on a complex mixture of 9 metals and 5 most commonly produced plastic types, showed that unlike with organic contaminants, the accumulation of metals on plastic debris does not differ greatly by polymer types. This phenomenon can be due to the fact that the adsorption process for metals is mediated through a biofilm, which composition does not vary significantly among plastic types. Still, HDPE tended to accumulate lesser concentrations of metals [47].

MPs' adsorption capacity for heavy metals often depends on their diverse surface functional groups. For instance, a study investigated the adsorption mechanisms of Cd^{2+} on various MPs (PA, PS, PVC, ABS, and PET) and identified the presence of C–O and N–H, attributing the highest adsorption capacity to PA compared to other MPs. Regarding PET, the presence of fillers such as flame retardants, silicate, and calcium carbonate, aimed at protecting it from aging and organism colonization, may hinder physical changes, resulting in a very low adsorption capacity for heavy metals [22].

Moreover, the dose and particle size of MPs are significant factors influencing metal adsorption. Microplastics with smaller particle sizes exhibited larger adsorption capacities due to their more prominent specific surface area. This increased contact area with pollutants significantly improved the adsorption performance of the plastics. A recent study indicated that, for PP, when the concentration exceeded $0,1\ mg/L$, the adsorption rate decreased. In another study, the copper ion adsorption capacity at a PS concentration of $0,1\ mg/L$ was significantly higher than at concentrations of $1,0$ and $10,0\ mg/L$, with agglomeration observed at $10,0\ mg/L$. This suggests that lower doses of metallic solutions provide more adsorption sites for MP particles, while higher doses may reach a certain coverage rate, impacting subsequent adsorption behavior. Regarding particle size, research demonstrated a notable decline in the adsorption of lead (Pb), copper (Cu), and cadmium (Cd) on MPs as particle size increased. Smaller particle size MPs offer a larger specific surface area and more adsorption sites, resulting in higher metal adsorption capacity [14] [42] [59].

The material surface Zeta potential, a crucial parameter for assessing the trends of repulsion or attraction between adsorbent and adsorbate, played a significant role. The low Zeta

potential of MPs facilitated the adsorption of cationic ions through electrostatic attraction and impeded the adsorption of anionic ions due to repulsion forces [22].

The adsorbent's pore size also plays a role, as observed in polyethylimide adsorption of lead and mercury. A larger pore size in the adsorbent leads to better adsorption effectiveness. Consequently, variations in pollutant adsorption by these plastics arise due to the impact of solubility, concentration, and dosage on the adsorption performance of microplastics. [59].

In most studies, MPs used were purchased directly [20]. However, aging significantly impacts metal adsorption on MPs. Predictions suggest the sorption capacity for Cd, Pb, Cu, and Zn ions on aged MPs can be $1-5$ times higher than on virgin ones, a finding supported by laboratory studies. Aging PVC accumulates more Cu and Zn, and aging HDPE, PVC, and PS enhance adsorption capacity for Ca, Cu, and Zn. The partition coefficient of Cr on aged PE is reported to be one order of magnitude higher than on virgin MPs. The aging process involves physical (crushing, weathering, abrasion) and chemical processes (UV oxidation precipitation, adsorption, surface waviness, cracks), resulting in a more uneven surface and larger specific area in MPs. Oxygen-containing functional groups generated after UV radiation exhibit a strong metal ion complexing ability (Figure 2.19). Precipitation of inorganic minerals and organic matter during aging modifies surface properties, creating active binding sites for various metal ions [14] [59] [38]. Chemical degradation of plastics involves bond breaking in the molecular backbone, with hydrolysis being a representative reaction. Hydrolysis requires labile functional groups like esters, forming ionized acids. This process increases the number of hydrolysable bonds, creating additional hydrophilic structures that enhance the degradation rate [56].

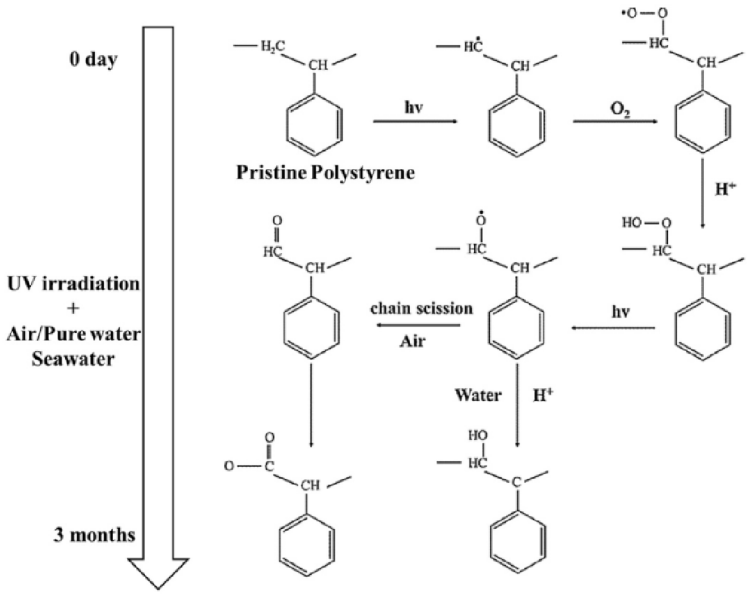

Figure 2.19: The weathering mechanism of PS microplastics under UV radiation, in conjunction with air, pure water, and seawater, involves complex processes leading to physical and chemical transformations. Taken from [22].

The crystallinity degree, representing the mass/volume fraction of crystalline polymers, varied among plastics, ranging from approximately $3,43$ % for PET to around 90 % for HDPE [22]. The crystalline, semicrystalline, and amorphous nature of polymers can impact the

rate of adsorption. Crystalline polymers tend to have reduced sorption capacity, as they require higher energy to destabilize ordered polymer chains. Conversely, the amorphous region exhibits greater sorption capacity due to the presence of randomly oriented polymer chains. Weathering processes can decrease the crystallinity of plastic surfaces due to increased cross-linking, thereby potentially increasing the sorption capacity of the polymers [42] [59] [37].

HMs chemical properties

The types of heavy metals affect surface potential and, consequently, their adsorption. Synergistic or competitive effects among metals are observed. In a solution with coexisting Pb, Cu, and Cd ($0,05\ mg/L$), the adsorption capacity is lower than in single-metal solutions, indicating competitive adsorption. However, coexisting heavy metals can also have a promoting effect; for instance, Cu and Pb coexisting increased the affinity of PA to Pb. Another study noted Zn^{2+} coexistence enhancing the adsorption of Cu^{2+} on PS. Additionally, the adsorption capacity of MPs increases with the initial Pb(II) concentration ($2 - 15\ mg/L$), suggesting a concentration-dependent effect. Studies confirm plastic production pellets adsorbing various heavy metals at 20 $\mu g/L$. Importantly, heavy metal Zn concentrations from 10^2 to 10^5 $\mu g/L$ lead to adsorption capacities ranging from 236 to 7171 $\mu g/g$ [14].

Environmental conditions

The layer of ocean water can undergo acidification due to the rapid absorption of increasing atmospheric CO_2, a phenomenon that has been reported for many decades. Therefore, the effects of pH should not be neglected [56]. Only the $pH < 7$ is being considered, as metal ions will precipitate under alkaline conditions. The adsorption capacity of MPs strengthens as pH increases [38]. Field tests have shown increased adsorption of Cd, Co, Ni, and Pb in river water with rising pH. This is attributed to the deprotonation of functional groups on the MPs' surface, enhancing electronegativity and adsorption sites. Another factor is the negative zeta potential of MPs when $pH > pHpzc$ (point of zero charge), with higher pH values generating more negative surface charge and increased electrostatic attraction to metal cations. However, excessively high pH may hinder adsorption due to passivation or precipitation. For instance, Pb(II) is mainly presented as Pb^{2+} at low pH and as $Pb(OH)^{+}$, $Pb(OH)_2$, $Pb(OH)^{-}_3$ at high pH [14] [59] [37].

Another study also demonstrated that the adsorption of certain heavy metals on MPs is pH-dependent. An increase in pH was found to enhance the adsorption amounts of Pb, Cd, Co, Ni, Cu, and Zn onto MPs, likely attributed to the increase in charged sites on MPs. In contrast, the adsorption of Cr(VI) onto MPs reduced with an increase in pH, possibly due to weak coulombic interactions between the oxyanionic form of Cr(VI) and MPs with reduced positive charge on their surface. Notably, pH had no influence on Cu adsorption [36].

Effective adsorption of metal cations on MPs occurs due to an increase in charged sites on MP surfaces at high pH. In conditions of low pH (< 7), where there is a substantial presence of H^+ ions, competition and replacement by these ions lead to reduced adsorption of metals

on MPs. An increase in pH was also found to significantly influence the adsorption of Cu and Pb in Musi river waters and the adjacent estuary in Indonesia [31].

Furthermore, salinity has diverse effects on the adsorption behavior between MPs and metals. In the experiment removing heavy metal ions, coexisting sodium ions rapidly occupied adsorption sites of heavy metals, thereby reducing the removal efficiency of heavy metals. Firstly, the ionic strength induced by NaCl, specifically Na^+, may compete with Cd^{2+} for adsorption sites, and Cl^- can restrict Cd^{2+} by forming complexes when coexisting. Salinity also induces electrostatic shielding, impacting the electrostatic adsorption behavior of metals. In a study evaluating the effect of ionic strength on Pb^{2+} adsorption at $0,01\ M$ and $0,1\ M$ NaCl, higher ionic strength was found to inhibit Pb^{2+} adsorption onto MPs. This may be attributed to increased salinity causing MP aggregation, reducing adsorption sites, and electrostatic screening between the negative surface and positive Pb(II) by salt [14] [59].

In contrast to the observation with pH, the adsorption of heavy metals (Cd, Cu, Co, Ni, and Pb, etc.) on MPs is inhibited by increasing ionic strength. However, high ionic strength was shown to increase Cr(VI) adsorption, possibly due to a reduction in the negative-negative (surface-chromate) repulsion between MP and Cr(VI). A few studies have demonstrated that salinity has no significant effects on MPs' adsorption of Cu and Pb [36].

The influence of ionic strength in the capture process can manifest in two ways: (1) Salting out effect, where increased ionic strength enhances the activity coefficient of hydrophobic organic compounds, decreasing solubility and promoting adsorption; (2) Extrusion effect, wherein ions penetrate the diffuse double layer on microplastic surfaces, diminishing repulsive forces and facilitating denser aggregation structures, potentially hindering adsorption [20].

In another study, increased salinity was reported to impact the aggregation of MP particles by compressing the electrical double layer, reducing repulsive forces, leading to „stacking effects," and ultimately causing aggregation of MPs. This aggregation resulted in reduced surface area and sorption capacity on the MPs [22].

In a study investigating the adsorption of cadmium, cobalt, chromium, copper, nickel, and lead onto high-density polyethylene under estuarine conditions, it was found that for cadmium, cobalt, nickel, and lead, adsorption decreased with increasing salinity. However, increasing pH led to increased adsorption, except for chromium in both cases. No effects of pH and salinity were observed on copper. The lower adsorption at acidic pH may be attributed to electrostatic repulsion between metal ions (Cd^{2+}) and the positively charged plastic surface [42]. In another study, increase in pH from 3 to 7 resulted in enhanced metal adsorptions, which was observed on Cu as well, unlike in the previous study [31].

Another important factor is the temperature. With increasing temperature, the adsorption performance of microplastics improves. This observation may be explained by considering that the adsorption process is an endothermic reaction, leading to an increase in spontaneity with rising temperatures. Examples include the adsorption of cadmium(II) by D152 resin, the adsorption of metal ions like Cu(II) by cross-linked polystyrene supported low-generation diethanolamine dendrimers, and the adsorption of precious metal ions on polyacrylonitrile-2-amino-2-thiazoline resin [59] [38] [22].

The adsorption of heavy metals by MPs is influenced by the metal concentration in the surrounding environment. A six-month field experiment demonstrated that the concentra-

tions of Cr, Mn, Cu, Zn, As, and Cd adsorbed on MPs were consistent with the trend of surrounding seawater concentrations. Similarly, a field study across six sandy beaches in Hong Kong revealed that MPs from the most polluted site contained higher concentrations of Cu, Fe, Ni, and Mn. This trend is also observed in the adsorption of heavy metals by MPs in soil; for example, a study in central China found strong correlations between the metal contents in soil and MP particles, indicating that the contents of Cd, Pb, Hg, and Mn in MPs were significantly influenced by their levels in soils [14].

The sorption behavior is also influenced by the dissolved organic matter in natural waters, as it competes with other sorbents, potentially through hydrophobic interactions. Dissolved organic matter may decrease sorption capability by reducing available sorption regions or may interact further with pollutants sorbed on the surface of plastic [42] [31] [22].

MPs can create an ecological niche for microorganisms by forming microbial biofilms, known as plastisphere. In the presence of heavy metals, microbial cells in biofilms can increase the production of extracellular polymeric substances (EPS) to shield themselves from the harsh environment. EPS, rich in ionizable functional groups like hydroxyl, phosphoric, carboxyl, and amine groups, plays a crucial role in biosorption of heavy metals. Additionally, EPS inhibits the diffusion of heavy metals within the matrix, lowering their concentration to sublethal levels and enabling the survival of exposed microbes, which develops tolerance or resistance to heavy metals (Figure 2.20) [38] [39] [36].

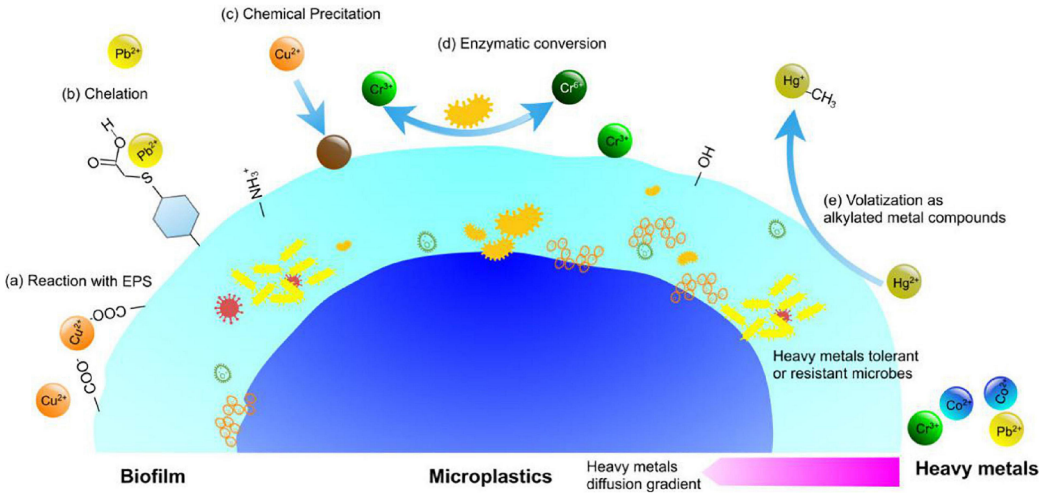

Figure 2.20: Mechanisms of biofilm involved in the interactions between MPs and heavy metals. (a) Reaction with extracellular polymeric substance (EPS) in the matrix; (b) chelation with proteins and peptides; (c) precipitation via chemical or biological agents; (d) enzymatic conversion; (e) volatilization as alkylated metal compounds. Taken from [38].

Compared to the marine environment, very few studies exist on the occurence and effects of microplastics in fresh water (rivers) and estuaries. However, catchments are direct and significant recipients of stormwater runoff and also both municipal and industrial effluents, making them a significant recipient of plastic debris. Since flow in rivers (non-tidal areas) is unidirectional, plastic debris present in rivers is likely to be less weathered than marine plastic debris, which has generally been suspended and beached for longer periods of time [27].

2.4.4 Combined effects of MPs and HMs on organisms and humans

Microplastics, along with hazardous chemicals adhered to their surfaces, have the potential to be ingested by organisms, resulting in the bioaccumulation of these substances. Microplastic ingestion provides a pathway for the transfer of metals, additives, and persistent organic pollutants to organisms through ingestion. Consequently, microplastics act as a multiple stressor to the organism [42] [31].

The combination of MPs with contaminants alters organism toxicity, crucial for understanding plastic behavior in the environment (Figure 2.21). Both MPs and heavy metals can individually exhibit toxicity, resulting in synergistic, antagonistic, or potentiating effects when combined. Synergistic effects amplify the combined impact, antagonistic effects occur as MPs reduce heavy metal concentrations, and potentiating effects enhance the toxicity of one chemical when added to another. Currently, synergistic and antagonistic effects are more common in aquatic environments [14].

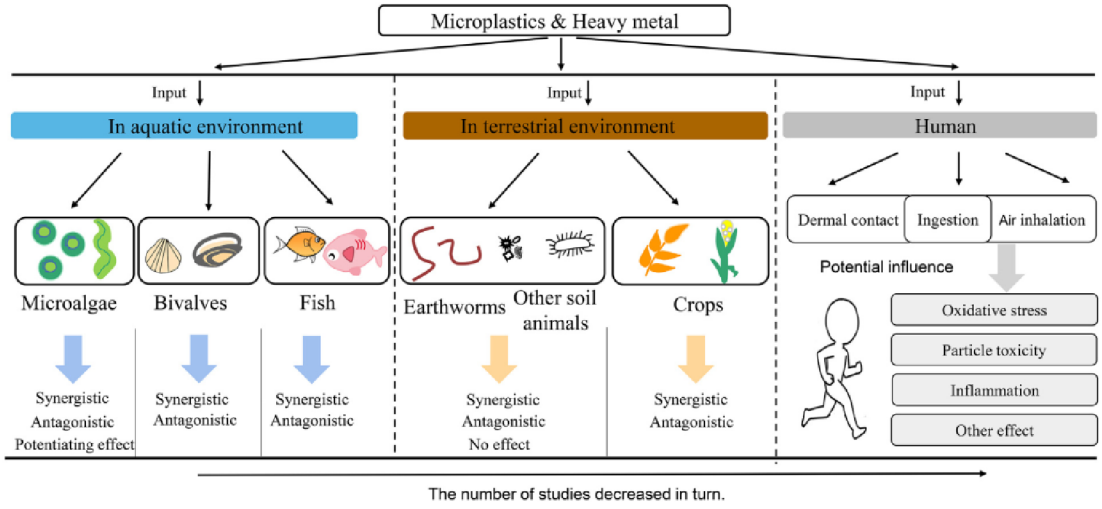

Figure 2.21: The combined effects of different microplastics (MPs) and heavy metals on organisms and humans are schematically depicted. Synergistic or antagonistic effects may occur when organisms are co-exposed to specific MPs and heavy metals. The combined toxicities on organisms can be chemical- and species-specific. Humans may be exposed to MPs and heavy metals through ingestion, inhalation, and dermal contact. The potential impact on humans is uncertain, requiring further investigation and efforts. Taken from [14].

Numerous studies confirm that MPs are readily ingested by aquatic and terrestrial biota, impacting their physiology, reproduction, and mortality. Acting as carriers, MPs transport adsorbed heavy metals into organism bodies, where these pollutants may be desorbed within the digestive systems. The interaction between MPs and heavy metals alters plastic surface properties, influencing the uptake and accumulation of both plastics and contaminants in exposed organisms. This results in diverse reactivity among organisms. Despite heavy metals commonly being present on MPs, few studies investigate the joint toxicity of MPs and heavy metals on organisms [14] [42] [31].

Heavy metals adsorbed on/in MPs may enter the human body through ingestion, inhalation, and dermal contact. MPs' toxicity depends on exposure concentration, particle com-

ponents, adsorbed contaminants, and individual factors. Critical dosage reaching systemic circulation, bioavailability, bioaccessibility, and adverse effects require careful evaluation. Toxicodynamic modeling suggested human threshold concentrations for 20 μm and 5 μm MPs. Cumulative exposure dosage measurements for MP and heavy metal mixtures are crucial for accurate health risk assessment. However, understanding the combined toxicity of MPs and heavy metals to humans is limited, necessitating further research to explore dosage-dependent effects on human health [14].

In a simulated human digestive system, the desorption behavior of Cr from both non-degradable MPs (PE, PP, PVC, and PS) and degradable MPs (PLA) was studied. The bioaccessibility of Cr was found to be higher for degradable MPs in gastric, small, and large intestinal phases compared to non-degradable MPs. This suggests that MPs, particularly degradable ones, could pose higher ecological risks when inadvertently ingested by organisms [31].

A recent study demonstrated that MPs act as vectors for Cr in a simulated human digestive system, increasing its bioaccessibility. Additionally, metal nanoparticles and MPs have been associated with cytotoxic effects on the human brain, epithelial cells, and colon-rectal differentiated cells [31].

2.5 Future prospects

The sorption of hydrophobic organic pollutants, such as polycyclic aromatic hydrocarbons, dioxins, phthalates and polychlorinated biphenyls has been weel studied and documented, as well as toxicity of heavy metals in the aquatic environment. Nevertheless, the MP-mediated transport of metals remains poorly understood [25].

Considering the prevalence and potential impacts of MPs in marine ecosystems, our understanding of the levels of heavy metals associated with MPs in marine environments is currently inadequate. Urgent measures need to be implemented, such as the establishment of environmental monitoring programs, to comprehensively assess the association of heavy metals with MPs [31].

While the toxicity of metals is well-studied, further research on bioavailability and ecological risks of metal contaminants on plastics is needed. The bioavailability of metals is influenced via the route of exposure (e.g., ingestion of plastic debris) and health effects will differ according to the mixture of metals and the species exposed, as well as other environmental factors [47].

Further studies are needed to clarify the role of microplastics as sinks or sources of metals. These studies should investigate the release of heavy metals from microplastics in various environments, such as the digestive tracts of fish and deposit feeders. Additionally, it is essential to assess whether the levels of metals found in microplastics can pose toxicity to the surrounding biota [9].

Many studies use no certified reference material (CRM), whereas other employ unsuited, non-matrix matched CRMs (such as water, soil, sewage sludge, etc.). Usage of such non- or poorly validated procedures leads to incomparable, hardly traceable or even inaccurate data. For accurate assessment of the data involving interactions between metals and microplastics,

thourough method validation and protocols are needed, including reference materials and inter-laboratory comparison tests [25] [38].

For instance, leaching/extraction protocols through weak acid have different degrees of selectivity towards different metals. The degree of desorption also varies between different polymer types according to their chemical composition. Aditionally, a variety of physical parameters, such as permeability, diffusion coefficients, solubility and polarity, as well as polymer-specific parameters (glass transition temperature and crystallization content) also play an important role in the sorption process and are crucial for the thourough assessment of this type of interaction [25].

Future studies should not only focus on the adsorption of single pollutants by MPs but also investigate adsorption in the presence of multiple coexisting pollutants in the complex actual environment. The physical and chemical properties of MPs undergo significant changes in the environment. Therefore, more attention should be given to understanding the interaction mechanisms between MPs and organic pollutants in natural conditions, as these may differ from laboratory settings [19].

In-depth studies on the adsorption behavior of MPs are limited, and there is a need for the development of a theoretical model to calculate the adsorption of organic pollutants by MPs. Current research methods and results may be inadequate for discussing the underlying mechanisms. Attention should be directed towards understanding the combined effects of MPs and organic pollutants on organisms for a comprehensive assessment of their impact [19].

In a recent study, an Artificial Neural Network (ANN) model for heavy metal adsorption on MPs was developed. This model predicted that laboratory studies can offer valuable insights into the sorption mechanisms of heavy metals on MPs in the world's aquatic environments [31].

Chapter 3

Experimental part

3.1 Materials and equipment

3.1.1 Materials

During the experimental part, following materials and chemicals were used:

- $NaCl$ (p.a.), Sigma-Aldrich
- $MgCl_2$ (p.a.), Sigma-Aldrich
- $NaSO_4$ (p.a.), Sigma-Aldrich
- $CaCl_2$ (p.a.), Sigma-Aldrich
- KCl (p.a.), Sigma-Aldrich
- $NaHCO_3$ (p.a.), Sigma-Aldrich
- KBr (p.a.), Sigma-Aldrich
- miliQ water (p.a.), Sigma-Aldrich
- nitric acid HNO_3 (65 % p.a.), PENTA
- milled polyethyleneterephtalate PET, Petka cz a.s.
- calibration standard Pb solution (c = $1 \pm 0,002\ g \cdot dm^{-3}$), Analytika, s r.o., ČR
- calibration standard Hg solution (c = $1 \pm 0,002\ g \cdot dm^{-3}$), ČMI CZ 9024 (1N)
- calibration standard Zn solution (c = $1 \pm 0,002\ g \cdot dm^{-3}$), ČMI CZ 9069 (1N)
- calibration standard Cu solution (c = $1 \pm 0,002\ g \cdot dm^{-3}$), ČMI CZ 9015 (1N)
- calibration standard Cd solution (c = $1 \pm 0,002\ g \cdot dm^{-3}$), Analytika, s r.o., ČR

	Pb	Zn	Cr	Cu	Cd
Lamp current (mA)	5	5	7	4	4
Fuel	acetylene	acetylene	acetylene	acetylene	acetylene
Support	air	air	$N_2O + O_2$	air	air
Flame stoichiometry	oxidizing	oxidizing	reducing	oxidizing	oxidizing
Wavelength (nm)	217	213,9	357,9	324,7	228,8
Fuel flow $(L \cdot min^{-1})$	1,1	1,2	4,2	1,1	1,2
Burner height (mm)	7	7	8	7	7

Table 3.1: Parameters of selected heavy metals measurement by *Solar M*6, *Thermo Analytic*.

Drying time (s)	60
Decomposition time (s)	120
Waiting time (s)	45
Absorbance blank threshold $(-)$	0,005
Decomposition time blank (s)	60

Table 3.2: Parameters of mercury measurements by AMA 254.

3.1.2 Equipment

During the experimental part, following equipment was used:

Atomic absorption spectroscope Solar M6

For the analysis of heavy metals solutions after the adsorption experiments, atomic adsorption spectroscope *Solar M*6, *Thermo Analytic* was used, in flame atomisation mode. The width of the burner used was 50 mm and the temperature was 22 $°C$. Solar AA software was used to set analysis parameters and recording of measured values. The parameters used can be seen in Table 3.1.

Advanced mercury analyzer AMA 254

Atomic absorption spectrometer AMA 254 was used for Hg measurements. It can be used in both solid and liquid matrices and is highly sensitive. It is a single-purpose atomic absorption spectrometer where the sample with Hg is incinerated and Hg-contaminated vapours are trapped on a gold or silver amalgamator. The settings for the measurement are stated in Table 3.2.

Fourier transform infrared spectroscope Alpha II (Bruker)

Fourier transform infared spectroscopy (*Alpha II*, *Bruker*) was used as an additional method for microplastic analysis after the adsorption experiments, in an ATR (attenuated

Number of scans	32
Wavelength range (cm^{-1})	4000 - 400
Scanning time (s)	40
Resolution (cm^{-1})	4

Table 3.3: Parameters of PET measurements by *Alpha II*, *Bruker*.

Compound	**Concentration** ($g \cdot L^{-1}$)
$NaCl$	24,53
$MgCl_2$	5,2
$NaSO_4$	4,09
$CaCl_2$	1,16
KCl	0,695
$NaHCO_3$	0,201
KBr	0,101

Table 3.4: Composition of artificial seawater.

total reflection) mode. Opus 8.1 software was subsequently used for spectra evaluation. The parameters for FTIR measurements by *Alpha II*, *Bruker* are stated in Table 3.3.

3.2 Experiment design

PET was first sieved into 2 fractions: $< 0,63\ \mu m$ and $0,63\ \mu m - 1\ mm$. Both fractions were subsequently divided and weighed into plastic containers (approximately 50 mg each) and stored in a cool, dry place for subsequent adsorption experiments.

The lab sea water was prepared, to simulate the conditions in real sea water. The chemical compositions used for mixing of artificial seawater are tabulated in Table 3.4 [52].

Calibration standard solutions of heavy metals (Pb, Zn, Cr, Cu, Cd) were prepared from stock heavy metals solutions with concentrations of $1,000 \pm 0,002\ g \cdot dm^{-3}$ in 3% nitric acid solution in ultrapure MiliQ water. Additionally, 95 % confidence intervals and specified prediction intervals were determined for all calibration dependencies.

In the adsorption experiments, a series of 10 heavy metals solutions with increasing concentrations were prepared for every metal in two versions: fresh and sea water and 40 ml of those were added into the plastic containers. The mixture was left for 72 hours on a shaker device. After the adsorption period, solutions were filtered ($0,22\ \mu m$ syringe filters (JET BIOFIL)) and diluted when needed. 4 PET samples of each series were dried and stored for further FTIR analysis.

- Lead solutions had concentrations of 4, 8, 12, 16, 20, 24, 28, 32, 36 and 40 $g \cdot dm^{-3}$.
- Mercury solutions had concentrations of 1, 2, 3, 5, 6, 7, 9, 10, 15 and 20 $g \cdot dm^{-3}$.
- Zinc solutions had concentrations of 1, 2, 3, 5, 6, 7, 9, 10, 15 and 20 $g \cdot dm^{-3}$.

- Copper solutions had concentrations of 1, 2, 3, 5, 6, 7, 9, 10, 15 and 20 $g \cdot dm^{-3}$.
- Cadmium solutions had concentrations of 1, 2, 3, 5, 6, 7, 9, 10, 15 and 20 $g \cdot dm^{-3}$.

The analysis sequence on *Solar M6* included measuring the blank, calibration series, and samples. Each metal's set of samples aimed to check for metal ion release from PET, nitric acid solution, or the containers used in adsorption experiments. Measurements included a 3 % HNO_3 solution and a 3 % HNO_3 solution with 50 mg of PET, left for 96 hours on a shaker. Concentrations were subsequently calculated for all metals - Pb, Zn, Cr, Cu, Cd, and adsorption isotherms were plotted.

Mercury was measured on *AMA* 354. Before the actual measurement, cleaning was performed by adding 100 μL of tap water, repeating until the absorbance value was below $0,005$. Subsequently, an analysis of liquid samples from sorption experiments was carried out for an unknown concentration of mercury, using 100 μL of the sample. The instrument was cleaned again using tap water at the end of the analysis.

The analysis of PET after adsorption experiments involved infrared spectrometry with Fourier transform. Both pure PET and PET after adsorption of heavy metal ions (concentration of 10 $mg \cdot L^{-1}$) were analyzed. The IR spectra were measured using an *Alpha II* with the attenuated total reflection (ATR) module. PET samples were air-dried before analysis to avoid interference from water bands in the central region of infrared radiation.

3.3 Data analysis

For automated data procession as well as charts and tables generation, a series of scripts in `python3` language were programmed, with the use of following libraries:

- `matplotlib` for charts construction,
- `pandas` for loading of csv data into python scripts,
- `sklearn` for R^2 score calculation,
- `scipy` for optimalization parameters of non-linear fittings, as well as analytical solutions of linear regressions,
- `numpy` for application of vector operations when calculating equations (for the purpose of speeding up calculations and optimizing curves)[1].

3.4 Calibrations

The calibration curves represent the absorbance dependence on concentration, expressed as a straight line equation ($y = a + bx$) through linear regression. Additionally, 95 % confidence intervals and prediction intervals were determined for all calibration dependencies. Calibration standard solutions of heavy metals from a stock solutions of heavy metals

[1] https://en.m.wikipedia.org/wiki/Single_instruction,_multiple_data

$(1,000 \pm 0,002\ g/L$ were prepared in a 3 % nitric acid solution in ultrapure MiliQ water for Pb, Zn, Cu and Cd. AMA 254 had already been calibrated, therefore no calibration series had to be prepared (Figure 3.2). Calibration series were prepared as follows:

- For Pb, the calibration series concentrations were $0, 5, 8, 10, 15,$ and $20\ mg \cdot L^{-1}$ (Figure 3.1).
- For Zn, the calibration series concentrations were $0, 0.4, 0.8, 1.2, 1.6,$ and $2\ mg \cdot L^{-1}$ (Figure 3.3).
- For Cu, the calibration series concentrations were $0, 2, 4, 6, 8,$ and $10\ mg \cdot L^{-1}$ (Figure 3.4).
- For Cd, the calibration series concentrations were $0, 0.4, 0.8, 1.2, 1.6,$ and $2\ mg \cdot L^{-1}$ (Figure 3.5).

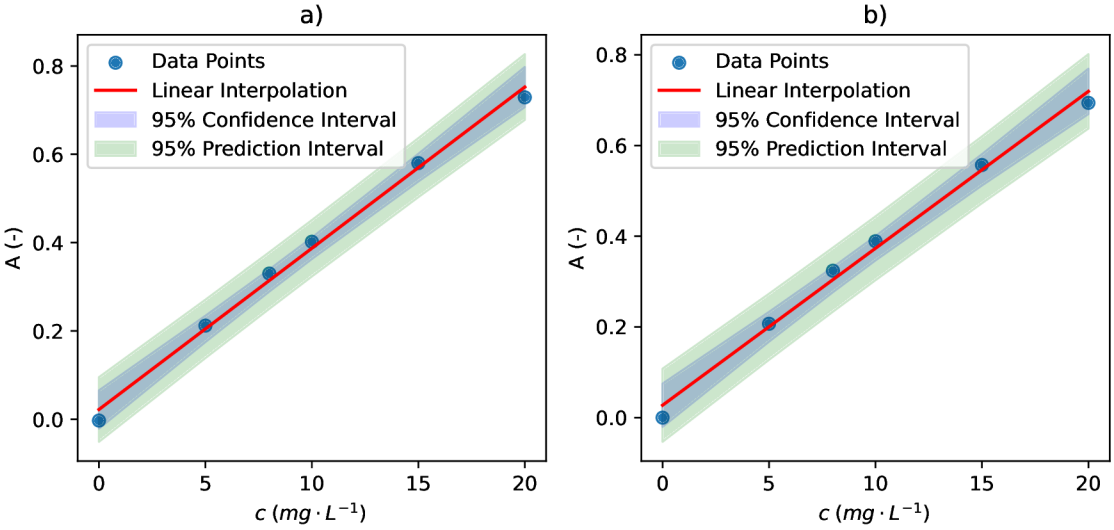

Figure 3.1: Pb calibration curves for fresh (a) and sea (b) water.

In tables Table 3.5 and Table 3.6, parameters of calibration curves are stated for heavy metals in fresh water and sea water, respectively. The limit of detection (LOD)[2] and limit of quantification (LOQ)[3] were calculated as multiple of the standard deviation of residuals (the differences between the observed signals and the signals predicted by the calibration curve) - 3 for the LOD and 10 for the LOQ.

[2]The limit of detection, according to IUPAC, expressed as the concentration or the quantity, is derived from the smallest measure that can be detected with reasonable certainty for a given analytical procedure [1].

[3]The quantitation limit of an individual analytical procedure is the lowest amount of analyte in a sample which can be quantitatively determined with suitable precision and accuracy [10].

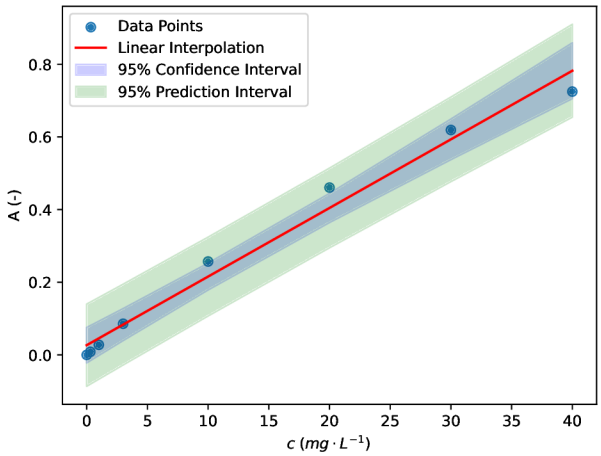

Figure 3.2: Hg calibration curve.

	Pb	Hg	Zn	Cu	Cd
Slope	0.036510	0.018884	0.534600	0.061600	0.247800
Intercept	0.022040	0.026770	0.024520	0.035330	0.009714
Coeficcient of correlation	0.997300	0.991250	0.998300	0.992200	0.998200
Coefficient of determination	0.994700	0.982576	0.996600	0.984500	0.996500
LOD $(\mathbf{mg \cdot L^{-1}})$	0.051980	0.108355	0.063570	0.079320	0.030090
LOQ $(\mathbf{mg \cdot L^{-1}})$	0.173300	0.361184	0.211900	0.264400	0.100300

Table 3.5: Parameters of calibration curves for Pb, Zn, Cu and Cd and fresh water.

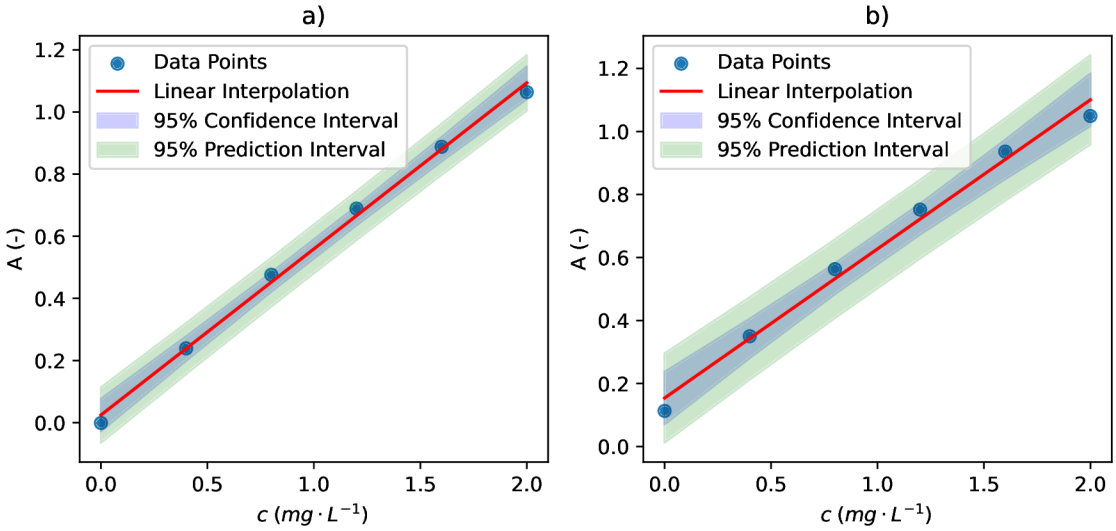

Figure 3.3: Zn calibration curves for fresh (a) and sea (b) water.

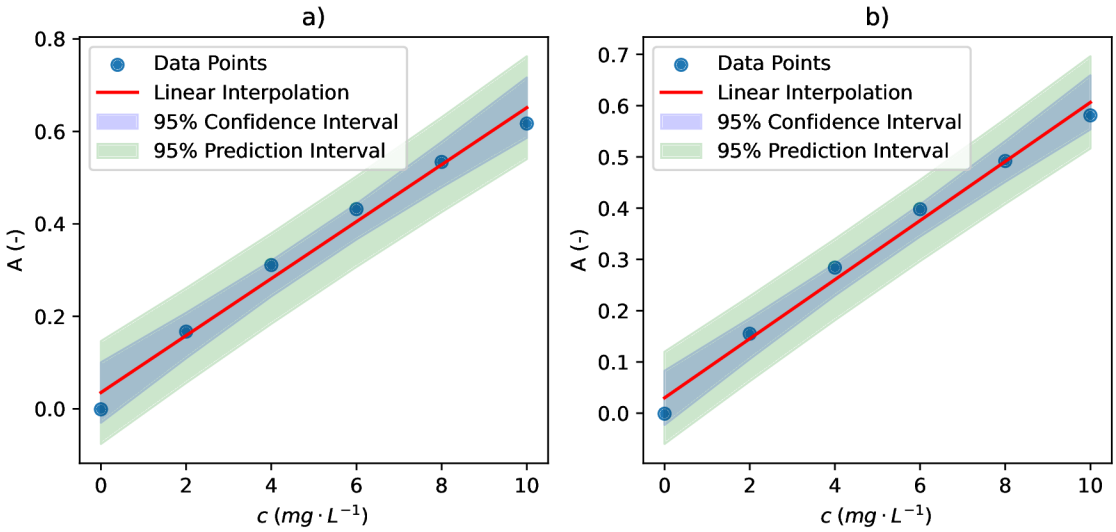

Figure 3.4: Cu calibration curves for fresh (a) and sea (b) water.

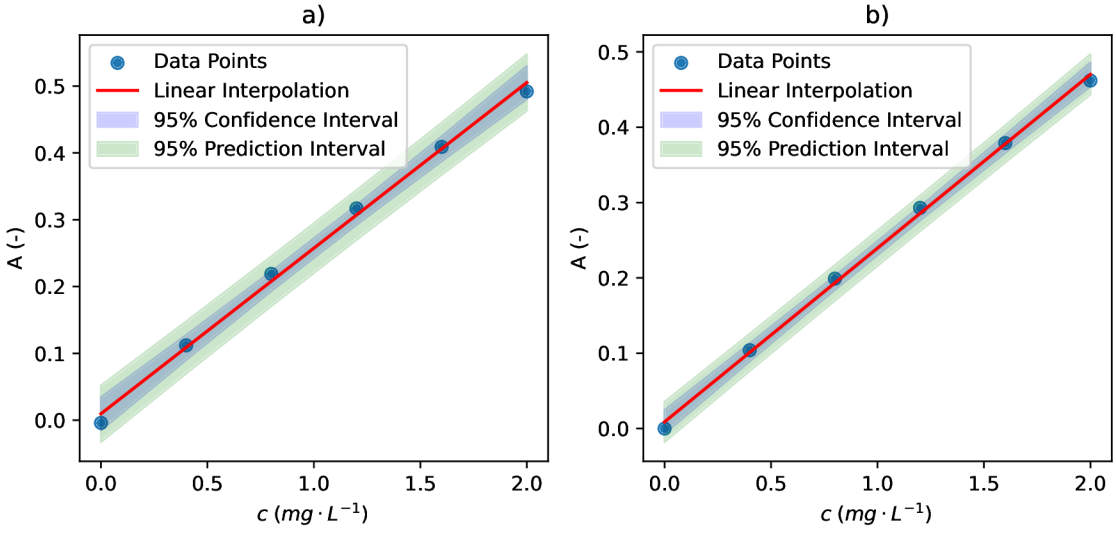

Figure 3.5: Cd calibration curves for fresh (a) and sea (b) water.

	Pb	**Hg**	**Zn**	**Cu**	**Cd**
Slope	0.034600	0.018884	0.473400	0.057640	0.230600
Intercept	0.027350	0.026770	0.153800	0.029950	0.008857
Coeficcient of correlation	0.996400	0.991250	0.994600	0.994200	0.999200
Coefficient of determination	0.992800	0.982576	0.989200	0.988300	0.998400
LOD ($\mathbf{mg \cdot L^{-1}}$)	0.057280	0.108355	0.101200	0.064130	0.018990
LOQ ($\mathbf{mg \cdot L^{-1}}$)	0.190900	0.361184	0.337200	0.213800	0.063290

Table 3.6: Parameters of calibration curves for Pb, Zn, Cr, Cu and Cd and sea water.

Chapter 4

Results and discussion

4.1 Adsorption experiments

4.1.1 Adsorption curves

Adsorption experiments of 5 heavy metals (Pb, Hg, Zn, Cu and Cd) were performed in both fresh and sea water (prepared in laboratory) on PET of two fractions - small ($< 0,63\ \mu m$) and big ($0,63\ \mu m - 1\ mm$). Adsorbed amount was calculated from the adsorbances of heavy metal solutions before and after the sorption experiments, adsjusted to the amount of plastic and the volume of the solution and plotted against the concentration of the post-experiment solutions. These data, fitted with logarithmic curve, can be observed in Figure 4.1 – Figure 4.5.

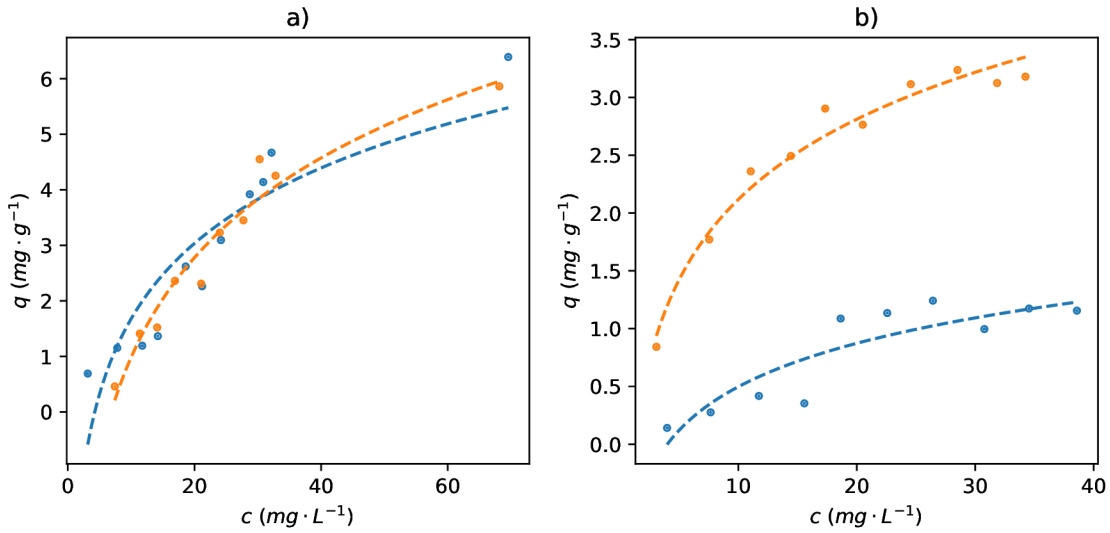

Figure 4.1: Measured data points of adsorption isotherms for Pb: a) fresh water, b) sea water; smaller PET fraction ($< 0,63\ \mu m$) - blue, bigger PET fraction ($0,63\ \mu m - 1\ mm$) - orange.

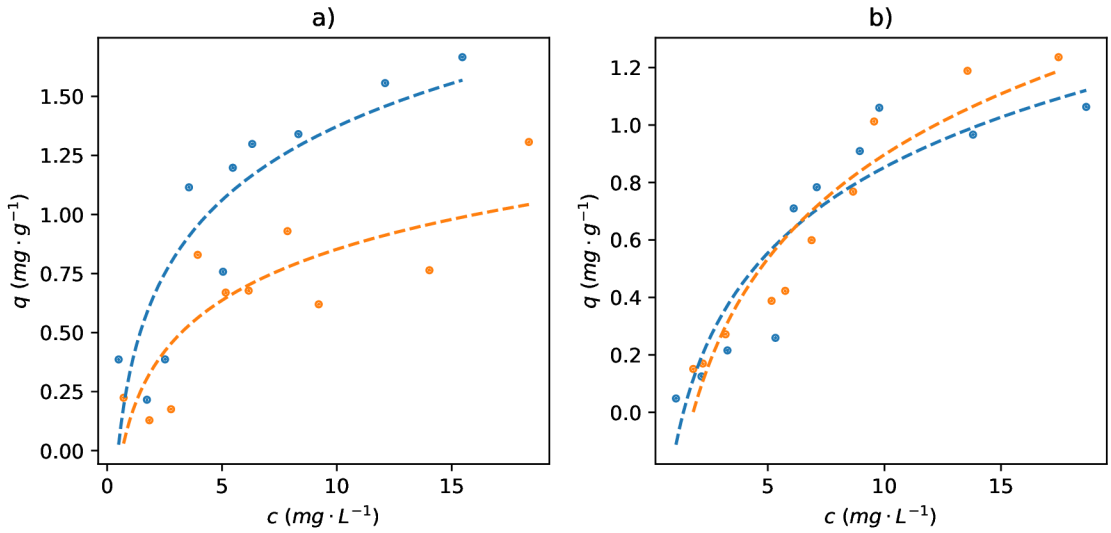

Figure 4.2: Measured data points of adsorption isotherms for Hg: a) fresh water, b) sea water; smaller PET fraction ($< 0,63\ \mu m$) - blue, bigger PET fraction ($0,63\ \mu m - 1\ mm$) - orange.

The differences between small and big fraction vary among the metals. For Pb, the bigger fraction adsorbed larger amounts of heavy metal. For Hg, the trend is the opposite. For Zn, the adsorption was more prominent for smaller fraction in the fresh water, and with bigger fraction in the sea water. For Cu, the difference is very small, negligable, with plotted adsorbed concentrations being in very close proximity of each other. Cd again shows clear difference between the small and big fractions, with the adsorption was more prominent for bigger fraction in the fresh water, and with smaller fraction in the sea water.

I hypothesized that the amount of metal adsorbed on smaller fraction would be much more significant compared to the bigger fraction due to a larger active surface area per unit mass and as a result, increased number of active sites available for interaction with the metal ions. However, the results of the experiments indicate other factors, which likely include surface chemistry and solution chemistry, also played a significant role.

All metals show considerably higher adsorbed amounts in fresh water than in the sea water. This corresponds with my hypothesis and can be primarily attributed to differences in solution chemistry. Sea water has higher ionic strength due to dissolved salts, which can compete with heavy metal ions for adsorption onto the PET surface. The pH also influence the speciation and availability of heavy metal ions for adsorption. In sea water, electrostatic repulsion can also be of great importance and complexes (such as $MeCl^{+}$, $MeCl^{0}{}_{2}$, $MeCl^{-}{}_{3}$, and $Me(OH)Cl^{0}$) are also likely to be formed, which further decreases the adsorption rate. MPs aggregation is yet another possible contributing factor.

Some of the adsorption curves (mainly Pb and Hg) clearly have not reached plateau stage yet and display a shape that indicates the active places on PET surface were not yet saturated. In such cases, the adsorption is likely still ongoing and the concentrations of the metals were too low to occupy all available binding sites. It is worth noting that the metals

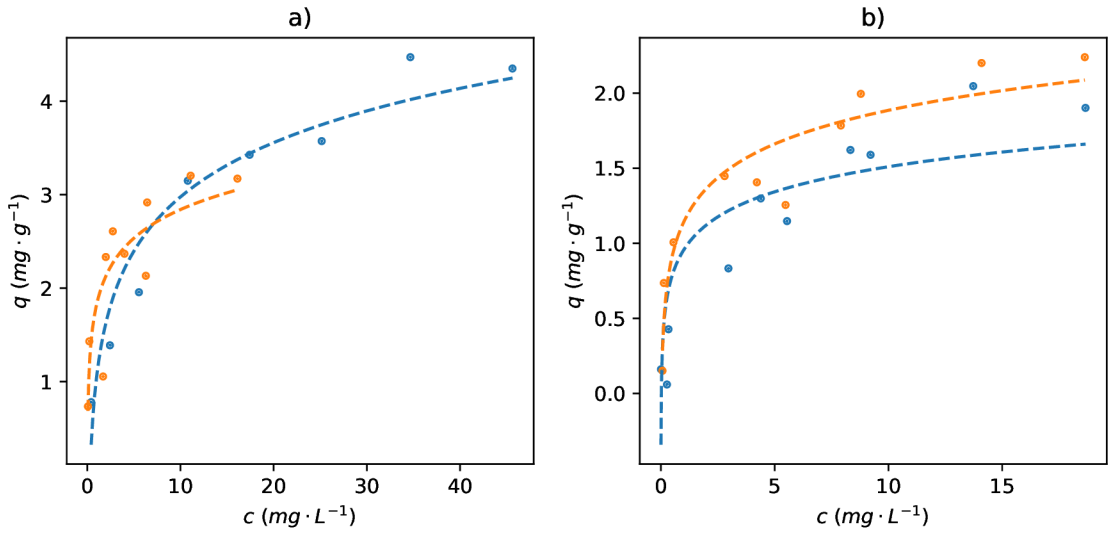

Figure 4.3: Measured data points of adsorption isotherms for Zn: a) fresh water, b) sea water; smaller PET fraction ($< 0,63\ \mu m$) - blue, bigger PET fraction ($0,63\ \mu m - 1\ mm$) - orange.

can also undergo different specific adsorption mechanisms, which can influence the shape of the curve.

4.1.2 Isotherms fitting

The calculated curves were fitted with Langmuir, Freundlich and Temkin adsorption isotherms. An example series of charts (for adsorption of Zn on smaller fraction in fresh water) can be seen in Figure 4.6. All other plotted series can be found in Appendix A.

The parameters of the isotherms were calculated in two ways. Firstly, linearized forms of the isotherms were used (Equation 4.1 for Langmuir isotherm, Equation 4.2 for Freundlich isotherm and Equation 4.3 for Temkin isotherm). Langmuir linearized isotherm was plotted as $c/q\ \ (g/L)$ against $c\ \ (mg/L)$, Freundlich linearized isotherm was plotted as $ln\ \ q\ \ (mg/g)$ against $ln\ \ c\ \ (mg/L)$ and Temkin linearized isotherm was plotted as $q\ \ (mg/g)$ against $ln\ \ c\ \ (mg/L)$. A linear least-squares regression was calculated using `scipy.stats.linregress` (see section 3.3) and parameters for isotherms were finally calculated from the regression equations. The Temkin models were determined with the $T = 298,15\ K$.

$$\frac{C}{q} = \frac{1}{K_l \cdot q_{\max}} + \frac{C}{q_{\max}} \tag{4.1}$$

$$\ln(q) = \ln(K_f) + \frac{1}{n}\ln(C) \tag{4.2}$$

$$q = \frac{RT}{b_t}\ln(C) + \frac{RT}{b_t}\ln(K_t) \tag{4.3}$$

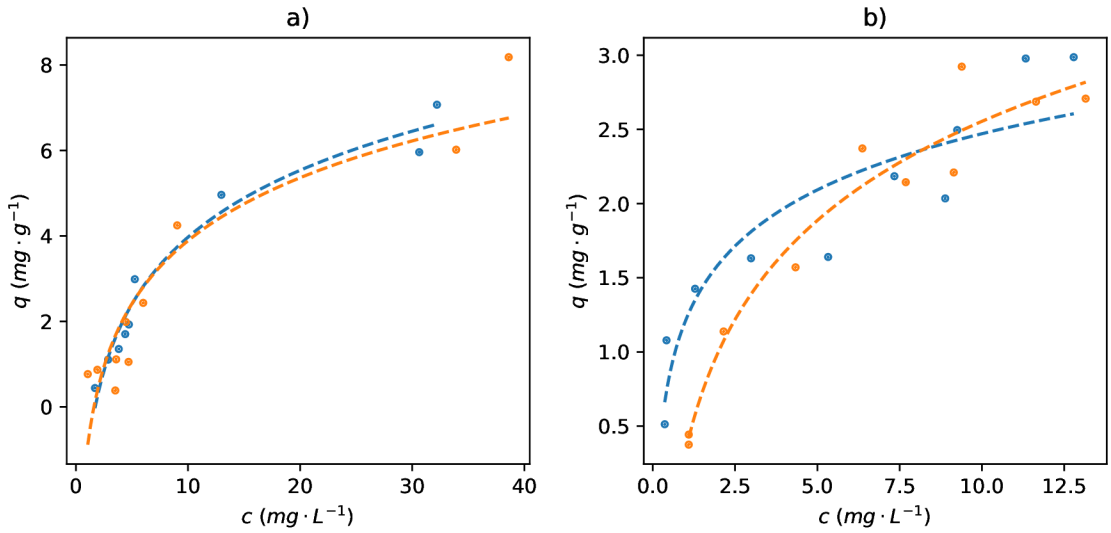

Figure 4.4: Measured data points of adsorption isotherms for Cu: a) fresh water, b) sea water; smaller PET fraction ($< 0,63\ \mu m$) - blue, bigger PET fraction ($0,63\ \mu m - 1\ mm$) - orange.

Secondly, parameters of the models were determined using `curve_fit` function from the `scipy.optimize` library that directly fitted the adsorption curves. The number of iterations was adjusted to 10000[1]. To perform the minimalization, the function uses Trust Region Reflective algorithm[2]. An example table of parameters of these fittings (for Zn) can be found in Table 4.1. Parameters for other metals can be found in Appendix B.

The isotherm fitting with the `curve_fit` has yielded higher R^2 values[3]and has proved to be more suitable than the linearised isotherms methods. This supports a known fact that fitting data directly is preferrable over fitting the transformed version of the data. This is due to linearisation and de-linearisation errors resulting from the nature of the transformation, which also affects the errors (e.g., the size of the „distance“ between the real point and its supposed value (determined by the fit) changes after de-linearisation). In another words, optimizing a curve to best fit the transformed (linearised) data does not necessarily yield the best fit of the original data after de-linearisation. Temkin isotherm is exeption, with values acquired with both methods being almost identical (there are subtle differences that have been lost when rounding the values up to 4 valid digits). In some cases of Pb adsorption (Figure A.1, Figure A.2, Figure A.4), the `curve_fit` function was unable to find a suitable fit even after adjusting the number of iterations.

Looking at the R^2 values of the best fit, Zn follows the Freundlich adsorption model the most, Hg and Cd follow the Langmuir adsorption model and Pb and Cu yield best results with Temkin adsorption model. Maximal measured adsorbed amounts ($mg \cdot g^{-1}$) are in most cases lower than the calculated maximal ones (suggesting the beforementioned trend of ongoing adsorption) and are as follows:

[1] To ensure convergence in cases when more prominent outliers were present. The default value is 500.

[2] https://optimization.cbe.cornell.edu/index.php?title=Trust-region_methods

[3] In some cases, calculated R^2 is negative – https://scikit-learn.org/stable/modules/generated/sklearn.metrics.r2_score.html#sklearn-metrics-r2-score.

Langmuir isotherm							
q_{max} (exp.)							
freshwater				seawater			
A		B		A		B	
4.472		3.204		2.046		2.239	
		q_{max}	K_l	R^2	a	b	R^2 (reg.)
linear fitting							
freshwater	A	4.882	0.1668	0.951	0.2048	1.228	0.9789
	B	3.389	0.7004	0.6087	0.295	0.4212	0.9413
seawater	A	2.438	0.2215	0.9527	0.4102	1.852	0.8206
	B	2.357	0.568	0.7724	0.4243	0.7469	0.956
non-linear fitting							
freshwater	A	5.024	0.1375	0.957	-	-	-
	B	2.995	1.378	0.6242	-	-	-
seawater	A	2.585	0.1874	0.9542	-	-	-
	B	1.966	1.588	0.8038	-	-	-
Freundlich isotherm							
		n	K_f	R^2	a	b	R^2 (reg.)
linear fitting							
freshwater	A	2.56	1.066	0.2002	0.3906	0.06363	0.9814
	B	3.917	1.611	-0.2551	0.2553	0.4768	0.7557
seawater	A	2.605	0.581	0.3957	0.3839	-0.543	0.6869
	B	2.736	0.8548	0.3144	0.3655	-0.1569	0.7957
non-linear fitting							
freshwater	A	2.736	1.15	0.9647	-	-	-
	B	4.104	1.672	0.772	-	-	-
seawater	A	2.266	0.5855	0.9466	-	-	-
	B	3.463	0.9807	0.9149	-	-	-
Temkin isotherm							
		b_t	K_t	R^2	a	b	R^2 (reg.)
linear fitting							
freshwater	A	2959	3.492	0.9305	0.8377	1.047	0.9305
	B	5608	61.88	0.7498	0.442	1.823	0.7498
seawater	A	1.028e+04	52.54	0.748	0.241	0.9549	0.748
	B	7663	34	0.899	0.3235	1.141	0.899
non-linear fitting							
freshwater	A	2959	3.492	0.9305	-	-	-
	B	5608	61.88	0.7498	-	-	-
seawater	A	1.028e+04	52.54	0.748	-	-	-
	B	7663	34	0.899	-	-	-

Table 4.1: Calculated parameters of adsorption isotherms for Zn, reg. = regression, exp. = experimental, A = small fraction, B = big fraction, – - does not apply.

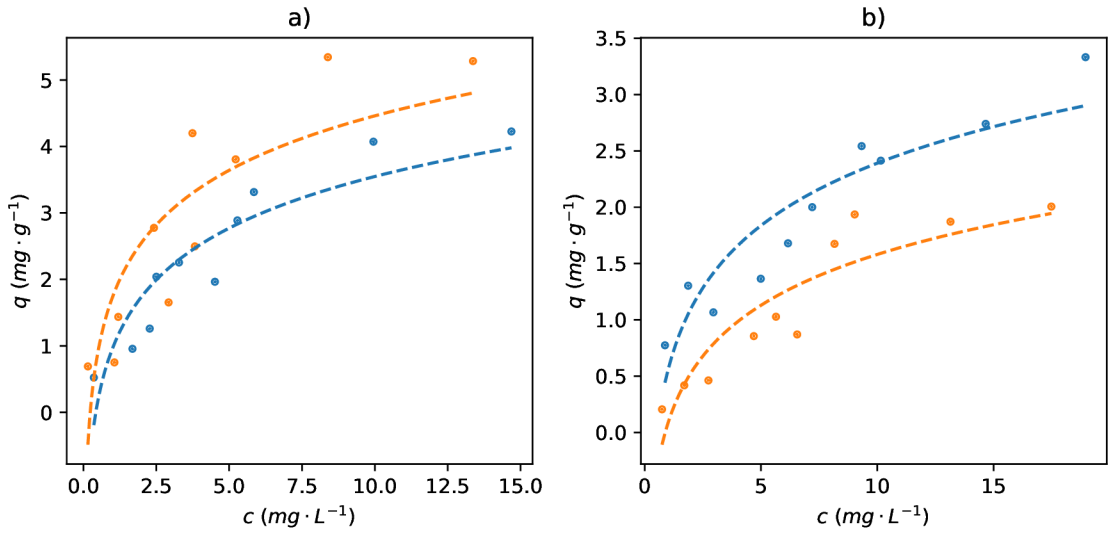

Figure 4.5: Measured data points of adsorption isotherms for Cd: a) fresh water, b) sea water; smaller PET fraction ($< 0,63\ \mu m$) - blue, bigger PET fraction ($0,63\ \mu m - 1\ mm$) - orange.

- On smaller fraction in freshwater: $Hg\ 1,666 < Cd\ 4,225 < Zn\ 4,472 < Pb\ 6,391 < Cu\ 7,069$.
- On bigger fraction in freshwater: $Hg\ 1,307 < Zn\ 3,204 < Cd\ 5,343 < Pb\ 5,862 < Cu\ 8,181$.
- On smaller fraction in seawater: $Hg\ 1,063 < Pb\ 1,242 < Zn\ 2,046 < Cu\ 2,987 < Cd\ 3,332$.
- On bigger fraction in seawater: $Hg\ 1,236 < Cd\ 2,006 < Zn\ 2,239 < Cu\ 2,923 < Pb\ 3,328$.

As can be seen, Pb exhibited a high adsorbed amount (except for adsorption of smaller fraction in seawater). On the contrary, Hg had the smallest amount of all metals in all tested conditions, while Zn showed medium amount in all cases. The adsorbed amounts of Cu were high. Cd exhibited low to medium amounts, wih the exception of adsorption on smaller fraction in seawater. All metals can be ordered according to the maximal adsorbed amounts as follows: Hg < Cd < Zn < Pb < Cu.

In all cases, the effect of the higher ionic strength prevails over the effect of larger active surface area, hindering the adsorption process. Considering individual metals, their adsorbed amounts in different conditions ascend as follows:

- Pb: A in seawater < B in seawater < B in freshwater < A in freshwater,
- Hg: A in seawater < B in seawater < B in freshwater < A in freshwater,
- Zn: A in seawater < B in seawater < B in freshwater < A in freshwater,

- Cu: B in seawater < A in seawater < A in freshwater < B in freshwater,
- Cd: B in seawater < A in seawater < A in freshwater < B in freshwater.

4.2 FTIR analysis

Next to the the adsorption experiments, FTIR analysis was also performed. FTIR spectra of smaller and bigger fraction were firstly measured as blanks and are depicted in Figure 4.7, with smaller fraction having a significantly stronger signal. This is likely due to higher surface area to volume ratio of small fraction, leading to more efficient absorption and scattering of incident IR radiation.

PET particles with adsorbed heavy metals from fresh water adsorption experiments (both fractions) were subsequently measured. The spectra of Pb are depicted in Figure 4.8 for small and Figure 4.9 for big fraction. All other spectra can be found in Appendix C.

All spectra were zoomed to their fingerprint region ($1500 - 400\ cm^{-1}$) which is unique to each individual compound. This „fingerprint“ represents the overall molecular structure unlike the functional group region, and was therefore chosen to examine the spectra of inorganic heavy metals.

For all pairs, a difference of signals of small and big fraction was calculated and plotted as a green line. It can be seen that the differences in spectra for small fraction are quite minimal, while the differences of signals for big fraction are much more distinct. In most cases, the signal with adsorbed heavy metals was higer than in the case of pure microplastic particles. As can be seen, the most notable changes are in the areas between $1500 - 1400\ cm^{-1}$ and $450 - 400\ cm^{-1}$.

It can be seen that FTIR spectra correspond with the findings subsection 4.1.1, with big differences between the fractions in adsorption curves also showing big differences in FTIR signal with the corresponding fraction.

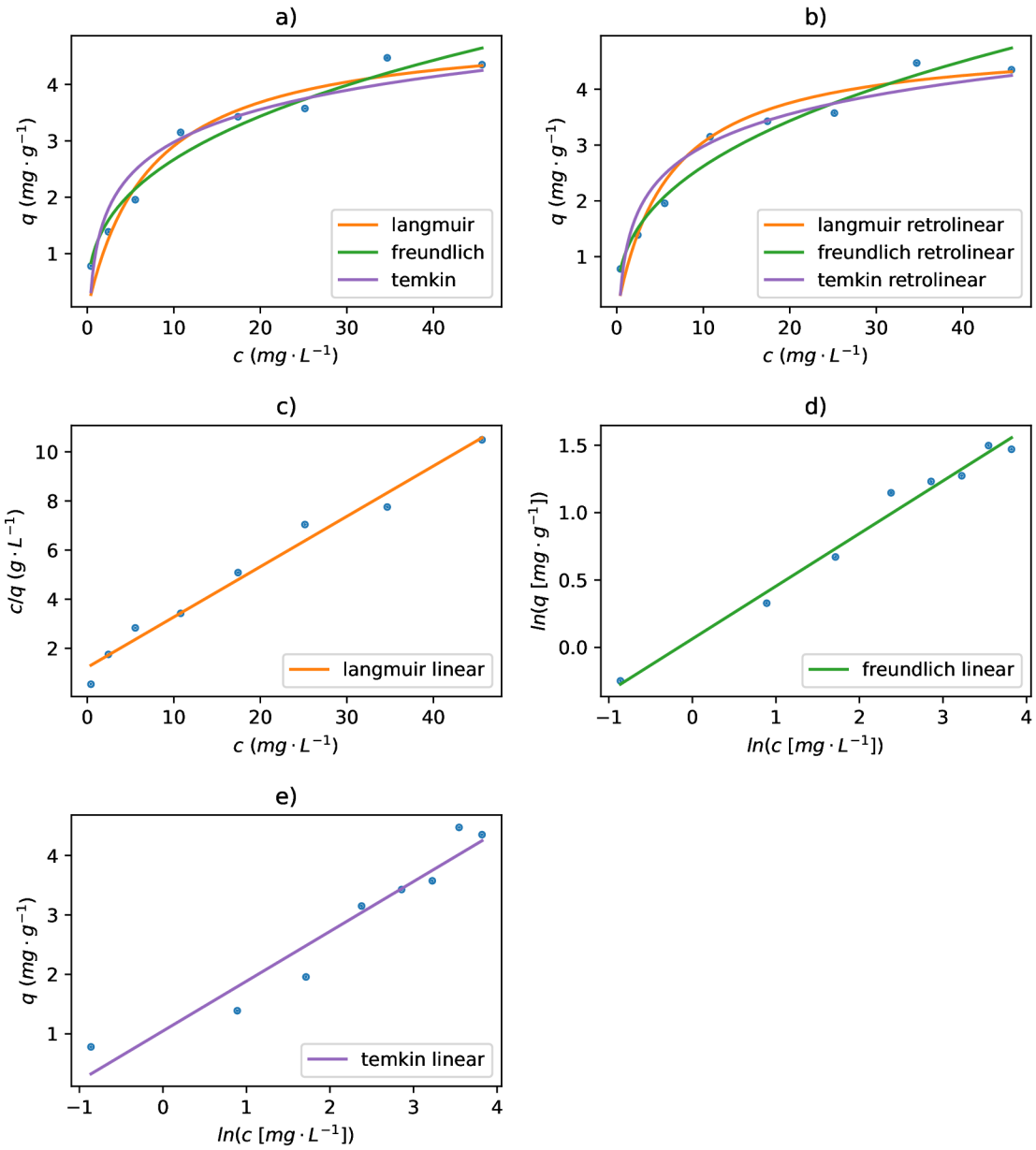

Figure 4.6: Adsorption isotherms and their linearised forms for adsorption of Zn on smaller fraction PET ($< 0,63\ \mu m$) in freshwater: a) adsorption isotherms constructed from non-linear fitting; b) adsorption isotherms constructed from linear fitting; c) Langmuir linear regression; d) Freundlich linear regression; e) Temkin linear regression.

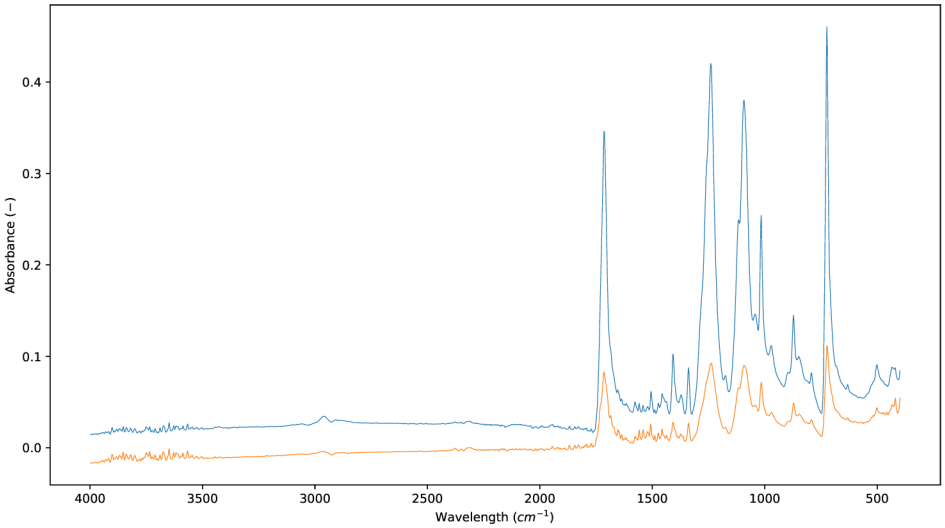

Figure 4.7: FTIR spectra of small fraction ($< 0,63\ \mu m$) - blue, and big fraction ($0,63\ \mu m - 1\ mm$) - orange - of PET.

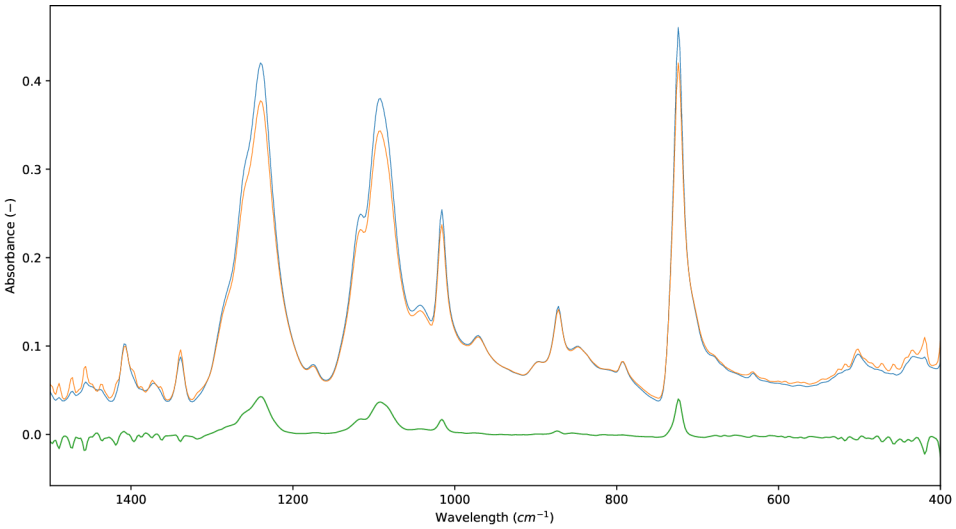

Figure 4.8: FTIR spectra of small fraction PET ($< 0,63\ \mu m$) - blue, small fraction PET with adsorbed Pb - orange, and visualized difference in adsorptions - green.

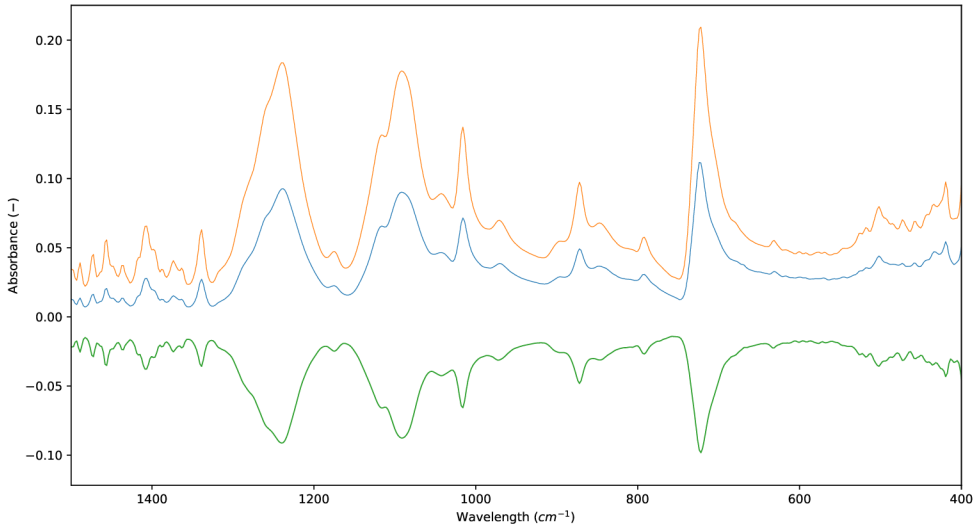

Figure 4.9: FTIR spectra of big fraction PET $(0,63\ \mu m - 1\ mm)$ - blue, big fraction PET with adsorbed Pb - orange, and visualized difference in adsorptions - green.

Chapter 5

Conclusion

Microplastics are a long-term, significant threat to the environment as well as organisms, and are nowadays ubiquitous in the environment. Among all environmental realms, the hydrosphere stands out as a primary reservoir for the majority of microplastics. Of particular concern is their capacity to adsorb toxic pollutants, including heavy metals, amplifying the risk they pose to ecosystems, which was explored further in this thesis.

Adsorption experiments were performed with 5 common heavy metals (Pb, Hg, Zn, Cu and Cd) and PET, a widespread polymer, with the use of atomic absorption spectrometry (AAS). Experiments were carried out in two laboratory prepared environments (fresh water and sea water), that aimed to stimulate real-world conditions. The polymer was used in two fractions - small fraction ($< 0,63\ \mu m$) and big fraction ($0,63\ \mu m - 1\ mm$) to illustrate impact of MP particles size on the adsorption process. These experiments were coupled with FTIR analysis (for fresh water) to further confirm the nature of ongoing processes.

The differences between small and big fraction varied among the metals, with no clear observable trend. This suggest that other factors than the size of the active surface of MPs, played more prominent role. With regards to the water conditions, increased ionic strength in sea water clearly hindered asorption process, which can be attributed to phenomena such as competition for adsorption sites, electrostatic repulsion, MPs aggregation and formation of complexes. All data have been fitted with Langmuir, Freundlich and Temkin adsorption isotherms lineary and non-lineary, with latter yielding better results. The determined preferred adsorption models vary - Zn follows the Freundlich adsorption model the most, Hg and Cd follow the Langmuir adsorption model, while Pb and Cu yield best results with Temkin adsorption model. Considering the maximal adsorbed amounts (and therefore, the adsorption capacity of PET for the given metal), metals can be ordered as follows: Hg $<$ Cd $<$ Zn $<$ Pb $<$ Cu. FTIR spectra correspond with the findings from the adsorption experiments, with differences between the fractions in adsorption curves corresponding to the differences in FTIR signal. The most notable changes can be observed in the areas between $1500 - 1400\ cm^{-1}$ and $450 - 400\ cm^{-1}$.

While the sorption of hydrophobic organic pollutants in aquatic environments is well-documented, the sorption of heavy metals remains poorly understood. The differences in adsoprtion processes for varying ionic strenght conditions demonstrate the importance of further research on the adsorption of heavy metals on microplastics with regard to the environmental conditions they occur in real life. This means considering the factors such

as environment and MPs condition, studying the HMs adsorption on MPs with regard to other entities present in the aquatic environment, such as other contaminants (i.e., organic pollutants), microorganisms and organic matter, among others, and using real, collected weathered microplastics, as those tend to have higher adsorption capacities. In some of the experiments, the adsorption curves have not fully reached the plateau stage yet, indicating higher concentrations might be needed in future experiments.

Bibliography

[1] Limit of detection. 3.0.1th ed. 2019. DOI: doi:10.1351/goldbook.L03540. Available at: https://doi.org/10.1351/goldbook.L03540.

[2] Microplastics with adsorbed contaminants: Mechanisms and Treatment. *Environmental Challenges*. 2021, vol. 3, p. 100042. DOI: https://doi.org/10.1016/j.envc.2021.100042. ISSN 2667-0100. Available at: https://www.sciencedirect.com/science/article/pii/S2667010021000214.

[3] Amobonye, A., Bhagwat, P., Raveendran, S., Singh, S. and Pillai, S. Environmental impacts of microplastics and nanoplastics. *Frontiers in Microbiology*. november 2021, vol. 12. DOI: 10.3389/fmicb.2021.768297.

[4] An, Q., Zhou, T., Wen, C. and Yan, C. The effects of microplastics on heavy metals bioavailability in soils: a meta-analysis. *Journal of Hazardous Materials*. 2023, vol. 460, p. 132369. DOI: https://doi.org/10.1016/j.jhazmat.2023.132369. ISSN 0304-3894. Available at: https://www.sciencedirect.com/science/article/pii/S0304389423016527.

[5] Artioli, Y. Adsorption. In: Jørgensen, S. E. and Fath, B. D., ed. *Encyclopedia of Ecology*. Oxford: Academic Press, 2008, p. 60–65. DOI: https://doi.org/10.1016/B978-008045405-4.00252-4. ISBN 978-0-08-045405-4. Available at: https://www.sciencedirect.com/science/article/pii/B9780080454054002524.

[6] Balali Mood, M., Naseri, K., Tahergorabi, Z., Khazdair, M. R. and Sadeghi, M. Toxic Mechanisms of Five Heavy Metals: Mercury, Lead, Chromium, Cadmium, and Arsenic. *Frontiers in Pharmacology*. 2021, vol. 12. DOI: 10.3389/fphar.2021.643972. ISSN 1663-9812. Available at: https://www.frontiersin.org/articles/10.3389/fphar.2021.643972.

[7] Bartkowiak, A. Influence of Heavy Metals on Quality of Raw Materials, Animal Products, and Human and Animal Health Status. In: Saleh, H. M. and Hassan, A. I., ed. *Environmental Impact and Remediation of Heavy Metals*. Rijeka: IntechOpen, 2022, chap. 3. DOI: 10.5772/intechopen.102497. Available at: https://doi.org/10.5772/intechopen.102497.

[8] Beaman, J., Bergeron, C., Benson, R., Cook, A.-M., Gallagher, K. et al. State of the Science White Paper: A Summary of Literature on the Chemical Toxicity of Plastics Pollution to Aquatic Life and Aquatic-Dependent Wildlife. *U.S.*

Environmental Protection Agency, Office of Water, Office of Science and Technology, Health and Ecological Criteria Division. december 2016.

[9] Brennecke, D., Duarte, B., Paiva, F., Caçador, I. and Canning Clode, J. Microplastics as vector for heavy metal contamination from the marine environment. *Estuarine, Coastal and Shelf Science*. 2016, vol. 178, p. 189–195. DOI: https://doi.org/10.1016/j.ecss.2015.12.003. ISSN 0272-7714. Available at: https://www.sciencedirect.com/science/article/pii/S027277141530158X.

[10] Bretnall, A. E. and Clarke, G. S. 11 - Validation of Analytical Test Methods. In: Ahuja, S. and Scypinski, S., ed. *Handbook of Modern Pharmaceutical Analysis*. Academic Press, 2011, vol. 10, p. 429–457. Separation Science and Technology. DOI: https://doi.org/10.1016/B978-0-12-375680-0.00011-5. ISSN 1877-1718. Available at: https://www.sciencedirect.com/science/article/pii/B9780123756800000115.

[11] Briffa, J., Sinagra, E. and Blundell, R. Heavy metal pollution in the environment and their toxicological effects on humans. *Heliyon*. 2020, vol. 6, no. 9, p. e04691. DOI: https://doi.org/10.1016/j.heliyon.2020.e04691. ISSN 2405-8440. Available at: https://www.sciencedirect.com/science/article/pii/S2405844020315346.

[12] C. Gerente, P. L. C. and McKay, G. Application of Chitosan for the Removal of Metals From Wastewaters by Adsorption—Mechanisms and Models Review. *Critical Reviews in Environmental Science and Technology*. Taylor & Francis. 2007, vol. 37, no. 1, p. 41–127. DOI: 10.1080/10643380600729089. Available at: https://doi.org/10.1080/10643380600729089.

[13] Campanale, C., Massarelli, C., Savino, I., Locaputo, V. and Uricchio, V. A Detailed Review Study on Potential Effects of Microplastics and Additives of Concern on Human Health. *International journal of environmental research and public health*. february 2020, vol. 17. DOI: 10.3390/ijerph17041212.

[14] Cao, Y., Zhao, M., Ma, X., Song, Y., Zuo, S. et al. A critical review on the interactions of microplastics with heavy metals: Mechanism and their combined effect on organisms and humans. *Science of The Total Environment*. 2021, vol. 788, p. 147620. DOI: https://doi.org/10.1016/j.scitotenv.2021.147620. ISSN 0048-9697. Available at: https://www.sciencedirect.com/science/article/pii/S0048969721026917.

[15] Chekkala, A., Mohapatra, S. and Tyagi, V. Microplastics in aquatic environment: Challenges and perspectives. *Chemosphere*. june 2021, vol. 282, p. 131151. DOI: 10.1016/j.chemosphere.2021.131151.

[16] Crawford, C. B. and Quinn, B. 4 - Physiochemical properties and degradation. In: Crawford, C. B. and Quinn, B., ed. *Microplastic Pollutants*. Elsevier, 2017, p. 57–100. DOI: https://doi.org/10.1016/B978-0-12-809406-8.00004-9. ISBN 978-0-12-809406-8. Available at: https://www.sciencedirect.com/science/article/pii/B9780128094068000049.

[17] Duis, K. and Coors, A. Microplastics in the aquatic and terrestrial environment: sources (with a specific focus on personal care products), fate and effects.

Environmental Sciences Europe. january 2016, vol. 28. DOI: 10.1186/s12302-015-0069-y.

[18] Dąbrowski, A. Adsorption — from theory to practice. *Advances in Colloid and Interface Science*. 2001, vol. 93, no. 1, p. 135–224. DOI: https://doi.org/10.1016/S0001-8686(00)00082-8. ISSN 0001-8686. Available at: https://www.sciencedirect.com/science/article/pii/S0001868600000828.

[19] Fu, L., Li, J., Wang, G., Luan, Y. and Dai, W. Adsorption behavior of organic pollutants on microplastics. *Ecotoxicology and Environmental Safety*. 2021, vol. 217, p. 112207. DOI: https://doi.org/10.1016/j.ecoenv.2021.112207. ISSN 0147-6513. Available at: https://www.sciencedirect.com/science/article/pii/S0147651321003183.

[20] Fu, Q., Tan, X., Ye, S., Ma, L., Gu, Y. et al. Mechanism analysis of heavy metal lead captured by natural-aged microplastics. *Chemosphere*. 2021, vol. 270, p. 128624. DOI: https://doi.org/10.1016/j.chemosphere.2020.128624. ISSN 0045-6535. Available at: https://www.sciencedirect.com/science/article/pii/S0045653520328198.

[21] Gao, F., Li, J., Sun, C., Zhang, L., Jiang, F. et al. Study on the capability and characteristics of heavy metals enriched on microplastics in marine environment. *Marine Pollution Bulletin*. 2019, vol. 144, p. 61–67. DOI: https://doi.org/10.1016/j.marpolbul.2019.04.039. ISSN 0025-326X. Available at: https://www.sciencedirect.com/science/article/pii/S0025326X19303005.

[22] Gao, X., Hassan, I., Peng, Y., Huo, S. and Ling, L. Behaviors and influencing factors of the heavy metals adsorption onto microplastics: A review. *Journal of Cleaner Production*. 2021, vol. 319, p. 128777. DOI: https://doi.org/10.1016/j.jclepro.2021.128777. ISSN 0959-6526. Available at: https://www.sciencedirect.com/science/article/pii/S0959652621029759.

[23] Hale, R. C., Seeley, M. E., Guardia, M. J. L., Mai, L. and Zeng, E. Y. A Global Perspective on Microplastics. *JGR Oceans*. 2020, vol. 125. DOI: https://doi.org/10.1029/2018JC014719. Available at: https://agupubs.onlinelibrary.wiley.com/doi/full/10.1029/2018JC014719.

[24] Han, R., Zhou, B., Huang, Y., Lu, X., Li, S. et al. Bibliometric overview of research trends on heavy metal health risks and impacts in 1989–2018. *Journal of Cleaner Production*. 2020, vol. 276, p. 123249. DOI: https://doi.org/10.1016/j.jclepro.2020.123249. ISSN 0959-6526. Available at: https://www.sciencedirect.com/science/article/pii/S0959652620332947.

[25] Hildebrandt, L., Au, M., Zimmermann, T., Ebeling, A., Ludwig, J. et al. A metrologically traceable protocol for the quantification of trace metals in different types of microplastic. *PLOS ONE*. july 2020, vol. 15, p. e0236120. DOI: 10.1371/journal.pone.0236120.

[26] Holmes, L. A., Turner, A. and Thompson, R. C. Adsorption of trace metals to plastic resin pellets in the marine environment. *Environmental Pollution*. 2012, vol. 160, p. 42–48. DOI: https://doi.org/10.1016/j.envpol.2011.08.052. ISSN 0269-7491. Available at: https://www.sciencedirect.com/science/article/pii/S0269749111005057.

[27] Holmes, L. A., Turner, A. and Thompson, R. C. Interactions between trace metals and plastic production pellets under estuarine conditions. *Marine Chemistry*. 2014, vol. 167, p. 25–32. DOI: https://doi.org/10.1016/j.marchem.2014.06.001. ISSN 0304-4203. Estuarine Biogeochemistry. Available at: https://www.sciencedirect.com/science/article/pii/S0304420314001017.

[28] Hui Qiu, B.-c. P. Q.-j. Z. W.-m. Z. . Q.-x. Z. Critical review in adsorption kinetic models. *Journal of Zhejiang University-SCIENCE A*. 2009, vol. 10, p. 716–724. DOI: https://doi.org/10.1631/jzus.A0820524. Available at: https://link.springer.com/article/10.1631/jzus.A0820524.

[29] Ivleva, N. P., Wiesheu, A. C. and Niessner, R. Microplastic in Aquatic Ecosystems. *Angewandte Chemie International Edition*. 2017, vol. 56, no. 7, p. 1720–1739. DOI: https://doi.org/10.1002/anie.201606957. Available at: https://onlinelibrary.wiley.com/doi/abs/10.1002/anie.201606957.

[30] Khalef, R. N., Hassan, A. I. and Saleh, H. M. Heavy Metal's Environmental Impact. In: Saleh, H. M. and Hassan, A. I., ed. *Environmental Impact and Remediation of Heavy Metals*. Rijeka: IntechOpen, 2022, chap. 1. DOI: 10.5772/intechopen.103907. Available at: https://doi.org/10.5772/intechopen.103907.

[31] Khalid, N., Aqeel, M., Noman, A., Khan, S. M. and Akhter, N. Interactions and effects of microplastics with heavy metals in aquatic and terrestrial environments. *Environmental Pollution*. 2021, vol. 290, p. 118104. DOI: https://doi.org/10.1016/j.envpol.2021.118104. ISSN 0269-7491. Available at: https://www.sciencedirect.com/science/article/pii/S0269749121016869.

[32] Kiran, Bharti, R. and Sharma, R. Effect of heavy metals: An overview. *Materials Today: Proceedings*. 2022, vol. 51, p. 880–885. DOI: https://doi.org/10.1016/j.matpr.2021.06.278. ISSN 2214-7853. CMAE'21. Available at: https://www.sciencedirect.com/science/article/pii/S221478532104668X.

[33] Kumar, R., Ivy, N., Bhattacharya, S., Dey, A. and Sharma, P. Coupled effects of microplastics and heavy metals on plants: Uptake, bioaccumulation, and environmental health perspectives. *Science of The Total Environment*. 2022, vol. 836, p. 155619. DOI: https://doi.org/10.1016/j.scitotenv.2022.155619. ISSN 0048-9697. Available at: https://www.sciencedirect.com/science/article/pii/S0048969722027152.

[34] Kutralam Muniasamy, G., Pérez Guevara, F., Martínez, I. E. and Shruti, V. Overview of microplastics pollution with heavy metals: Analytical methods, occurrence, transfer risks and call for standardization. *Journal of Hazardous Materials*. 2021, vol. 415, p. 125755. DOI: https://doi.org/10.1016/j.jhazmat.2021.125755. ISSN 0304-3894. Available at: https://www.sciencedirect.com/science/article/pii/S0304389421007196.

[35] Li, W., Lo, H.-S., Wong, H.-M., Zhou, M., Wong, C.-Y. et al. Heavy metals contamination of sedimentary microplastics in Hong Kong. *Marine Pollution Bulletin*. 2020, vol. 153, p. 110977. DOI: https://doi.org/10.1016/j.marpolbul.2020.110977. ISSN 0025-326X. Available at: https://www.sciencedirect.com/science/article/pii/S0025326X20300953.

[36] Liu, G., Dave, P. H., Kwong, R. W. M., Wu, M. and Zhong, H. Influence of Microplastics on the Mobility, Bioavailability, and Toxicity of Heavy Metals: A Review. *Bulletin of Environmental Contamination and Toxicology*. 2021, vol. 107, p. 710–721. DOI: https://doi.org/10.1007/s00128-021-03339-9. Available at: https://link.springer.com/article/10.1007/s00128-021-03339-9.

[37] Liu, S., Huang, J., Zhang, W., Shi, L., Yi, K. et al. Microplastics as a vehicle of heavy metals in aquatic environments: A review of adsorption factors, mechanisms, and biological effects. *Journal of Environmental Management*. 2022, vol. 302, p. 113995. DOI: https://doi.org/10.1016/j.jenvman.2021.113995. ISSN 0301-4797. Available at: https://www.sciencedirect.com/science/article/pii/S0301479721020570.

[38] Liu, S., Shi, J., Wang, J., Dai, Y., Li, H. et al. Interactions Between Microplastics and Heavy Metals in Aquatic Environments: A Review. *Frontiers in Microbiology*. 2021, vol. 12. DOI: 10.3389/fmicb.2021.652520. ISSN 1664-302X. Available at: https://www.frontiersin.org/journals/microbiology/articles/10.3389/fmicb.2021.652520.

[39] Liu, Y., Zhang, K., Xu, S., Yan, M., Tao, D. et al. Heavy metals in the "plastisphere" of marine microplastics: adsorption mechanisms and composite risk. *Gondwana Research*. 2022, vol. 108, p. 171–180. DOI: https://doi.org/10.1016/j.gr.2021.06.017. ISSN 1342-937X. Plastisphere and its impact on Earth's environment and life. Available at: https://www.sciencedirect.com/science/article/pii/S1342937X21001982.

[40] Mao, R., Lang, M., Yu, X., Wu, R., Yang, X. et al. Aging mechanism of microplastics with UV irradiation and its effects on the adsorption of heavy metals. *Journal of Hazardous Materials*. 2020, vol. 393, p. 122515. DOI: https://doi.org/10.1016/j.jhazmat.2020.122515. ISSN 0304-3894. Available at: https://www.sciencedirect.com/science/article/pii/S0304389420305045.

[41] Mitra, S., Chakraborty, A. J., Tareq, A. M., Emran, T. B., Nainu, F. et al. Impact of heavy metals on the environment and human health: Novel therapeutic insights to counter the toxicity. *Journal of King Saud University - Science*. 2022, vol. 34, no. 3, p. 101865. DOI: https://doi.org/10.1016/j.jksus.2022.101865. ISSN 1018-3647. Available at: https://www.sciencedirect.com/science/article/pii/S1018364722000465.

[42] Naqash, N., Prakash, S., Kapoor, D. and Singh, R. Interaction of freshwater microplastics with biota and heavy metals: a review. *Environmental Chemistry Letters*. 2020, vol. 18, p. 1813–1824. DOI: https://doi.org/10.1007/s10311-020-01044-3. Available at: https://link.springer.com/article/10.1007/s10311-020-01044-3.

[43] Nerland, I. L., Halsband, C., Allan, I. J. and Thomas, K. V. Microplastics in marine environments: Occurrence, distribution and effects. In:. 2014. Available at: https://api.semanticscholar.org/CorpusID:132310485.

[44] Nisticò, R. Polyethylene terephthalate (PET) in the packaging industry. *Polymer Testing*. 2020, vol. 90, p. 106707. DOI:

https://doi.org/10.1016/j.polymertesting.2020.106707. ISSN 0142-9418. Available at: https://www.sciencedirect.com/science/article/pii/S0142941820310333.

[45] Piccin, J., Dotto, G. and PINTO, L. Adsorption isotherms and thermochemical data of FDandC RED N° 40 Binding by chitosan. *Brazilian Journal of Chemical Engineering*. june 2011, vol. 28, p. 295–304. DOI: 10.1590/S0104-66322011000200014.

[46] Ratner, B. 9.21 - Polymeric Implants. In: Matyjaszewski, K. and Möller, M., ed. *Polymer Science: A Comprehensive Reference*. Amsterdam: Elsevier, 2012, p. 397–411. DOI: https://doi.org/10.1016/B978-0-444-53349-4.00230-2. ISBN 978-0-08-087862-1. Available at: https://www.sciencedirect.com/science/article/pii/B9780444533494002302.

[47] Rochman, C., Hentschel, B. and Teh, S. Long-Term Sorption of Metals Is Similar among Plastic Types: Implications for Plastic Debris in Aquatic Environments. *PloS one*. january 2014, vol. 9, p. e85433. DOI: 10.1371/journal.pone.0085433.

[48] Sun, Y., Yuan, J., Zhou, T., Zhao, Y., Yu, F. et al. Laboratory simulation of microplastics weathering and its adsorption behaviors in an aqueous environment: A systematic review. *Environmental Pollution*. 2020, vol. 265, p. 114864. DOI: https://doi.org/10.1016/j.envpol.2020.114864. ISSN 0269-7491. Available at: https://www.sciencedirect.com/science/article/pii/S0269749119365765.

[49] Tchounwou, P., Yedjou, C., Patlolla, A. and Sutton, D. Heavy Metal Toxicity and the Environment. *EXS*. september 2012, vol. 101, p. 133–64. DOI: 10.1007/978-3-7643-8340-4_6.

[50] Tursi, A., Baratta, M., Easton, T., Chatzisymeon, E., Chidichimo, F. et al. Microplastics in aquatic systems, a comprehensive review: origination, accumulation, impact, and removal technologies. *RSC Advances*. october 2022, vol. 12, p. 28318. DOI: 10.1039/d2ra04713f.

[51] Ungureanu, E. L. and Mustatea, G. Toxicity of Heavy Metals. In: Saleh, H. M. and Hassan, A. I., ed. *Environmental Impact and Remediation of Heavy Metals*. Rijeka: IntechOpen, 2022, chap. 2. DOI: 10.5772/intechopen.102441. Available at: https://doi.org/10.5772/intechopen.102441.

[52] Uy, E. E. S., Adajar, M. A. Q. and Dungca, J. R. VOLUME CHANGE BEHAVIOR OF SEA WATER EXPOSED COAL ASH USING HYPERBOLIC MODEL. *GEOMATE Journal*. Jun. 2019, vol. 16, no. 58, p. 97–103. Available at: https://geomatejournal.com/geomate/article/view/2718.

[53] Vieira, Y., Lima, E. C., Foletto, E. L. and Dotto, G. L. Microplastics physicochemical properties, specific adsorption modeling and their interaction with pharmaceuticals and other emerging contaminants. *Science of The Total Environment*. 2021, vol. 753, p. 141981. DOI: https://doi.org/10.1016/j.scitotenv.2020.141981. ISSN 0048-9697. Available at: https://www.sciencedirect.com/science/article/pii/S0048969720355108.

[54] Wang, J., Peng, J., Tan, Z., Gao, Y., Zhan, Z. et al. Microplastics in the surface sediments from the Beijiang River littoral zone: Composition, abundance, surface textures and interaction with heavy metals. *Chemosphere*. 2017, vol. 171, p. 248–258.

DOI: https://doi.org/10.1016/j.chemosphere.2016.12.074. ISSN 0045-6535. Available at: https://www.sciencedirect.com/science/article/pii/S0045653516318069.

[55] Xu, S., Ma, J., Ji, R., Pan, K. and Miao, A.-J. Microplastics in aquatic environments: Occurrence, accumulation, and biological effects. *Science of The Total Environment*. 2020, vol. 703, p. 134699. DOI: https://doi.org/10.1016/j.scitotenv.2019.134699. ISSN 0048-9697. Available at: https://www.sciencedirect.com/science/article/pii/S004896971934690X.

[56] Yu, F., Yang, C., Zhu, Z., Bai, X. and Ma, J. Adsorption behavior of organic pollutants and metals on micro/nanoplastics in the aquatic environment. *Science of The Total Environment*. 2019, vol. 694, p. 133643. DOI: https://doi.org/10.1016/j.scitotenv.2019.133643. ISSN 0048-9697. Available at: https://www.sciencedirect.com/science/article/pii/S0048969719335685.

[57] Yu, H., Zhang, Z., Zhang, Y., Fan, P., Xi, B. et al. Metal type and aggregate microenvironment govern the response sequence of speciation transformation of different heavy metals to microplastics in soil. *Science of The Total Environment*. 2021, vol. 752, p. 141956. DOI: https://doi.org/10.1016/j.scitotenv.2020.141956. ISSN 0048-9697. Available at: https://www.sciencedirect.com/science/article/pii/S0048969720354851.

[58] Yuan, W., Zhou, Y., Chen, Y., Liu, X. and Wang, J. Toxicological effects of microplastics and heavy metals on the Daphnia magna. *Science of The Total Environment*. 2020, vol. 746, p. 141254. DOI: https://doi.org/10.1016/j.scitotenv.2020.141254. ISSN 0048-9697. Available at: https://www.sciencedirect.com/science/article/pii/S0048969720347835.

[59] Zhao, M., Huang, L., Arulmani, S. R. B., Yan, J., Wu, L. et al. Adsorption of Different Pollutants by Using Microplastic with Different Influencing Factors and Mechanisms in Wastewater: A Review. *Nanomaterials*. 2022, vol. 12, no. 13. DOI: 10.3390/nano12132256. ISSN 2079-4991. Available at: https://www.mdpi.com/2079-4991/12/13/2256.

[60] Zhou, Y., Liu, X. and Wang, J. Characterization of microplastics and the association of heavy metals with microplastics in suburban soil of central China. *Science of The Total Environment*. 2019, vol. 694, p. 133798. DOI: https://doi.org/10.1016/j.scitotenv.2019.133798. ISSN 0048-9697. Available at: https://www.sciencedirect.com/science/article/pii/S0048969719337398.

Appendix A

Isotherms fitting

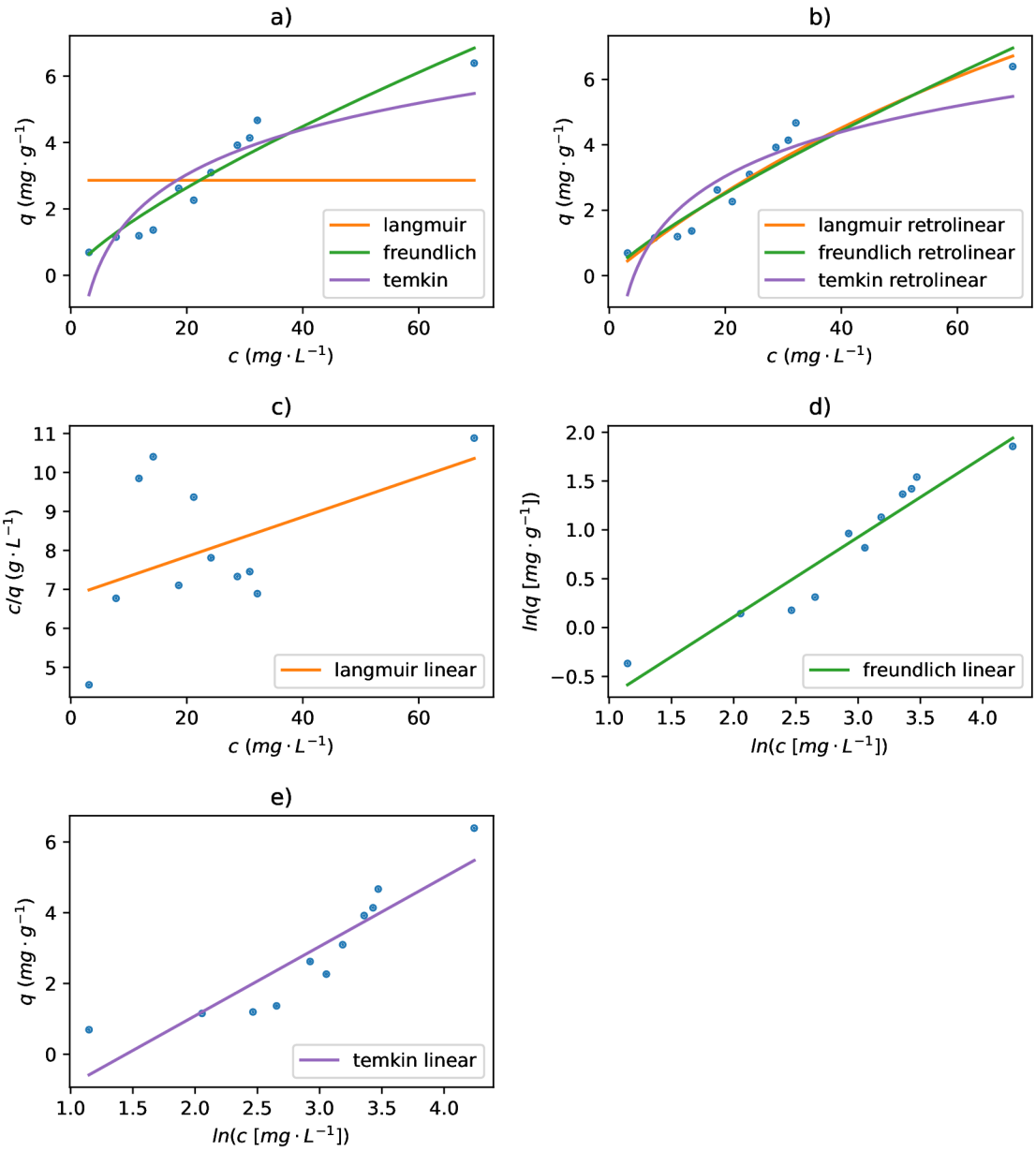

Figure A.1: Adsorption isotherms and their linearised forms for adsorption of Pb on smaller fraction PET ($< 0,63\ \mu m$) in freshwater: a) adsorption isotherms constructed from non-linear fitting; b) adsorption isotherms constructed from linear fitting; c) Langmuir linear regression; d) Freundlich linear regression; e) Temkin linear regression.

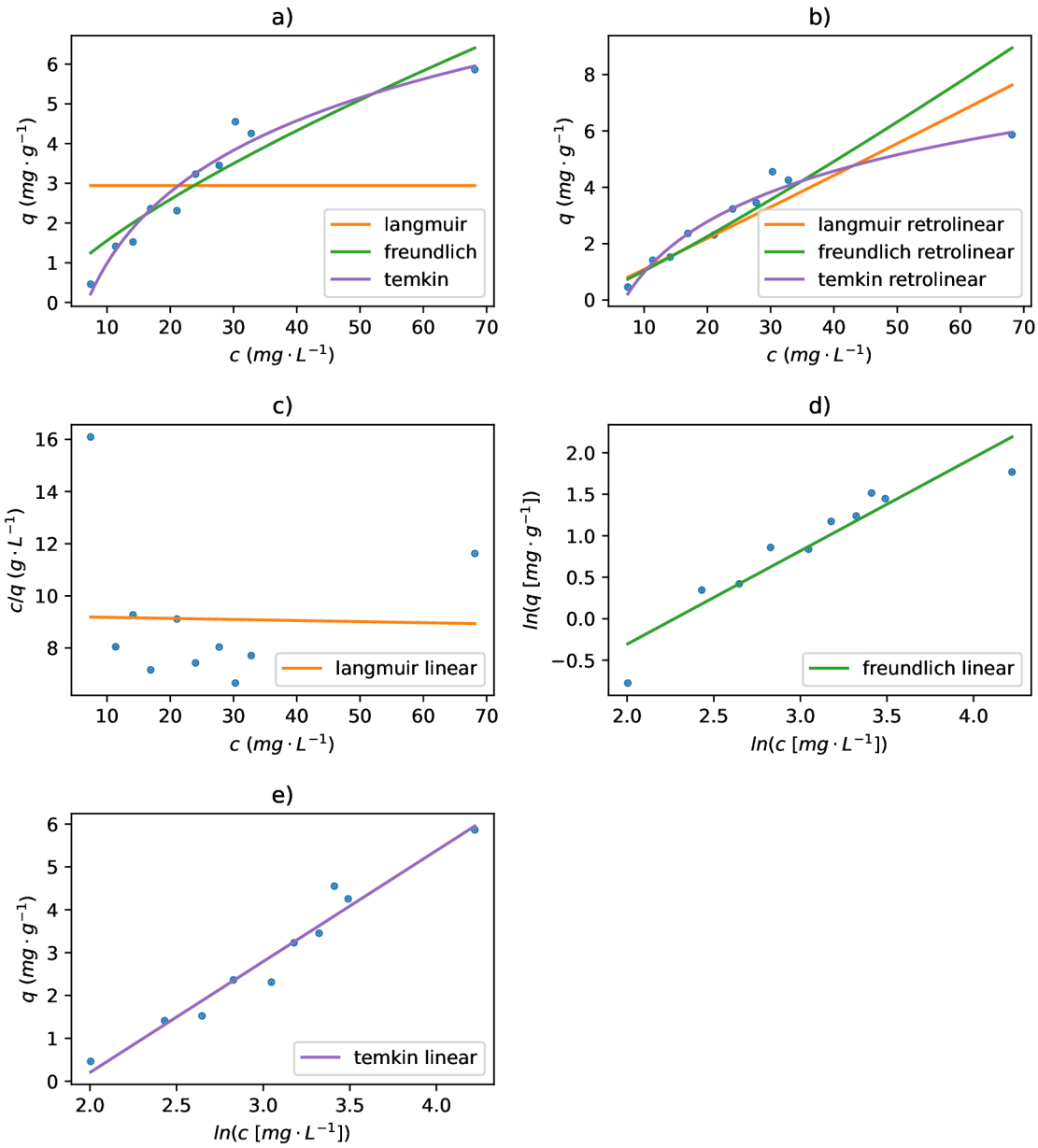

Figure A.2: Adsorption isotherms and their linearised forms for adsorption of Pb on bigger fraction PET ($0,63\ \mu m - 1\ mm$) in freshwater: a) adsorption isotherms constructed from non-linear fitting; b) adsorption isotherms constructed from linear fitting; c) Langmuir linear regression; d) Freundlich linear regression; e) Temkin linear regression.

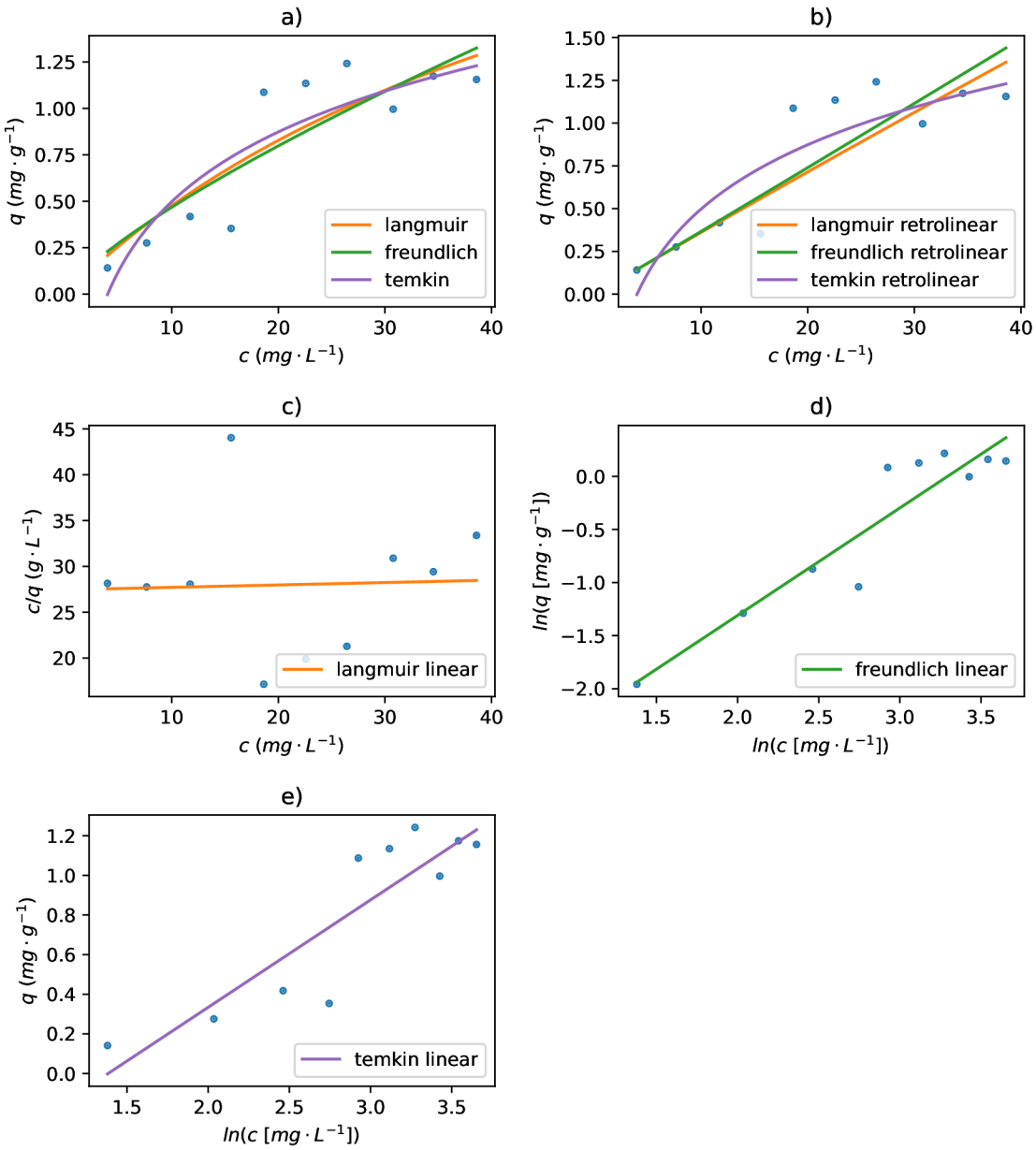

Figure A.3: Adsorption isotherms and their linearised forms for adsorption of Pb on smaller fraction PET ($< \ 0,63 \ \mu m$) in seawater: a) adsorption isotherms constructed from non-linear fitting; b) adsorption isotherms constructed from linear fitting; c) Langmuir linear regression; d) Freundlich linear regression; e) Temkin linear regression.

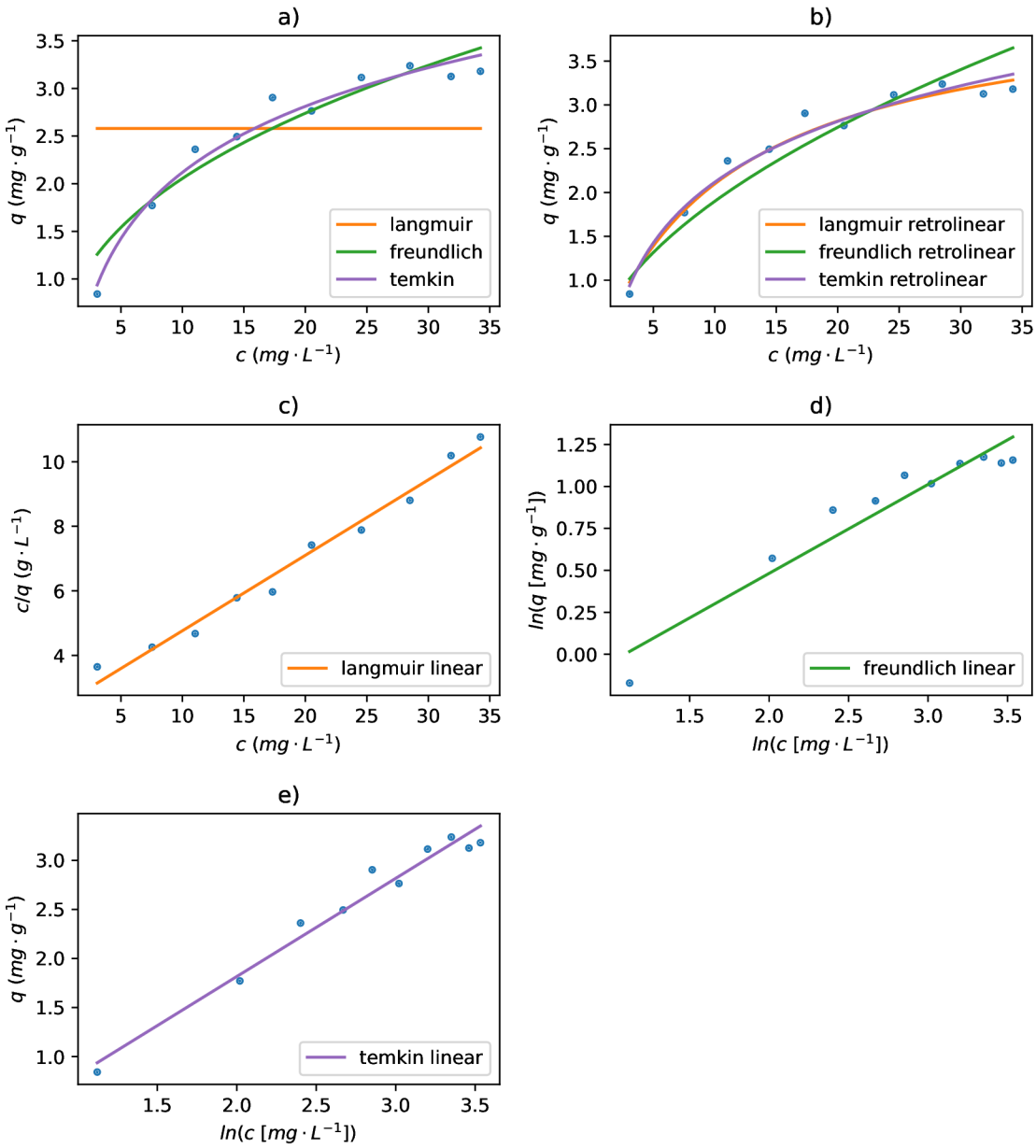

Figure A.4: Adsorption isotherms and their linearised forms for adsorption of Pb on bigger fraction PET ($0,63\ \mu m - 1\ mm$) in seawater: a) adsorption isotherms constructed from non-linear fitting; b) adsorption isotherms constructed from linear fitting; c) Langmuir linear regression; d) Freundlich linear regression; e) Temkin linear regression.

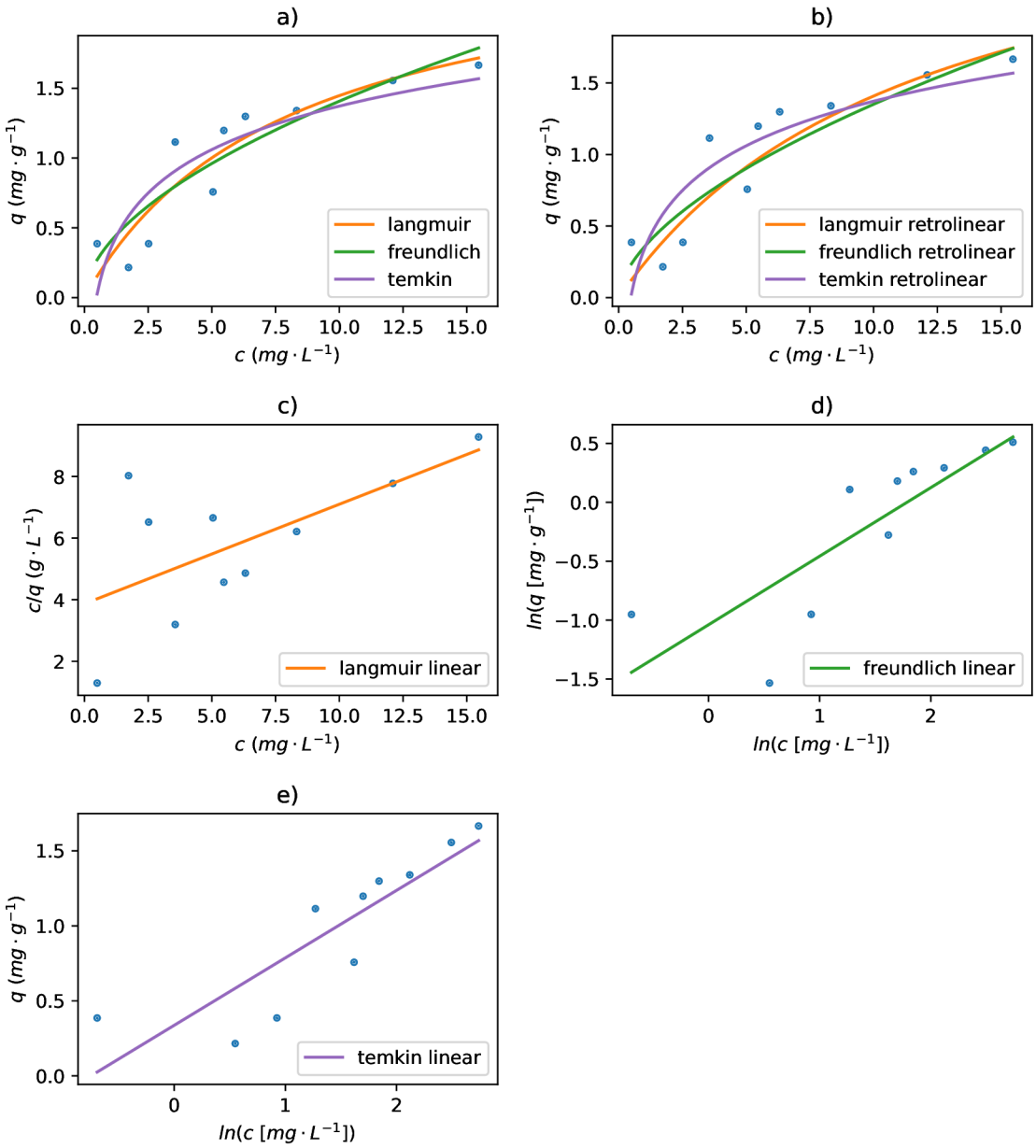

Figure A.5: Adsorption isotherms and their linearised forms for adsorption of Hg on smaller fraction PET ($< \ 0,63 \ \mu m$) in freshwater: a) adsorption isotherms constructed from non-linear fitting; b) adsorption isotherms constructed from linear fitting; c) Langmuir linear regression; d) Freundlich linear regression; e) Temkin linear regression.

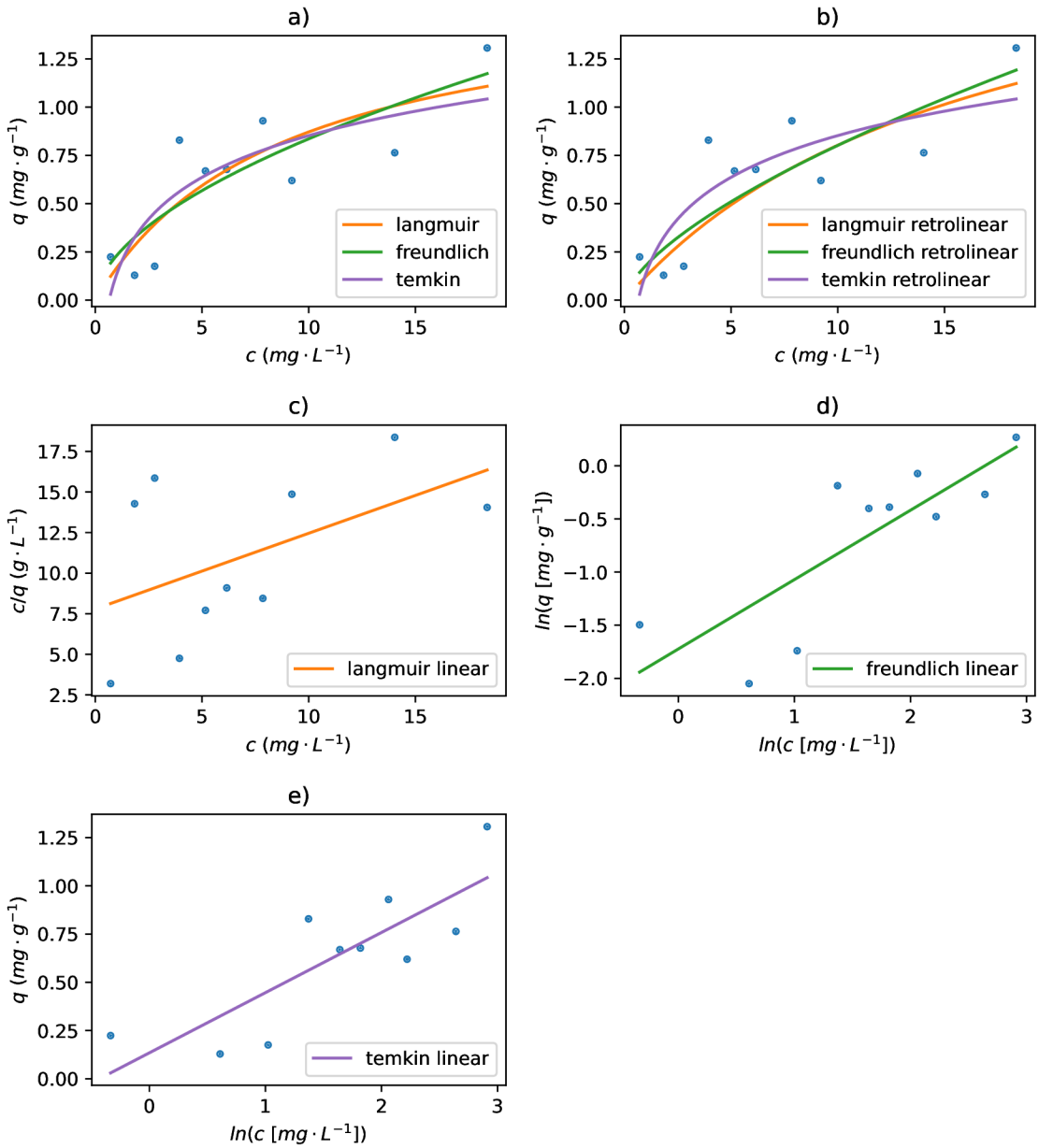

Figure A.6: Adsorption isotherms and their linearised forms for adsorption of Hg on bigger fraction PET ($0,63\ \mu m - 1\ mm$) in freshwater: a) adsorption isotherms constructed from non-linear fitting; b) adsorption isotherms constructed from linear fitting; c) Langmuir linear regression; d) Freundlich linear regression; e) Temkin linear regression.

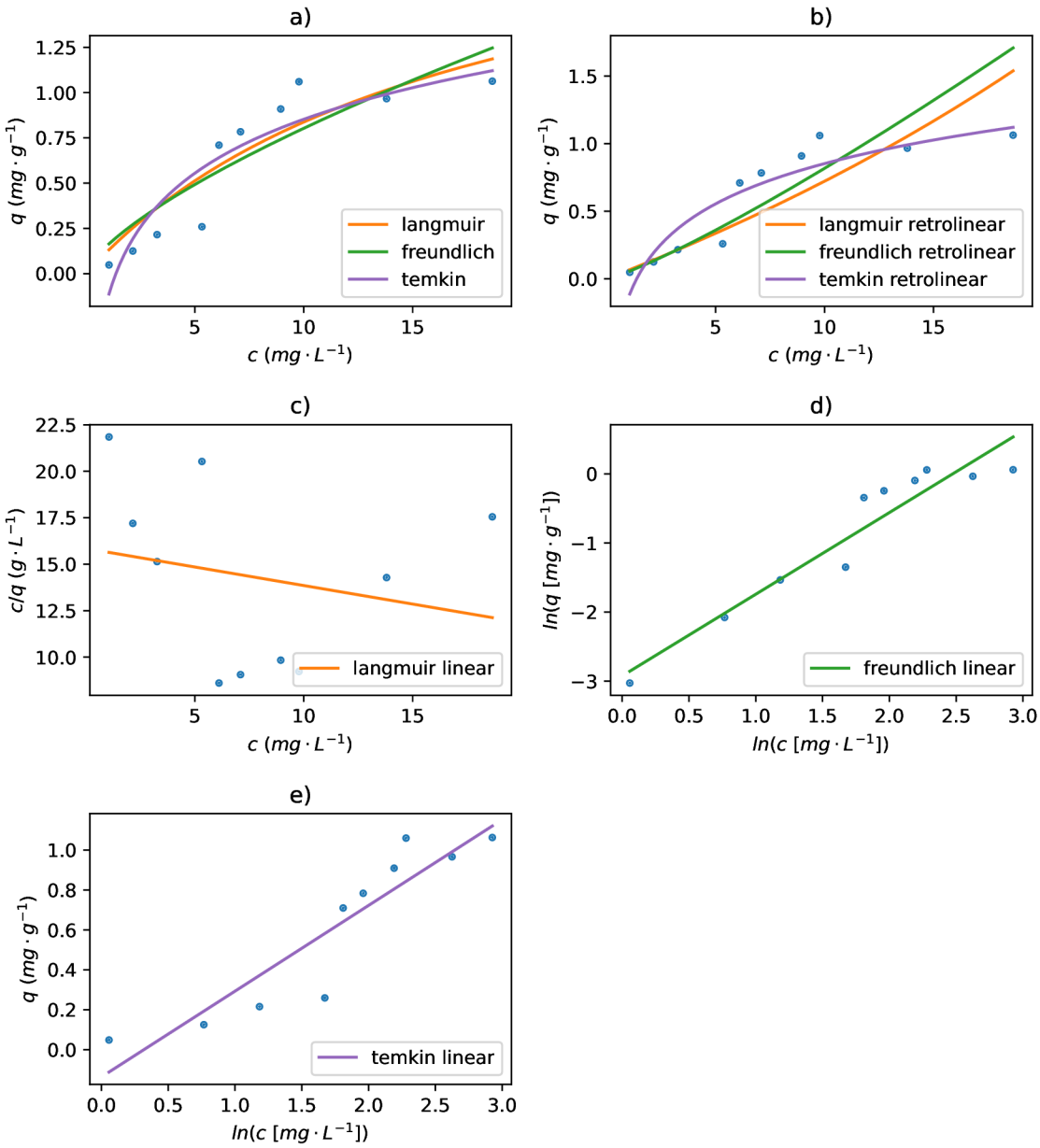

Figure A.7: Adsorption isotherms and their linearised forms for adsorption of Hg on smaller fraction PET ($< \ 0,63 \ \mu m$) in seawater: a) adsorption isotherms constructed from non-linear fitting; b) adsorption isotherms constructed from linear fitting; c) Langmuir linear regression; d) Freundlich linear regression; e) Temkin linear regression.

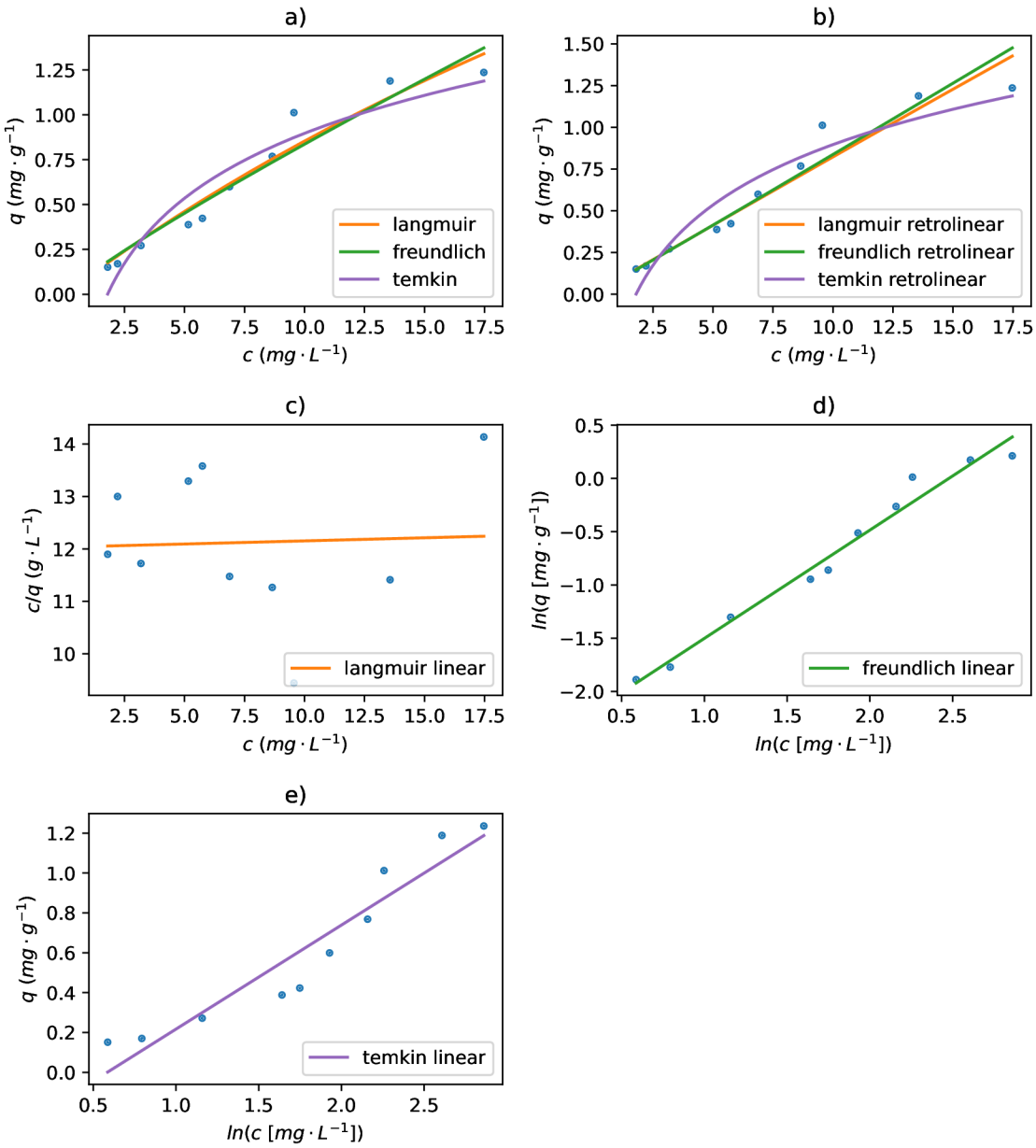

Figure A.8: Adsorption isotherms and their linearised forms for adsorption of Hg on bigger fraction PET ($0,63\ \mu m - 1\ mm$) in seawater: a) adsorption isotherms constructed from non-linear fitting; b) adsorption isotherms constructed from linear fitting; c) Langmuir linear regression; d) Freundlich linear regression; e) Temkin linear regression.

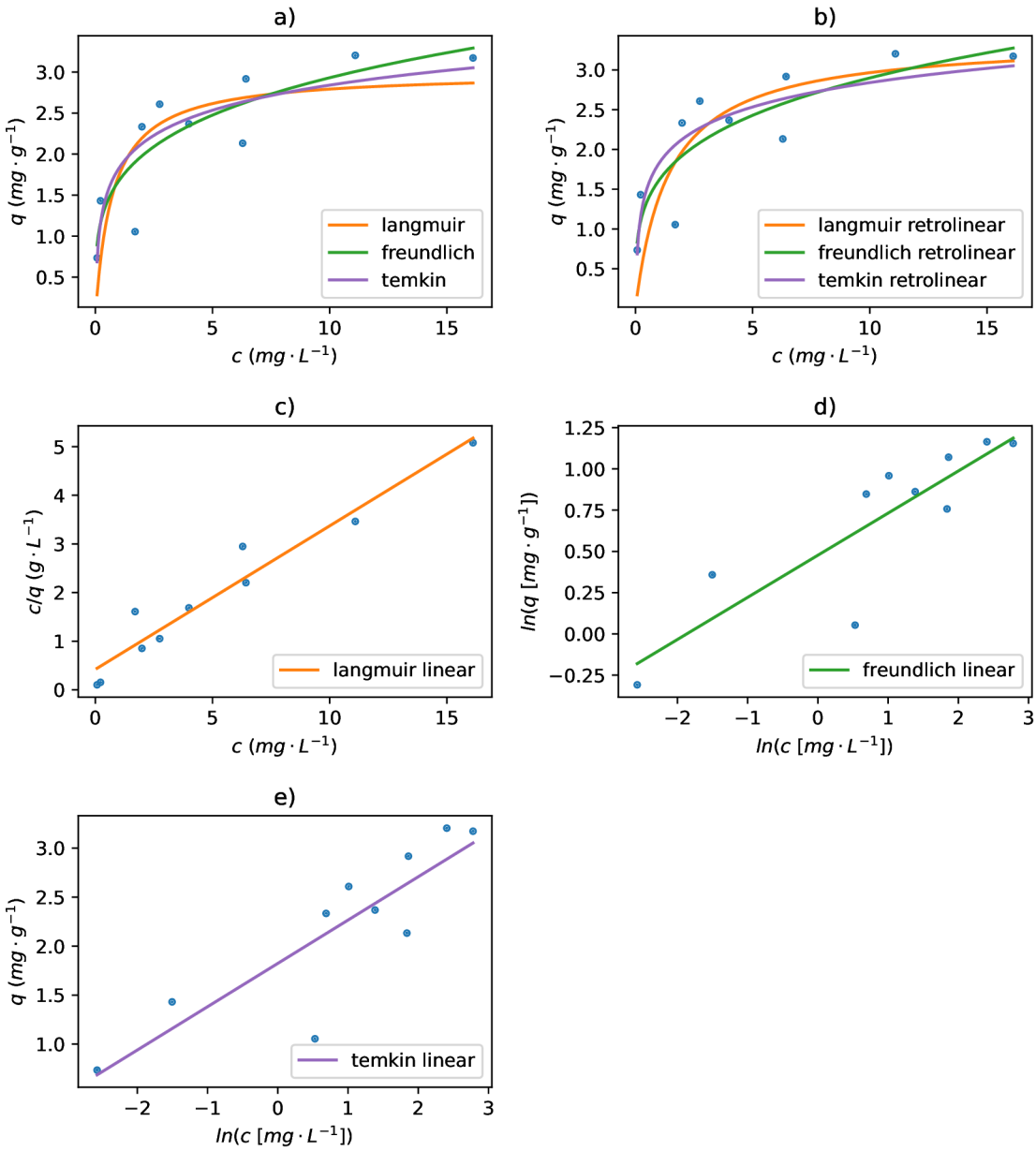

Figure A.9: Adsorption isotherms and their linearised forms for adsorption of Zn on bigger fraction PET ($0,63\ \mu m - 1\ mm$) in freshwater: a) adsorption isotherms constructed from non-linear fitting; b) adsorption isotherms constructed from linear fitting; c) Langmuir linear regression; d) Freundlich linear regression; e) Temkin linear regression.

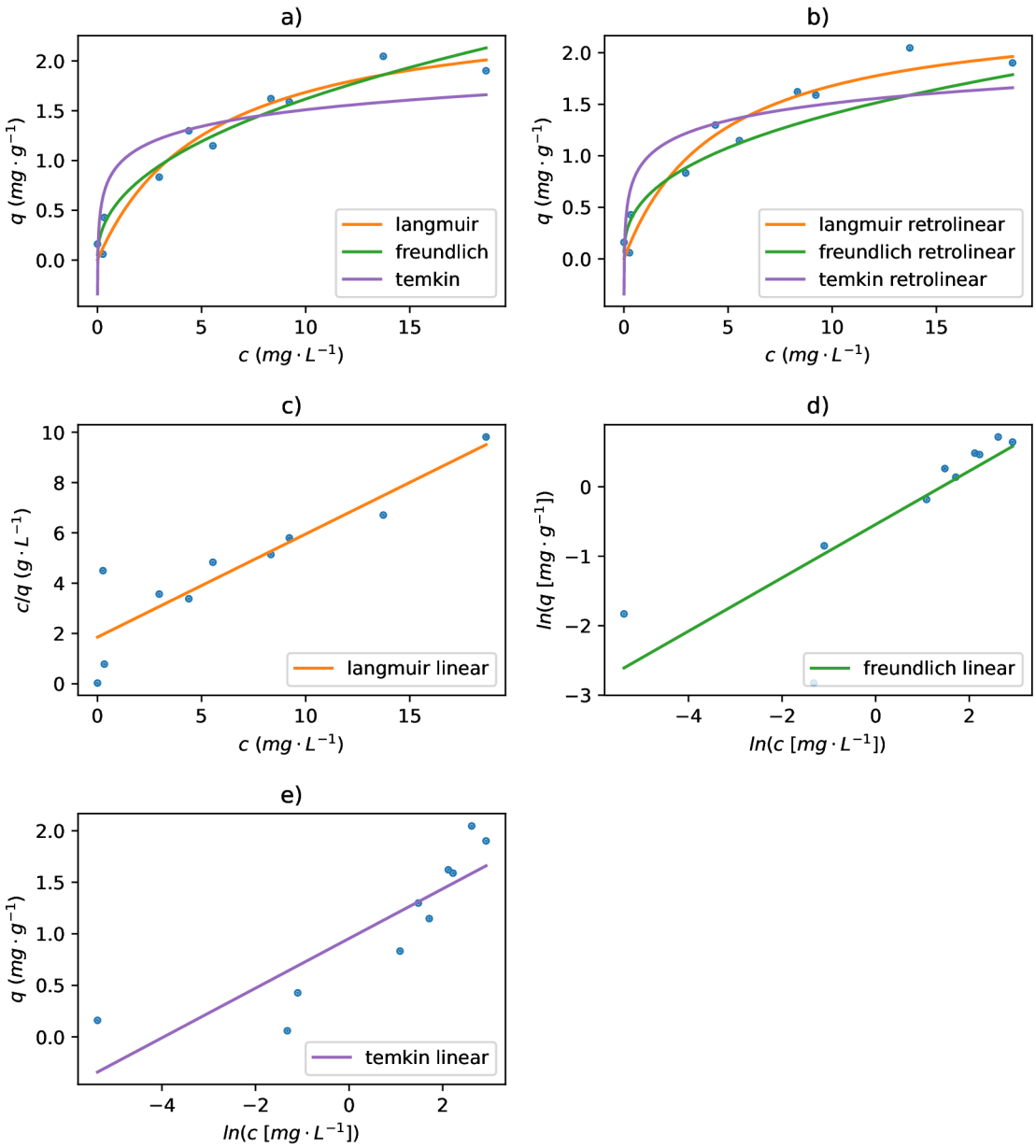

Figure A.10: Adsorption isotherms and their linearised forms for adsorption of Zn on smaller fraction PET ($< \ 0,63 \ \mu m$) in seawater: a) adsorption isotherms constructed from non-linear fitting; b) adsorption isotherms constructed from linear fitting; c) Langmuir linear regression; d) Freundlich linear regression; e) Temkin linear regression.

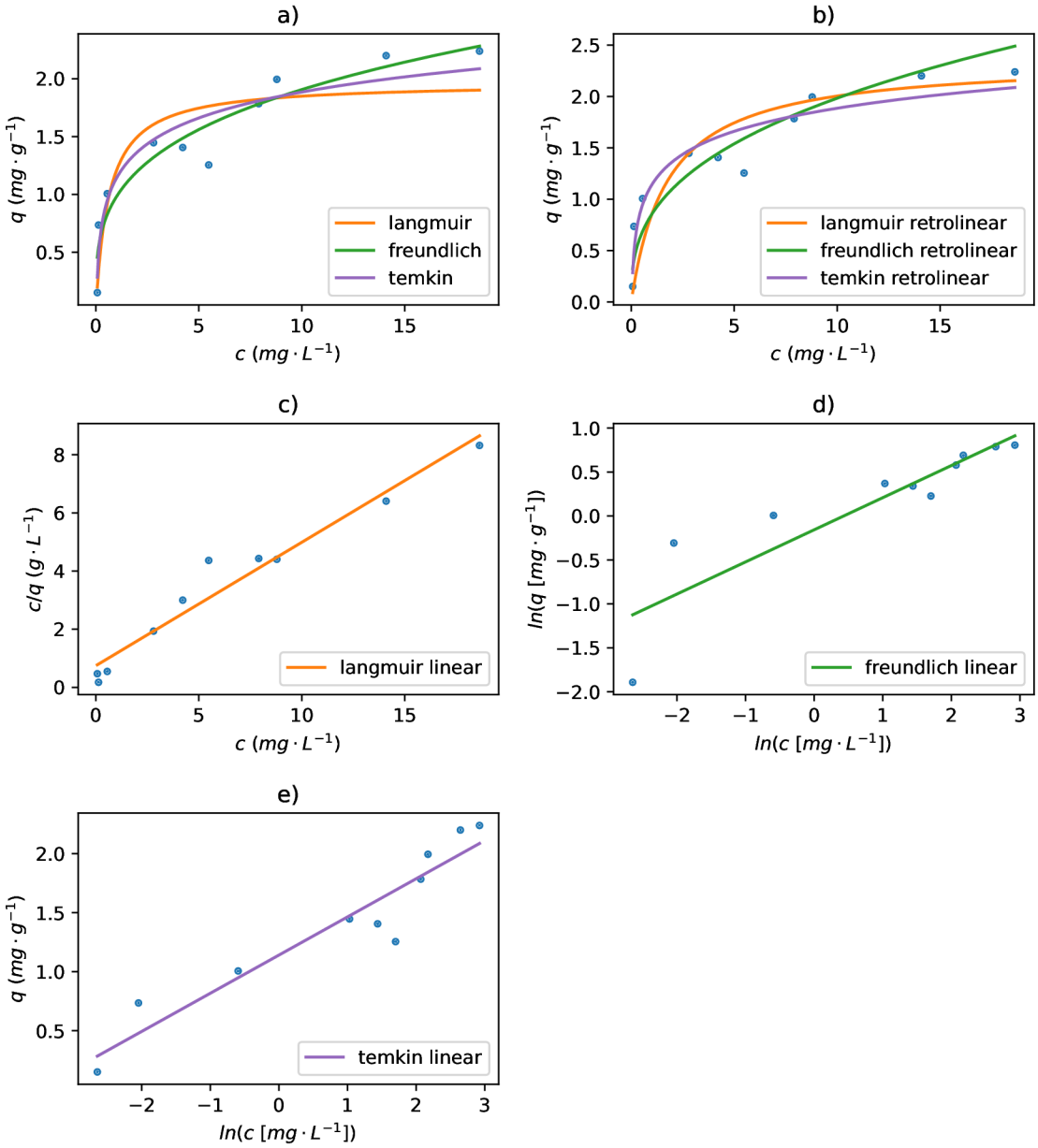

Figure A.11: Adsorption isotherms and their linearised forms for adsorption of Zn on bigger fraction PET ($0,63\ \mu m - 1\ mm$) in seawater: a) adsorption isotherms constructed from non-linear fitting; b) adsorption isotherms constructed from linear fitting; c) Langmuir linear regression; d) Freundlich linear regression; e) Temkin linear regression.

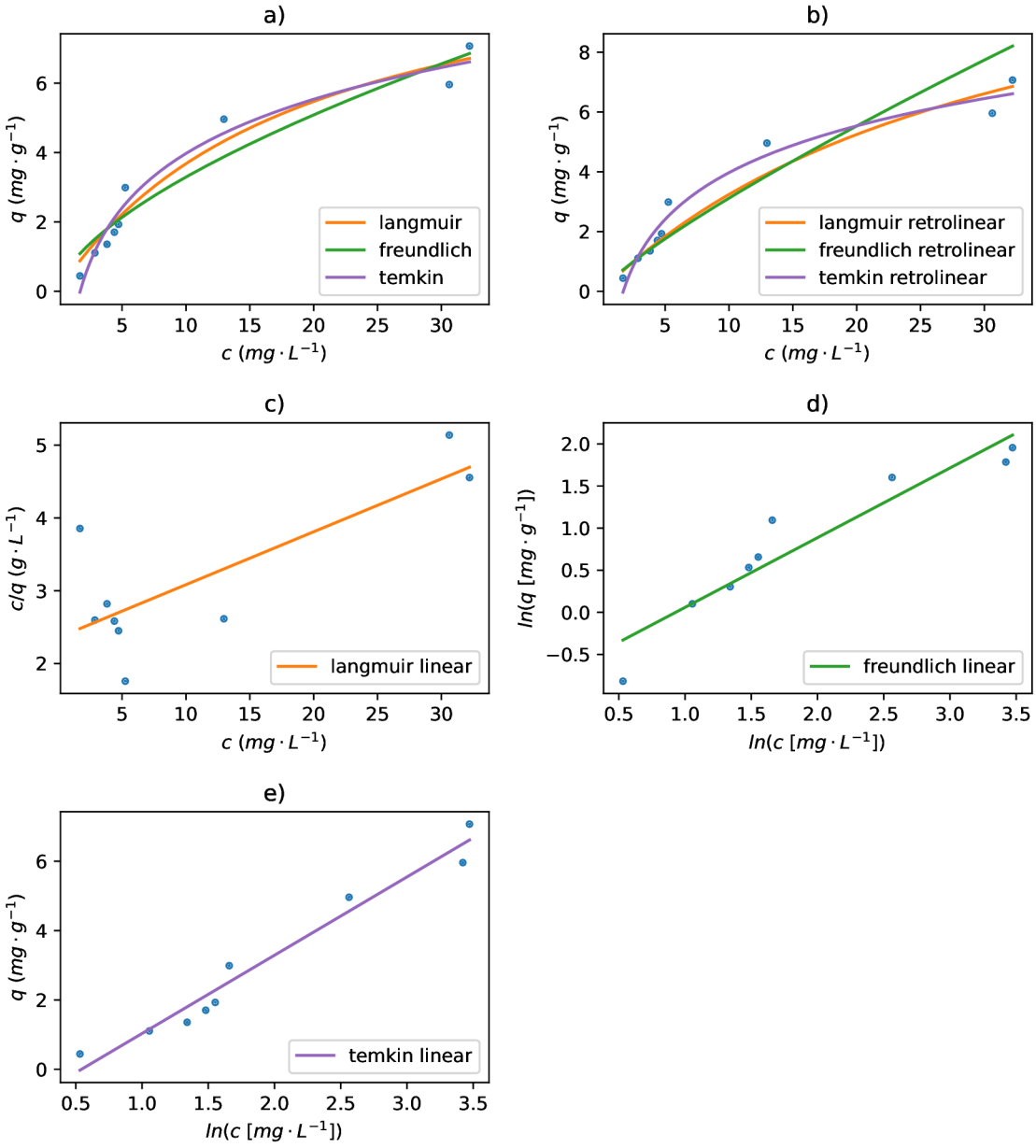

Figure A.12: Adsorption isotherms and their linearised forms for adsorption of Cu on smaller fraction PET ($< 0,63\ \mu m$) in freshwater: a) adsorption isotherms constructed from non-linear fitting; b) adsorption isotherms constructed from linear fitting; c) Langmuir linear regression; d) Freundlich linear regression; e) Temkin linear regression.

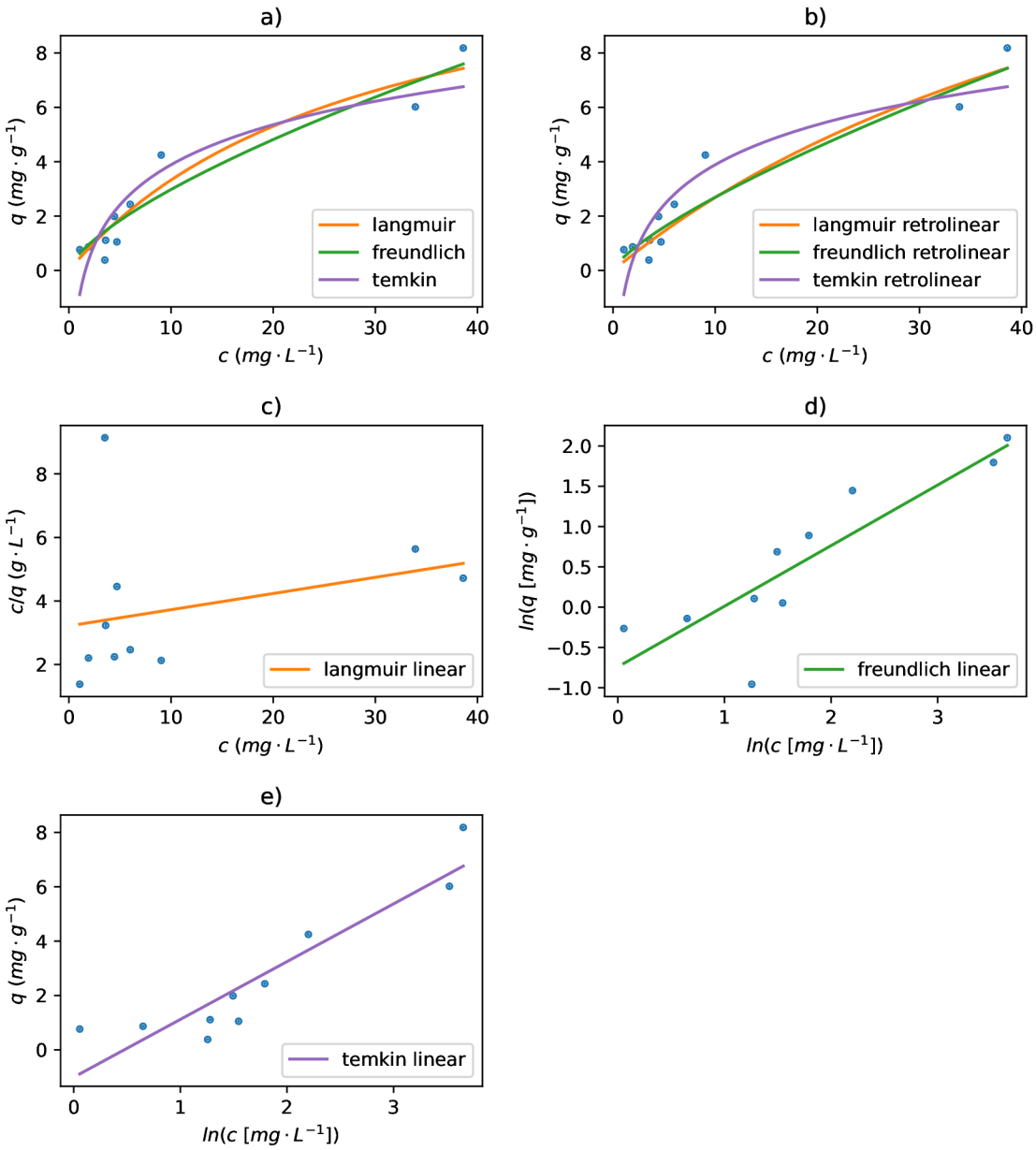

Figure A.13: Adsorption isotherms and their linearised forms for adsorption of Cu on bigger fraction PET ($0,63\ \mu m - 1\ mm$) in freshwater: a) adsorption isotherms constructed from non-linear fitting; b) adsorption isotherms constructed from linear fitting; c) Langmuir linear regression; d) Freundlich linear regression; e) Temkin linear regression.

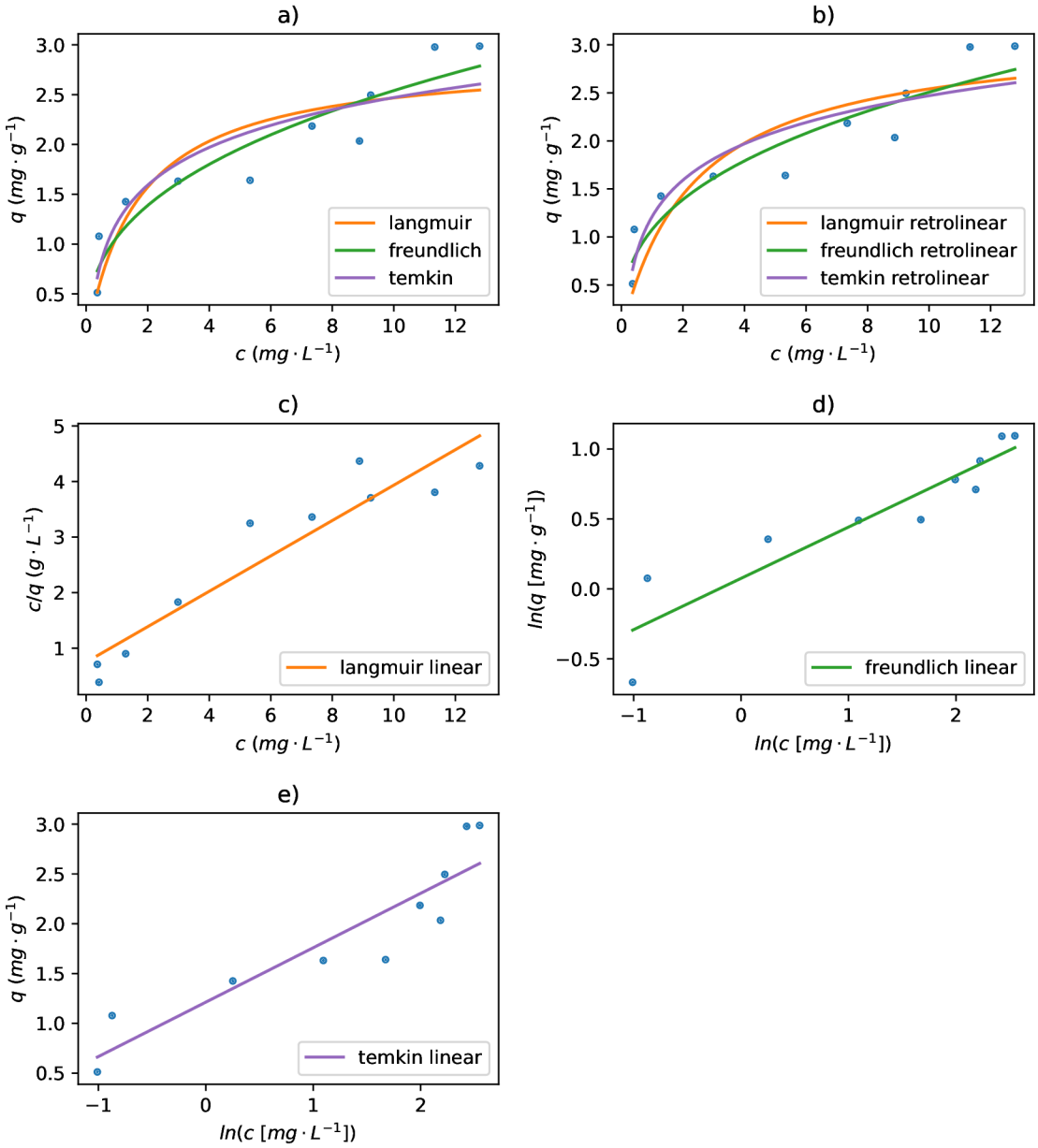

Figure A.14: Adsorption isotherms and their linearised forms for adsorption of Cu on smaller fraction PET ($< 0,63\ \mu m$) in seawater: a) adsorption isotherms constructed from non-linear fitting; b) adsorption isotherms constructed from linear fitting; c) Langmuir linear regression; d) Freundlich linear regression; e) Temkin linear regression.

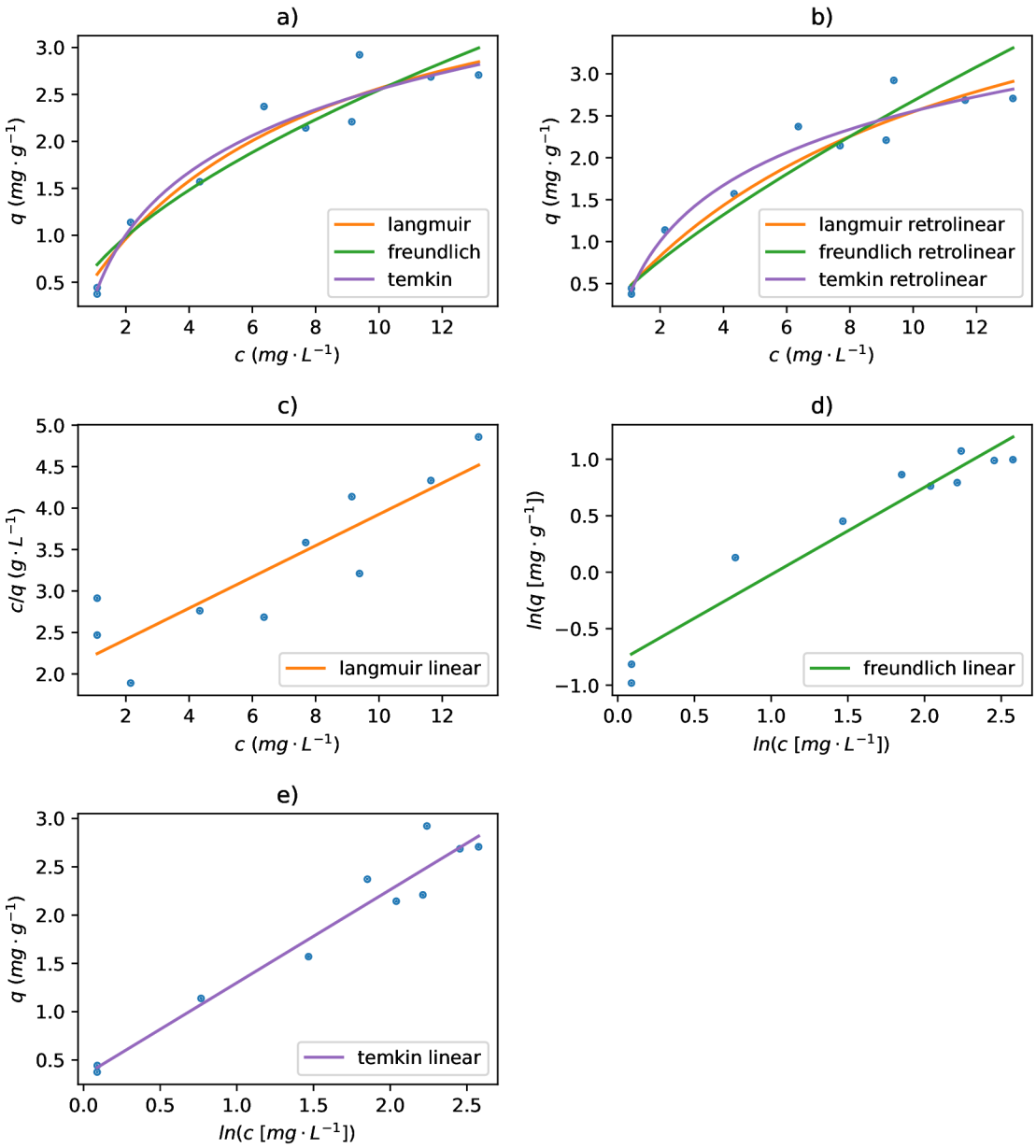

Figure A.15: Adsorption isotherms and their linearised forms for adsorption of Cu on bigger fraction PET ($0,63\ \mu m - 1\ mm$) in seawater: a) adsorption isotherms constructed from non-linear fitting; b) adsorption isotherms constructed from linear fitting; c) Langmuir linear regression; d) Freundlich linear regression; e) Temkin linear regression.

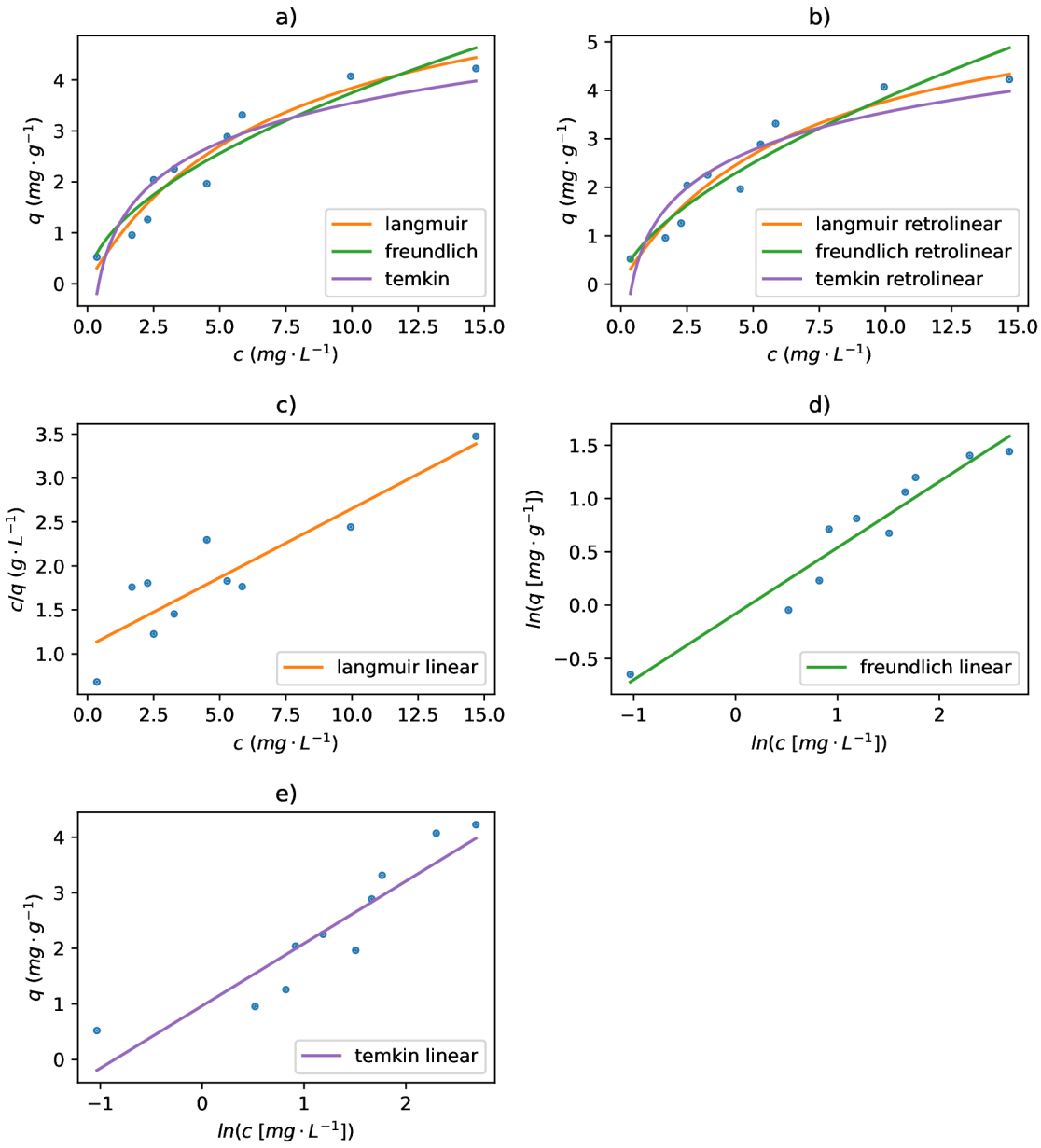

Figure A.16: Adsorption isotherms and their linearised forms for adsorption of Cd on smaller fraction PET ($< 0,63\ \mu m$) in freshwater: a) adsorption isotherms constructed from non-linear fitting; b) adsorption isotherms constructed from linear fitting; c) Langmuir linear regression; d) Freundlich linear regression; e) Temkin linear regression.

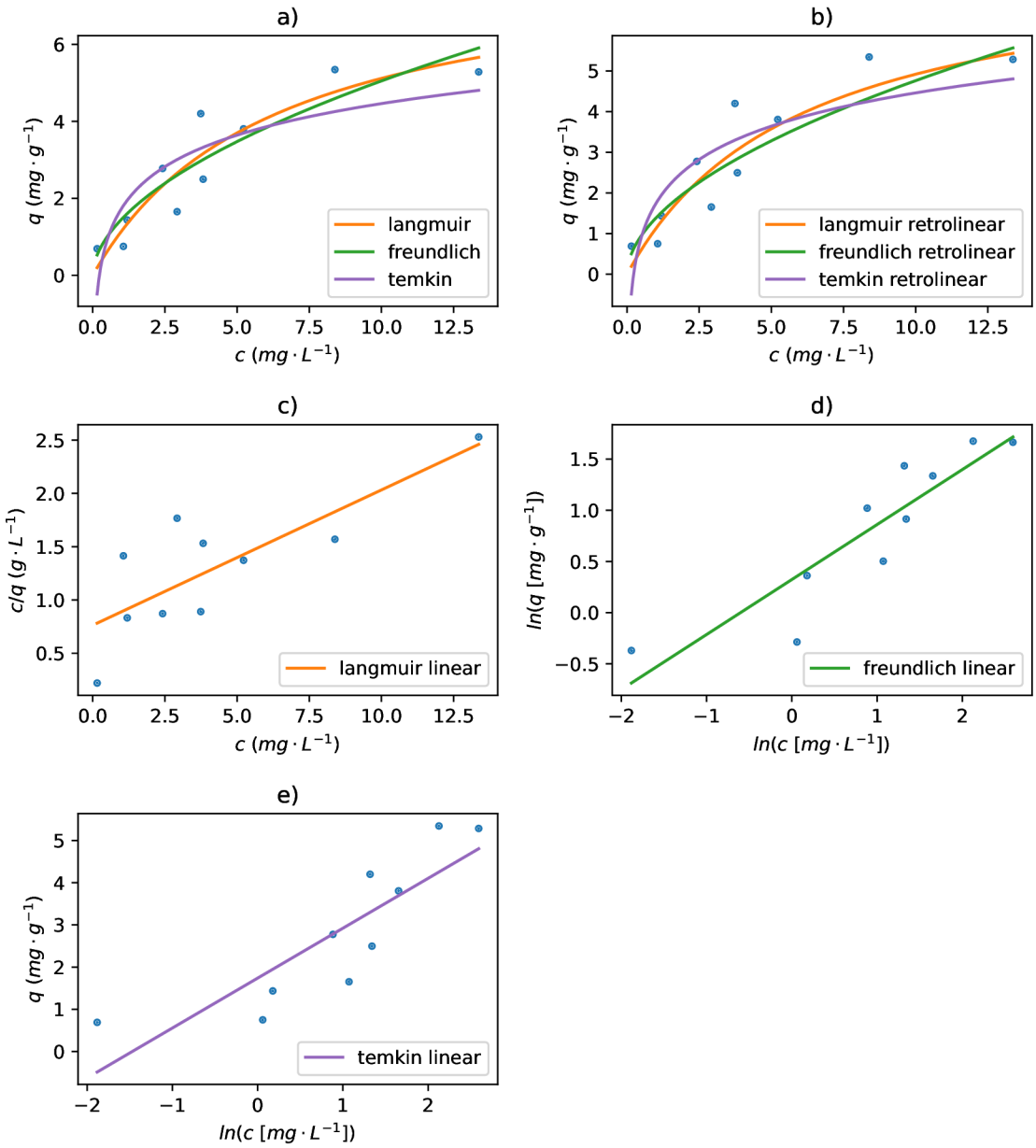

Figure A.17: Adsorption isotherms and their linearised forms for adsorption of Cd on bigger fraction PET ($0,63\ \mu m - 1\ mm$) in freshwater: a) adsorption isotherms constructed from non-linear fitting; b) adsorption isotherms constructed from linear fitting; c) Langmuir linear regression; d) Freundlich linear regression; e) Temkin linear regression.

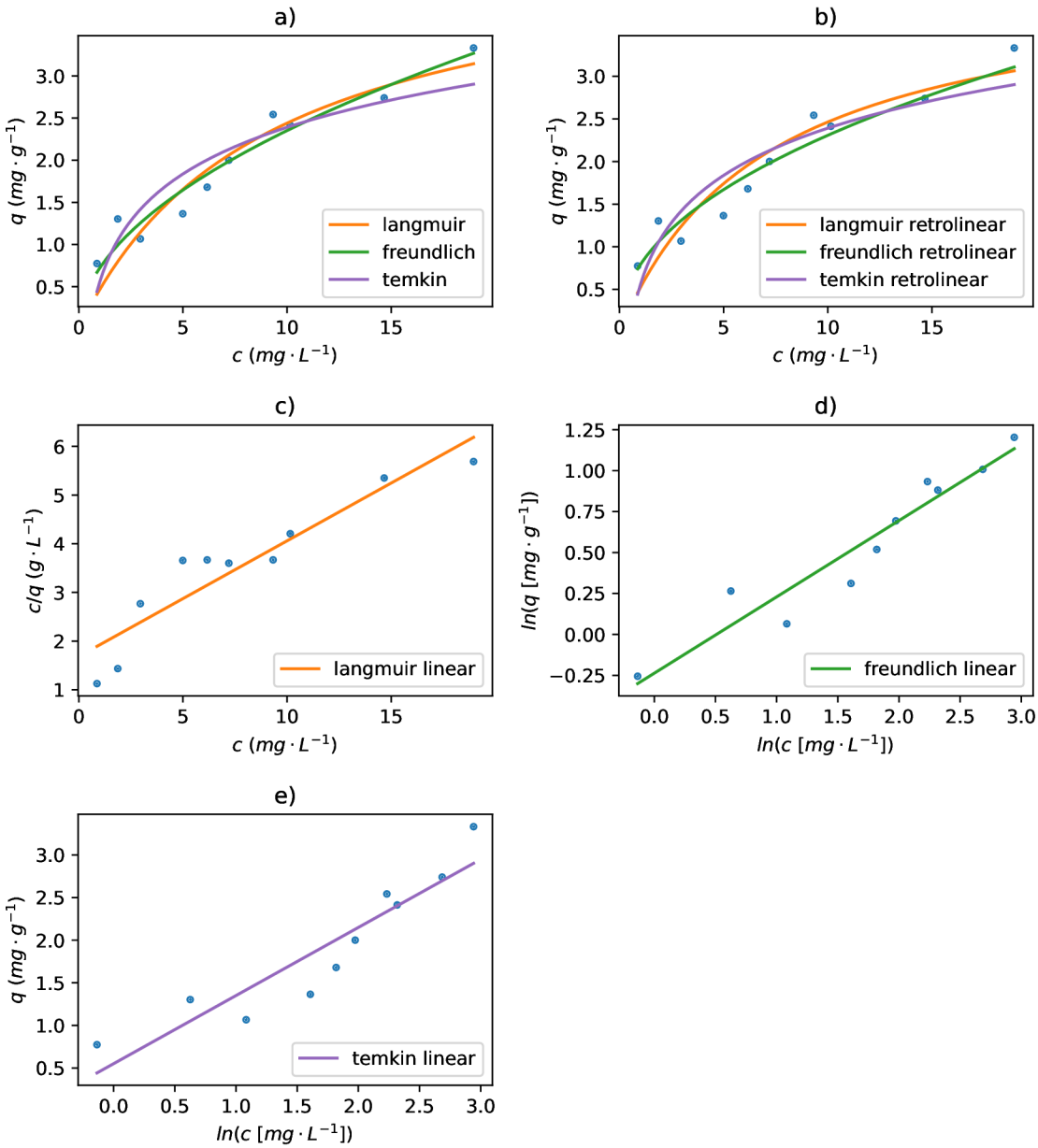

Figure A.18: Adsorption isotherms and their linearised forms for adsorption of Cd on smaller fraction PET ($< 0,63\ \mu m$) in seawater: a) adsorption isotherms constructed from non-linear fitting; b) adsorption isotherms constructed from linear fitting; c) Langmuir linear regression; d) Freundlich linear regression; e) Temkin linear regression.

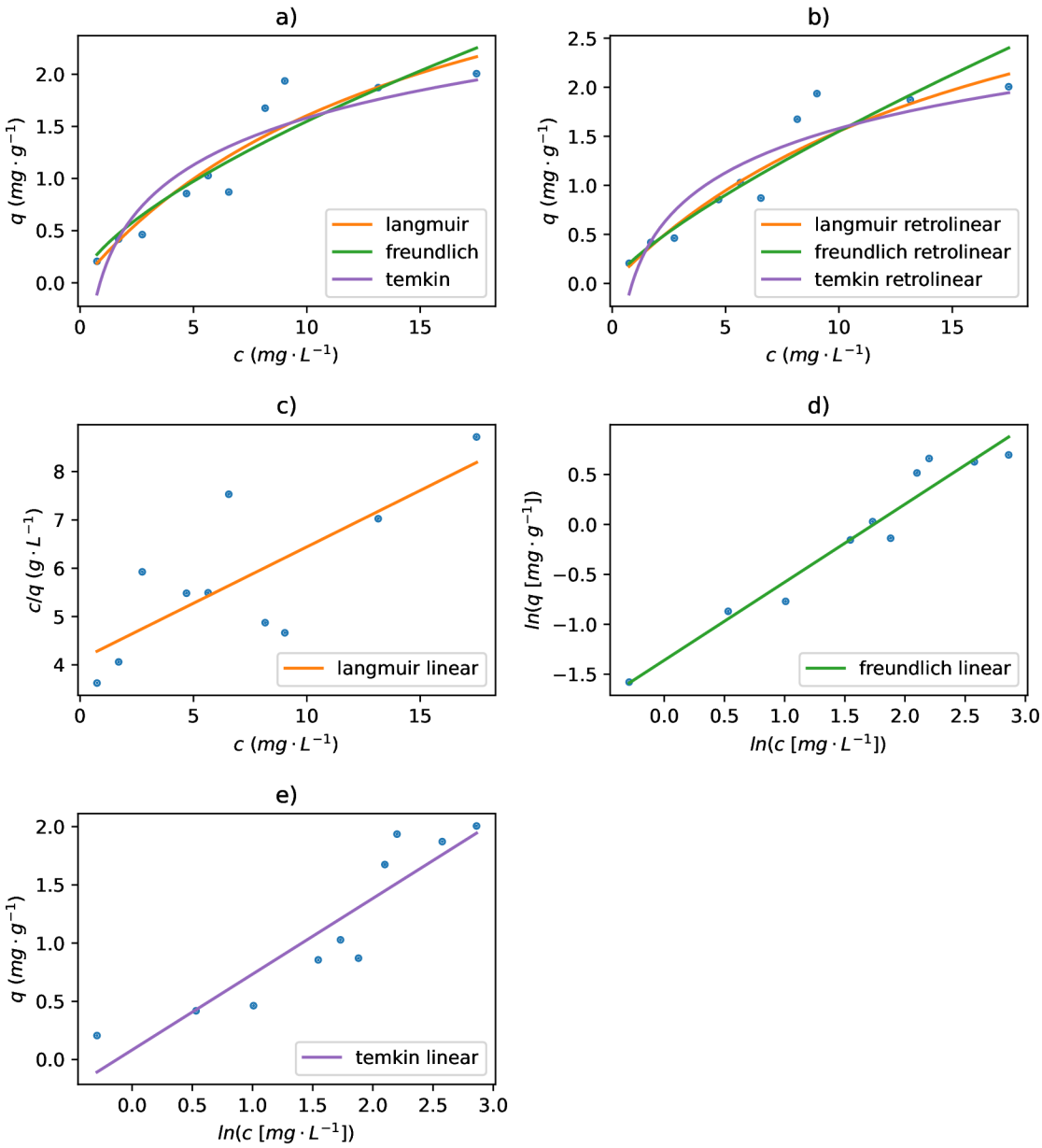

Figure A.19: Adsorption isotherms and their linearised forms for adsorption of Cd on bigger fraction PET ($0,63\ \mu m - 1\ mm$) in seawater: a) adsorption isotherms constructed from non-linear fitting; b) adsorption isotherms constructed from linear fitting; c) Langmuir linear regression; d) Freundlich linear regression; e) Temkin linear regression.

Appendix B

Isotherms parameters

Langmuir isotherm							
q_{max} (exp.)							
freshwater				seawater			
A		B		A		B	
6.391		5.862		1.242		3.238	
		q_{max}	K_l	R^2	a	b	R^2 (reg.)
linear fitting							
freshwater	A	19.68	0.007443	0.9369	0.05081	6.826	0.2313
	B	-240.6	-0.0004508	0.7566	-0.004156	9.219	0.000636
seawater	A	38.16	0.0009548	0.7314	0.02621	27.45	0.001581
	B	4.276	0.09647	0.9725	0.2339	2.424	0.9812
non-linear fitting							
freshwater	A	2.864	-6.797e+06	-2.675e-08	-	-	-
	B	2.942	-6.705e+06	-1.679e-08	-	-	-
seawater	A	3.16	0.01776	0.7882	-	-	-
	B	2.579	-1.785e+07	-3.26e-08	-	-	-
Freundlich isotherm							
		n	K_f	R^2	a	b	R^2 (reg.)
linear fitting							
freshwater	A	1.225	0.2181	-1.123	0.8162	-1.523	0.9195
	B	0.8897	0.07777	-2.21	1.124	-2.554	0.8842
seawater	A	0.9875	0.03561	-0.4486	1.013	-3.335	0.878
	B	1.887	0.5612	-1.204	0.5299	-0.5778	0.919
non-linear fitting							
freshwater	A	1.308	0.2672	0.9234	-	-	-
	B	1.356	0.2846	0.8851	-	-	-
seawater	A	1.297	0.07927	0.7667	-	-	-
	B	2.411	0.7908	0.9123	-	-	-
Temkin isotherm							
		b_t	K_t	R^2	a	b	R^2 (reg.)
linear fitting							
freshwater	A	1265	0.2356	0.8209	1.959	-2.832	0.8209
	B	957.4	0.1463	0.9541	2.589	-4.976	0.9541
seawater	A	4574	0.2506	0.7893	0.542	-0.75	0.7893
	B	2478	0.8314	0.9693	1	-0.1847	0.9693
non-linear fitting							
freshwater	A	1265	0.2356	0.8209	-	-	-
	B	957.4	0.1463	0.9541	-	-	-
seawater	A	4574	0.2506	0.7893	-	-	-
	B	2478	0.8314	0.9693	-	-	-

Table B.1: Calculated parameters of adsorption isotherms for Pb, reg. = regression, exp. = experimental, A = small fraction, B = big fraction, – - does not apply.

Langmuir isotherm							
q_{max} (exp.)							
freshwater				seawater			
A		B		A		B	
1.666		1.307		1.063		1.236	
		q_{max}	K_l	R^2	a	b	R^2 (reg.)
linear fitting							
freshwater	A	3.095	0.08354	0.8245	0.3231	3.868	0.4023
	B	2.145	0.0598	0.6627	0.4662	7.796	0.2618
seawater	A	-5.014	-0.01259	0.5869	-0.1994	15.85	0.04789
	B	84.45	0.000984	0.9329	0.01184	12.03	0.001855
non-linear fitting							
freshwater	A	2.608	0.1247	0.8454	-	-	-
	B	1.641	0.1133	0.7074	-	-	-
seawater	A	2.28	0.05804	0.84	-	-	-
	B	5.652	0.01779	0.9491	-	-	-
Freundlich isotherm							
		n	K_f	R^2	a	b	R^2 (reg.)
linear fitting							
freshwater	A	1.718	0.3536	0.7452	0.5822	-1.04	0.6856
	B	1.532	0.1784	0.6156	0.6527	-1.724	0.657
seawater	A	0.8459	0.05372	-0.5662	1.182	-2.924	0.9111
	B	0.9841	0.08065	0.04015	1.016	-2.518	0.9768
non-linear fitting							
freshwater	A	1.817	0.3963	0.8228	-	-	-
	B	1.79	0.231	0.7044	-	-	-
seawater	A	1.418	0.1582	0.7975	-	-	-
	B	1.125	0.1081	0.9407	-	-	-
Temkin isotherm							
		b_t	K_t	R^2	a	b	R^2 (reg.)
linear fitting							
freshwater	A	5513	2.116	0.7598	0.4496	0.3371	0.7598
	B	7947	1.539	0.6757	0.3119	0.1345	0.6757
seawater	A	5768	0.7276	0.8449	0.4297	-0.1366	0.8449
	B	4749	0.5574	0.9076	0.522	-0.3051	0.9076
non-linear fitting							
freshwater	A	5513	2.116	0.7598	-	-	-
	B	7947	1.539	0.6757	-	-	-
seawater	A	5768	0.7276	0.8449	-	-	-
	B	4749	0.5574	0.9076	-	-	-

Table B.2: Calculated parameters of adsorption isotherms for Hg, reg. = regression, exp. = experimental, A = small fraction, B = big fraction, – - does not apply.

Langmuir isotherm							
q_{max} (exp.)							
freshwater				seawater			
A		B		A		B	
7.069		8.181		2.987		2.923	
		q_{max}	K_l	R^2	a	b	R^2 (reg.)
linear fitting							
freshwater	A	13.76	0.03084	0.9358	0.07268	2.357	0.6196
	B	19.62	0.01585	0.8985	0.05097	3.216	0.08981
seawater	A	3.141	0.4241	0.7791	0.3184	0.7506	0.8937
	B	5.303	0.09248	0.9288	0.1886	2.039	0.7746
non-linear fitting							
freshwater	A	10.68	0.05248	0.956	-	-	-
	B	13.07	0.0342	0.9218	-	-	-
seawater	A	2.877	0.6017	0.7871	-	-	-
	B	4.388	0.1406	0.9406	-	-	-
Freundlich isotherm							
		n	K_f	R^2	a	b	R^2 (reg.)
linear fitting							
freshwater	A	1.208	0.4632	-0.8092	0.8279	-0.7695	0.8969
	B	1.33	0.4769	-0.3667	0.7518	-0.7405	0.7514
seawater	A	2.727	1.078	0.746	0.3667	0.0749	0.8565
	B	1.295	0.4525	-0.7957	0.7723	-0.7929	0.9345
non-linear fitting							
freshwater	A	1.594	0.7764	0.9292	-	-	-
	B	1.444	0.6049	0.9135	-	-	-
seawater	A	2.66	1.069	0.8886	-	-	-
	B	1.691	0.653	0.9098	-	-	-
Temkin isotherm							
		b_t	K_t	R^2	a	b	R^2 (reg.)
linear fitting							
freshwater	A	1098	0.5809	0.9644	2.257	-1.226	0.9644
	B	1167	0.6237	0.8505	2.125	-1.003	0.8505
seawater	A	4538	9.213	0.8423	0.5463	1.213	0.8423
	B	2573	1.417	0.95	0.9634	0.336	0.95
non-linear fitting							
freshwater	A	1098	0.5809	0.9644	-	-	-
	B	1167	0.6237	0.8505	-	-	-
seawater	A	4538	9.213	0.8423	-	-	-
	B	2573	1.417	0.95	-	-	-

Table B.3: Calculated parameters of adsorption isotherms for Cu, reg. = regression, exp. = experimental, A = small fraction, B = big fraction, – - does not apply.

Langmuir isotherm							
q_{max} (exp.)							
freshwater				seawater			
A		B		A		B	
4.225		5.343		3.332		2.006	
		q_{max}	K_l	R^2	a	b	R^2 (reg.)
linear fitting							
freshwater	A	6.368	0.145	0.9323	0.157	1.083	0.8119
	B	7.877	0.1664	0.8587	0.1269	0.7631	0.6386
seawater	A	4.21	0.141	0.8936	0.2375	1.685	0.8705
	B	4.283	0.05684	0.8919	0.2335	4.107	0.5804
non-linear fitting							
freshwater	A	6.644	0.1371	0.9337	-	-	-
	B	8.289	0.1613	0.8635	-	-	-
seawater	A	4.638	0.111	0.8994	-	-	-
	B	4.092	0.06443	0.8964	-	-	-
Freundlich isotherm							
		n	K_f	R^2	a	b	R^2 (reg.)
linear fitting							
freshwater	A	1.614	0.9231	-0.5845	0.6195	-0.08	0.9245
	B	1.861	1.382	-0.4643	0.5374	0.3234	0.8105
seawater	A	2.146	0.7891	0.4464	0.466	-0.2369	0.9176
	B	1.279	0.2565	0.158	0.7817	-1.361	0.9466
non-linear fitting							
freshwater	A	1.818	1.056	0.9083	-	-	-
	B	1.853	1.458	0.837	-	-	-
seawater	A	1.942	0.7188	0.944	-	-	-
	B	1.492	0.3307	0.8716	-	-	-
Temkin isotherm							
		b_t	K_t	R^2	a	b	R^2 (reg.)
linear fitting							
freshwater	A	2210	2.367	0.8463	1.121	0.9663	0.8463
	B	2097	4.352	0.7263	1.182	1.739	0.7263
seawater	A	3103	1.995	0.8573	0.7988	0.5518	0.8573
	B	3809	1.135	0.835	0.6508	0.08253	0.835
non-linear fitting							
freshwater	A	2210	2.367	0.8463	-	-	-
	B	2097	4.352	0.7263	-	-	-
seawater	A	3103	1.995	0.8573	-	-	-
	B	3809	1.135	0.835	-	-	-

Table B.4: Calculated parameters of adsorption isotherms for Cd, reg. = regression, exp. = experimental, A = small fraction, B = big fraction, – - does not apply.

Appendix C

FTIR spectra

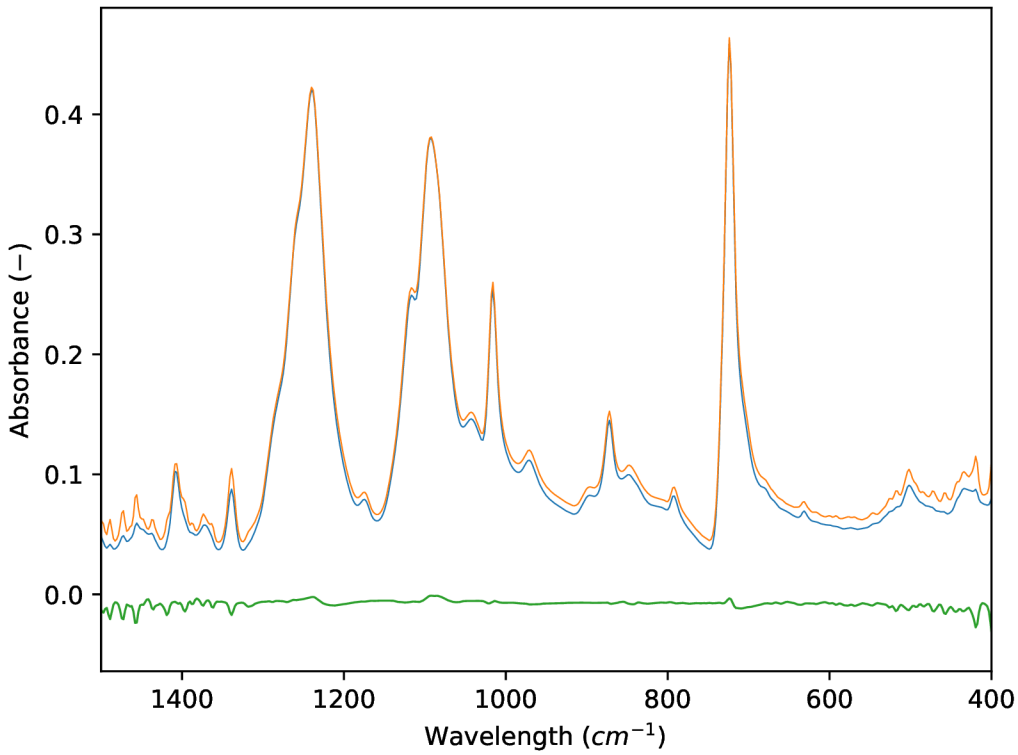

Figure C.1: FTIR spectra of small fraction PET ($< 0,63\ \mu m$) - blue, small fraction PET with adsorbed Hg - orange, and visualized difference in adsorptions - green.

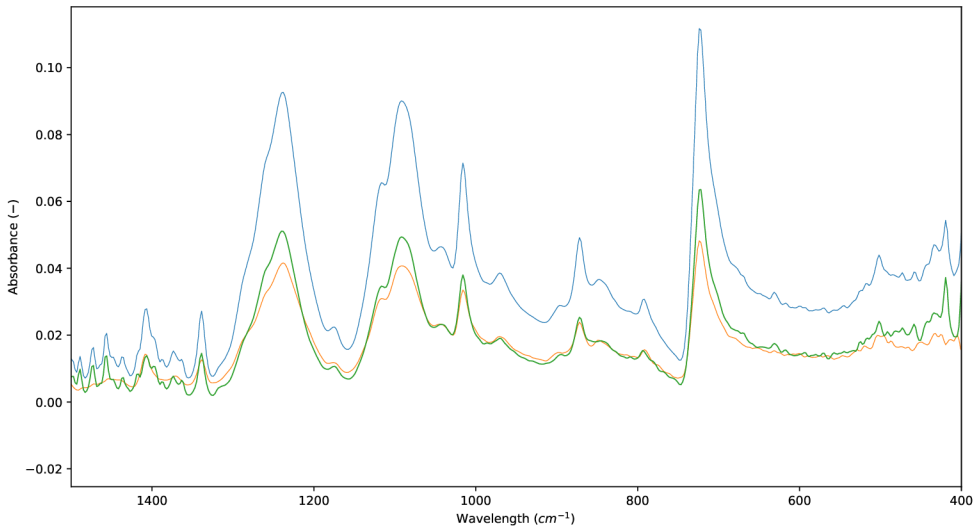

Figure C.2: FTIR spectra of big fraction PET $(0,63\ \mu m - 1\ mm)$ - blue, big fraction PET with adsorbed Hg - orange, and visualized difference in adsorptions - green.

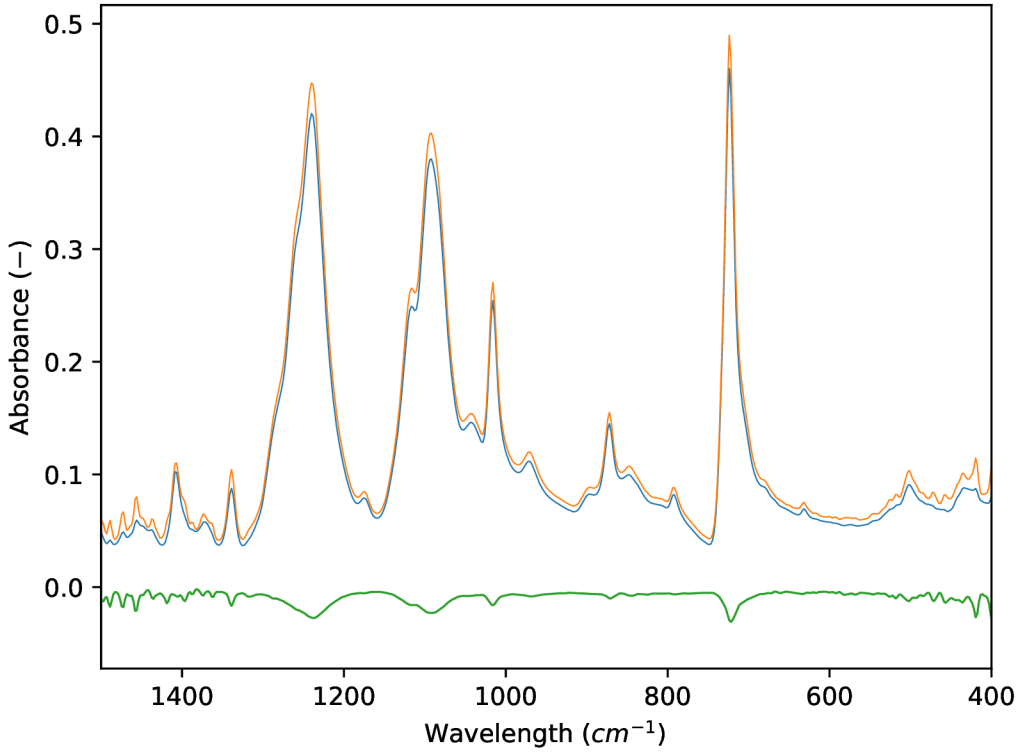

Figure C.3: FTIR spectra of small fraction PET $(< 0,63\ \mu m)$ - blue, small fraction PET with adsorbed Zn - orange, and visualized difference in adsorptions - green.

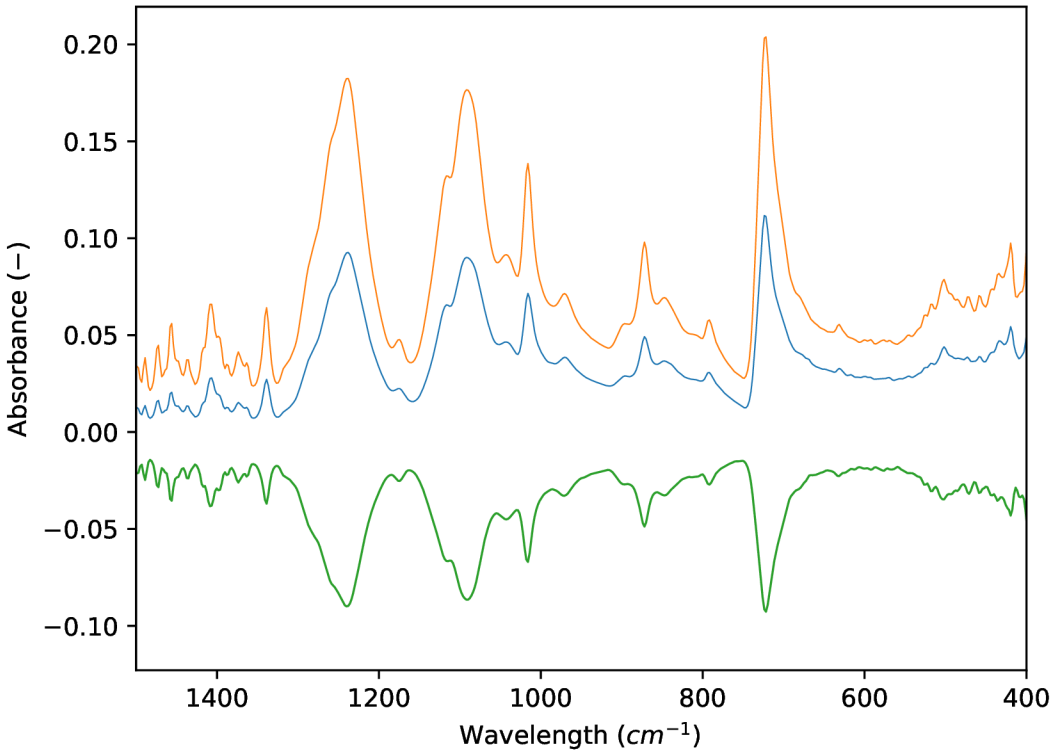

Figure C.4: FTIR spectra of big fraction PET ($0,63\ \mu m - 1\ mm$) - blue, big fraction PET with adsorbed Zn - orange, and visualized difference in adsorptions - green.

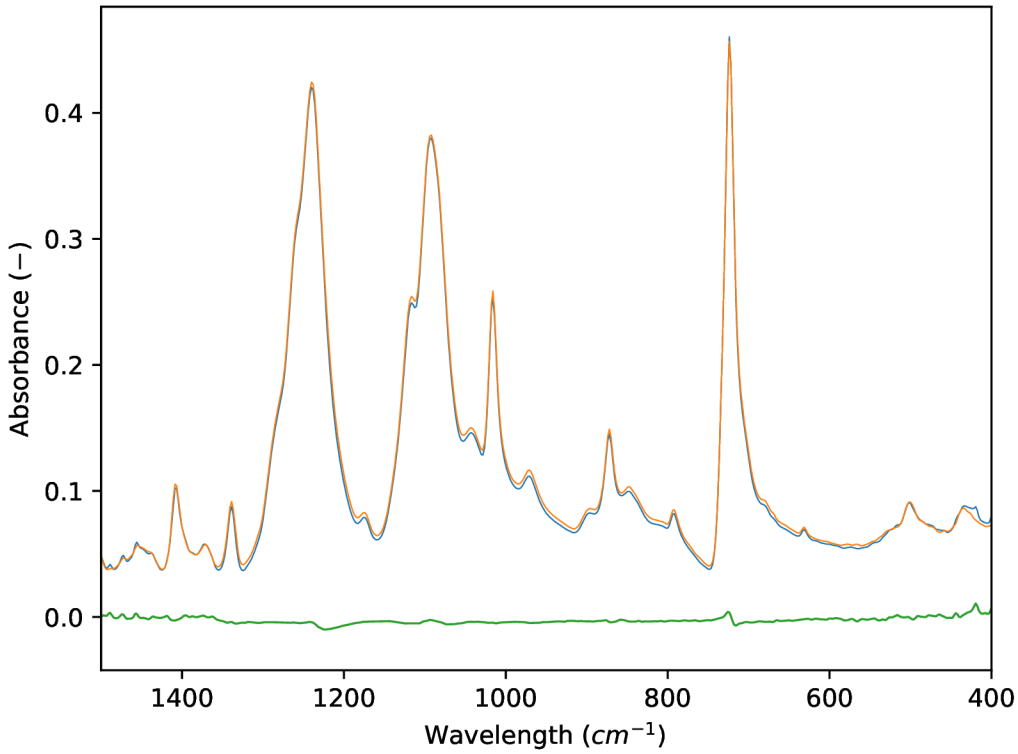

Figure C.5: FTIR spectra of small fraction PET ($< 0,63\ \mu m$) - blue, small fraction PET with adsorbed Cu - orange, and visualized difference in adsorptions - green.

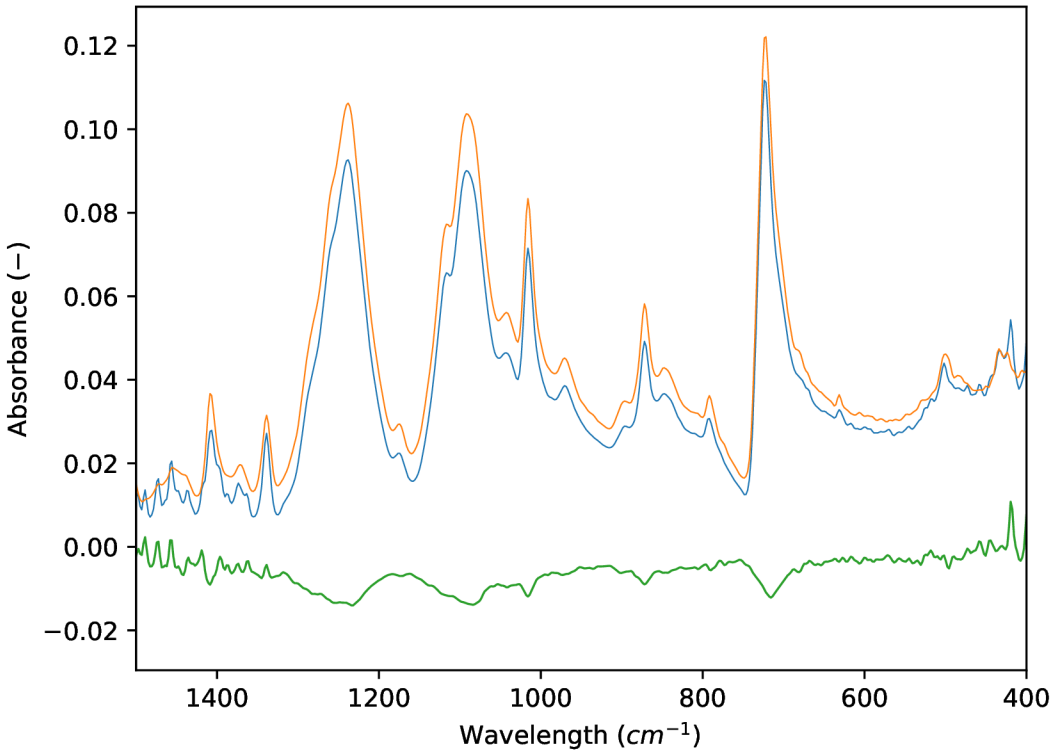

Figure C.6: FTIR spectra of big fraction PET $(0,63\ \mu m - 1\ mm)$ - blue, big fraction PET with adsorbed Cu - orange, and visualized difference in adsorptions - green.

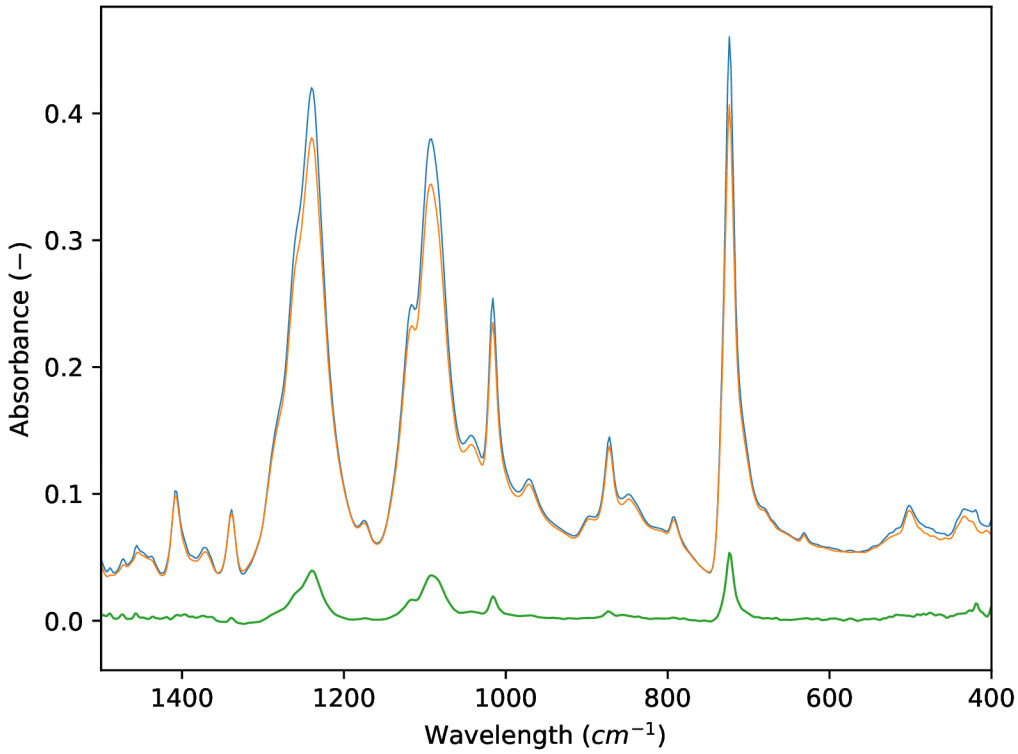

Figure C.7: FTIR spectra of small fraction PET ($< 0,63\ \mu m$) - blue, small fraction PET with adsorbed Cd - orange, and visualized difference in adsorptions - green.

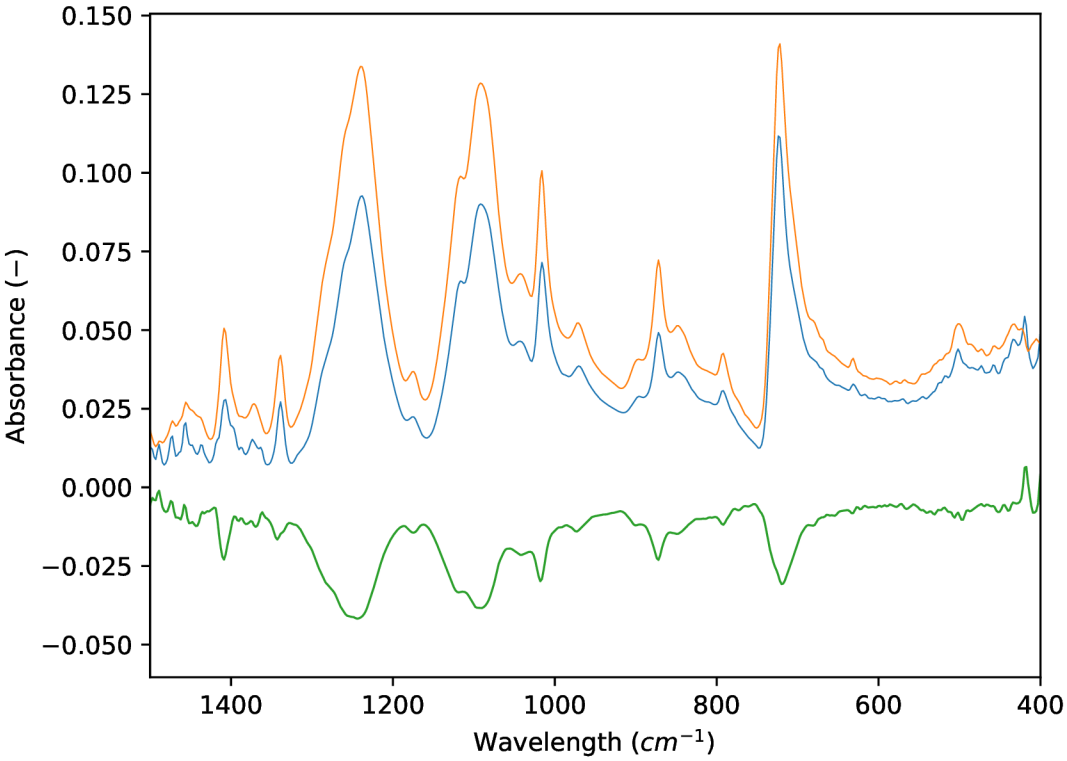

Figure C.8: FTIR spectra of big fraction PET ($0,63\ \mu m - 1\ mm$) - blue, big fraction PET with adsorbed Cd - orange, and visualized difference in adsorptions - green.